Relationship among EEG patterns, spatial memory and cell loss in neural degeneration induced by kainic acid or dexamethasone and in aging rats

Acharaporn Issuriya

A Thesis Submitted in Partial Fulfillment of the Requirements for the Degree of

Doctor of Philosophy in Physiology

Prince of Songkla University

2014

Thesis Title Relationship among EEG patterns, spatial memory and cell loss in neural degeneration induced by kainic acid or dexamethasone andin aging rats

Author Acharaporn Issuriya

Major Program Physiology

Major advisor:

…….
(Asst. Prof. Dr. Ekkasit Kumarnsit)

Co-advisors:

…….
(Asst. Prof. Dr. Uraporn Vongvatcharanon)

…….
(Asst. Prof. Dr. Chatchai Wattanapiromsakul)

Examining Committees:

……..……..……..… Chairperson
(Asst. Prof. Dr. Kitja Sawangjaroen)

……..……..……..… Committee
(Asst. Prof. Dr. Ekkasit Kumarnsit)

……..……..……..… Committee
(Asst. Prof. Dr. Uraporn Vongvatcharanon)

……..……..……..… Committee
(Prof. M.D. Anan Srikiatkhachorn)

……..……..……..… Committee
(Dr. Pennapa Chonpathompikunlert)

The Graduate School, Prince of Songkla University, has approved this thesis as partial fulfillment of the requirements for the degree of doctor of Philosophy in Physiology

.....

(Assoc. Prof. Dr. Teerapol Srichana)

Dean of Graduate School

This is to certify that he work here submitted is the result of the candidate's own investigation. Due acknowledgement has been made of any assistance received

……

(Asst. Prof. Dr. Ekkasit Kumarnsit)

Advisor

……

(Miss Acharaporn Issuriya)

Candidate

I hereby certify that this work has not been accepted in substance for any degree, and is not being currently submitted in candidature for any degree.

…….

(Miss Acharaporn Issuriya)

Candidate

ชื่อวิทยานิพนธ์ ความสัมพันธ์ของรูปแบบคลื่นไฟฟ้าสมอง spatial memory และการลดลงของเซลล์ในภาวะเสื่อมของระบบประสาทที่ถูกชักนำโดย kainic acid หรือ dexamethasone และในหนูขาวใหญ่แก่

ผู้เขียน นางสาวอัจฉราภรณ์ อิสสุริยะ

สาขาวิชา สรีรวิทยา

ปีการศึกษา 2557

บทคัดย่อ

การเสื่อมของระบบประสาทเกิดล่วงหน้าความบกพร่องทางกายภาพและเชาว์ปัญญาเป็นเวลานาน การค้นพบตัวบ่งชี้ทางชีวภาพในการทำงานของสมองที่สัมพันธ์กับโรคสมองเสื่อมจะเพิ่มวิธีจัดการกับโรคได้ และสามารถระบุสัญญาณจากพยาธิสภาพของสมองให้เร็วที่สุดเท่าที่เป็นไปได้ การศึกษาครั้งนี้มีจุดมุ่งหมายเพื่อระบุความแตกต่างของสมองที่เสื่อมใน 3 รูปแบบจากการชักนำด้วย dexamethasone หรือ kainic acid และการแก่ตามปกติโดยใช้เทคนิคการตรวจวัดคลื่นไฟฟ้าสมอง ผลการศึกษาแสดงให้เห็นว่าการชักนำด้วย dexamethasone มีผลเพิ่มการทำงานของคลื่นไฟฟ้าสมองส่วน parietal cortex ในช่วงความถี่ต่ำโดยเฉพาะอย่างยิ่งคลื่น theta ตั้งแต่วันที่ 11 หลังการชักนำ และในวันที่ 21 พบการลดลงของเวลาการนอนหลับแบบ REM sleep และมีการเพิ่มจำนวนของ pathological sleep spindle ด้วย ส่วนการชักนำด้วย kainic acid มีผลเพิ่มเพิ่มการทำงานของคลื่นไฟฟ้าสมองช่วงความถี่ delta เช่นดียวกันแต่มีการลดลงของคลื่น theta ลดเวลาในการตื่นและนอนหลับแบบ REM sleep แต่เพิ่มเวลาการนอนหลับแบบ SWS sleep นอกจากนี้หนูแก่ตามปกติพบการเปลี่ยนแปลงเล็กน้อยคือการลดลงของการทำงานของคลื่นไฟฟ้าสมองช่วงความถี่ delta นอกจากนี้เมื่อวิเคราะห์ความสัมพันธ์การเปลี่ยนแปลงของคลื่นไฟฟ้าสมองกับเนื่อเยื่อสมองและพฤติกรรมการเรียนรู้จดจำ พบว่ามีความสัมพันธ์ระหว่างปัจจัยเหล่านี้อย่างชัดเจน โดยเฉพาะอย่างยิ่งข้อมูลจากการศึกษารูปแบบคลื่นไฟฟ้าสมองกับรูปแบบการนอนหลับมีความสัมพันธ์กับผลทดสอบพฤติกรรมการเรียนรู้ที่ค่อนข้างสูงกว่าข้อมูลจากเนื่อเยื้อวิทยาของสมอง การศึกษานี้ชี้ให้เห็นถึงความไวของเทคนิคการตรวจวัดคลื่นไฟฟ้าสมองในงานวิจัยการเสื่อมของระบบประสาท ด้วยคุณสมบัติที่มีค่าใช้จ่ายถูกและไม่ลุกล้ำร่างกาย วิธีนี้จึงเหมาะกับการใช้ที่ถี่เพื่อตรวจวัดการเปลี่ยนแปลงและรักษาภาวะสมองเสื่อมแต่เนิ่น

Thesis title	Relationship among EEG patterns, spatial memory and cell loss in neural degeneration induced by kainic acid or dexamethasone and in aging rats
Author	Miss Acharaporn Issuriya
Major Program	Physiology
Academic Year	2014

ABSTRACT

Neurodegeneration precedes the onset of physical and cognitive impairments by many years. The discovery of the earliest biomarkers in brain activity linked to the risk of getting the neurodegenerative diseases could improve the way the diseases are addressed. It is critical to identify traces of brain pathology to intervene as early as possible. This study aimed to distinguish brain oscillation of 3 different models of neurodegeneration from that of controls by using electroencephalography (EEG) technique. Neurodegeneration was induced with treatment of either dexamethasone or kainic acid and in spontaneous aged rats. The results showed that dexamethasone significantly increased parietal slow wave activity especially in Theta oscillation from as early as day 11. Dexamethasone also reduced REM sleep and increased pathological sleep spindle on day 21. Kainic acid also had similar effects in increasing slow Delta wave but specifically decreased Theta activity. Kainic acid suppressed awake and REM stages and enhanced SWS sleep. Minimal change was observed in spontaneous aged rats when only reduction of frontal Delta oscillation was detected. Moreover, matching of these changes in electrical brain activity with histological data and learning & memory behavior performances resulted in great correlations. In particular, EEG data and sleep patterns were found have relatively greater correlations with cognitive decline than histological data. Ultimately, the EEG study was capable to distinguish electrical brain oscillation induced by 3 different models where other techniques including histology or behavioral observation seemed unable. This study indicates the sensitivity of EEG study for neurodegenerative research. With non-invasive and inexpensive qualities, EEG technique is suitable for frequent use to detect early signs and allow for early intervention of neurodegeneration.

ACKNOWLEDGEMENT

I would like to express my sincere gratitude to my advisor Asst. Prof. Dr. Ekkasit Kumarnsit whose guidance and support were needed in the difficult time of this thesis work since the start until the end for the continuous encouragements and valuable suggestions. His guidance also helped me in all the time of research and writing of this thesis.

I am also deeply honored to my co-advisors: Asst. Prof. Dr. Uraporn Vongvatcharanon and Asst. Prof. Dr. Chatchai Wattanapiromsakul for their help to finish my research. I would also like to express special thanks Assoc. Prof. Dr. Siriphun Hiranyachattada who acted as a president of Physiology graduate study for valuable criticisms, suggestions and corrections until I completed this thesis.

I also wish to thank all lecturers, scientists and staffs in the department of physiology, Faculty of Science for all the supports. Moreover, I thank Southern Laboratory Animal Facility, Prince of Songkla University for providing experimental animals of my research. In addition, I am grateful to the financial support of graduate school, Prince of Songkla University. My sincere thanks also goes to all of my colleagues/friends that are not possible to be listed here, for whom I have great regard.

Finally, my graduation would not be achieved without best wish from my family. Their great support and understanding kept me positive and working hard until the completion of this study. I have to thank them for the greatest love, their patience, understanding, and support throughout these years.

Acharaporn Issuriya

TABLE OF CONTENTS

TABLE OF CONTENTS (Continued)

TABLE OF CONTENTS (Continued)

TABLE OF CONTENTS (Continued)

TABLE OF CONTENTS (Continued)

LIST OF TABLES

LIST OF FIGURES

LIST OF FIGURES (Continued)

LIST OF FIGURES (Continued)

LIST OF FIGURES (Continued)

LIST OF FIGURES (Continued)

LIST OF ABBREVIATIONS AND SYMBOLS

μ	micro, mu
μm	micrometer
μl	microliter
μV	micro volt
^{o}C	degree Celsius
%	percentage
Ca^{2+}	calcium ion
H_2O_2	hydrogen peroxide
NO	nitric oxide
O_2^-	superoxide anion
OH^-	hydroxyl radical
ACh	acetylcholine
ACTH	adrenocorticotropic hormone
AIF	apoptotic-inducing factor
ANOVA	analysis of variance
AMPA	α-amino-3-hydroxy-5-methyl-4-isoxazolepropionic acid
ATP	adenosine tri phosphate
AW	awake
EEG	electroencephalography
EMG	electromyography
CA	cornu ammonis
cAMP	cyclic adenosine monophosphate
CB	cerebellum
cm	centimeter

LIST OF ABBREVIATIONS AND SYMBOLS (continued)

CNS	central nervous system
CRH	corticotropin-releasing hormone
dB	decibel
DG	dentate gyrus
DNA	deoxyribonucleic acid
Dx	dexamethasone
FC	frontal cortex
FFT	fast Fourier transforms
g	gram
GCs	glucocorticoid hormone
GCr	glucocorticoid receptor
GFAP-ir	glial fibrillary acidic protein immuno-reactivity
GRs	glucocorticoid receptor
HPA	hypothalamic-pituitary-adrenal axis
hr(s)	hour(s)
Hz	hertz
i.c.v.	intracerebroventricular
i.m.	intramuscular
i.p.	intraperitoneal
KA	kainic acid
kg	kilogram
LTP	long term potentiation
mΔΨ	mitochondrial membrane potential
M	molar
mg	milligram
min	minutes

LIST OF ABBREVIATIONS AND SYMBOLS (continued)

MPT	mitochondrial permeability transition pores
MRs	mineral glucocorticoid receptor
NMDA	N-Methyl-D-Aspartate
nmol	nanomol
PC	parietal cortex
p	p-value
PBS	phosphate buffer saline solution
PVN	paraventricular nucleus
R^2	R-square
REM	rapid eyes movement sleep
RNS	reactive nitrogen species
ROS	reactive oxygen species
SA%	spontaneous alternation percentage
SWS	slow wave sleep

BACKGROUND AND RATIONALE

Neurodegenerative diseases characterized by physical and cognitive impairments are found to have great impact to overall life quality. Progressive memory degradation and loss of language and motor skills among other things inevitably bring difficulties and sufferings to patients. The increasing amount of people affected by the diseases has been expected within the very near future. This would cost extremely high estimated budget in terms of research or health and care for population mass.

It is known that brain pathology that causes the symptoms precedes the onset of noticeable physical and cognitive declines with an unbelievable interval. Neurodegeneration associated with the diseases starts years before the appearance of dementia. In terms of brain therapy, even if the drugs are effective, the intervention has to be started well before the diseases begin to show debilitating symptoms. Anyway, it is controversial with extreme uncertainty when no diagnosis with acceptable accuracy has been developed.

To fight against neurodegenerative diseases, it is not to restore afflicted people to normal cognitive function. Instead, great attempt must be for preventing them in people who are at risk. To do that, high accuracy of the test is essential to help diagnose the diseases before large brain areas are severely damaged. The early detection would make early intervention very possible. Thus, short term goal is to search for reliable biomarkers that predict brain degeneration. Therefore, it would be practical for screening potential sufferers early enough. Up to date, advanced brain imaging techniques seem to be promising. Some of previous reports claimed that it is possible to identify definitive evidence of neurodegenerative pathologies such as amyloid plaque formation or T-tau protein. However, the translation of this technology into a routine checkup for people who might be at risk is relatively impractical due to access limit and expensive fees. The most important point is that it has not been conclusive.

CHAPTER 1

GENERAL INTRODUCTION

AND

REVIEW OF LITERATURE

General introduction

Neurodegeneration is a fundamental component of several central nervous system disorders that distress human population. The rate of neurodegenerative disorders is progressively increasing due to a growing proportion of aging population. Neurodegenerative diseases often affect mental performance or memory processing lead to memory loss, unusual behavior, personality changes and a decline in thinking abilities (Ganguly and Guha, 2008; Myhrer, 2003). Neurodegenerative diseases are irremediable conditions that result in progressive degeneration and/or decrease of nerve cells. Neurodegeneration causes problems with movement or ataxias and mental functioning or dementias. The development of disease is due to complicated interactions between individual activating genetic traits and several factors, such as aging, sex hormones, cardiovascular disorders and stressful life events (Esch et al., 2002; Hoenicka, 2006; Winner et al., 2011).

One of many neurodegenerative evaluations in *in vivo* studies is electroencephalographic (EEG) recording. It was demonstrated that dementia and other neurological disorders left characteristic signatures on EEG tracings. Many EEG studies on neurodegenerative diseases were aimed to find such markers that identify and predict Alzheimer's disease (Schmidt et al., 2013), REM sleep behavior disorder (Rodrigues et al., 2013), Parkinson's disease (Hansen et al., 2013), dementia with Lewy bodies (Andersson et al., 2008), Huntington's disease (van der Hiele et al., 2007) and Creutzfeldt–Jakob disease (Lv et al., 2013) through the analysis of sleep architecture and micro-structure or quantitative EEG analyses. Quantitative analysis of EEG signals in resting subjects is inexpensive and potentially useful neurophysiological access to the study normal aging and dementia. Several research groups have tried to diagnose biomarkers of EEG signals in demented patients. The dependable biomarkers that can be used for early diagnosis and tracking disease advancement are the basement of the development of treatments for neurodegenerative diseases and the early diagnosis is highly desirable before neurodegeneration becomes severe and disseminate.

Review of literature

1. Neurodegeneration

Neurodegeneration is the term for the progressive loss of function or structure of neuronal cell including destruction of neurons as a result of neurodegenerative processes. Neurodegeneration can be found in many different levels of neuronal circuitry ranging from molecular to systemic. The failure of neuronal networks and the death of neurons have been implicated in the pathogenesis of several neurodegenerative disorders through certain cellular processes such as protein degradation and mitochondrial biology (Everse and Coates, 2009; Palop et al., 2006).

Neurodegenerative diseases are heterogeneous groups of disorders that cause progressive loss of motor and cognitive function and characterized by gradually progressive, selective loss of anatomically or physiologically related neuronal systems. A number of factors have been proposed to trigger neurodegenerative disease, including protein over-expression, pathogenic mutations, aging, oxidative stress, impaired autophagy, inflammation, toxin, and excitotoxicity (Bains and Shaw, 1997; Fiskum et al., 2003; Heidenreich, 2003).

2. Stress

2.1 General knowledge of stress

Stress is an unavoidable condition of the human experience that includes both major life events and the problems associated with daily life (McEwen, 2002). The changing environment demands a continuous adaptation to external and internal challenges and environmental stimuli, obvious defensive responses, also termed stress responses, enable the organism to manage with novel conditions via the activation of complex neuroendocrine, metabolic and behavioral processes (Abraham et al., 2001). Stressful induce the release of stress hormones, including glucocorticoids and catecholamines (De Boer et al., 1990; McCarty and Gold, 1981).

Stress-related sensory information is transmitted to corticotropin-releasing hormone (CRH) secreting neurons in the paraventricular nucleus (PVN) of the hypothalamus to initiate the neuroendocrine stress cascade. CRH then stimulates the release of the adrenocorticotropic hormone (ACTH) from the pituitary, which in turn leads to the secretion of glucocorticoids (GCs; cortisol in human, corticosterone in rats) from the adrenal cortex as an end point of the activation of the hypothalamic-pituitary-adrenal (HPA) axis (Abraham et al., 2001) (Fig. 1.1). The action of CRH on ACTH release is mightily potentiated by vasopressin that is co-produced in augmentation amounts when the hypothalamic paraventricular neurons are chronically activated. Inasmuch as vasopressin stimulates ACTH release in humans, oxytocin inhibits it (Swaab et al., 2005). Major actions of GCs in the brain are multifold, as they facilitate the ability of the organism to cope with, adapt to, and recover after stressful stimuli. Primarily, the GC feedback maintains the basal activity of the HPA system and facilitates the termination of stress-induced HPA activation (Whitnall, 1993). Importantly, GCs also influence emotional, learning & memory processes, and is involved in the coordination of circadian events, such as the sleep-wake cycle and food intake (Bradbury et al., 1998; Dallman et al., 1995; Roozendaal et al., 1999). Stress also has effects on functions behavior that are interposed by the hippocampus. Exposure to the stress resulted in deficits in working memory indicative of hippocampal dysfunction (Diamond et al., 1996).

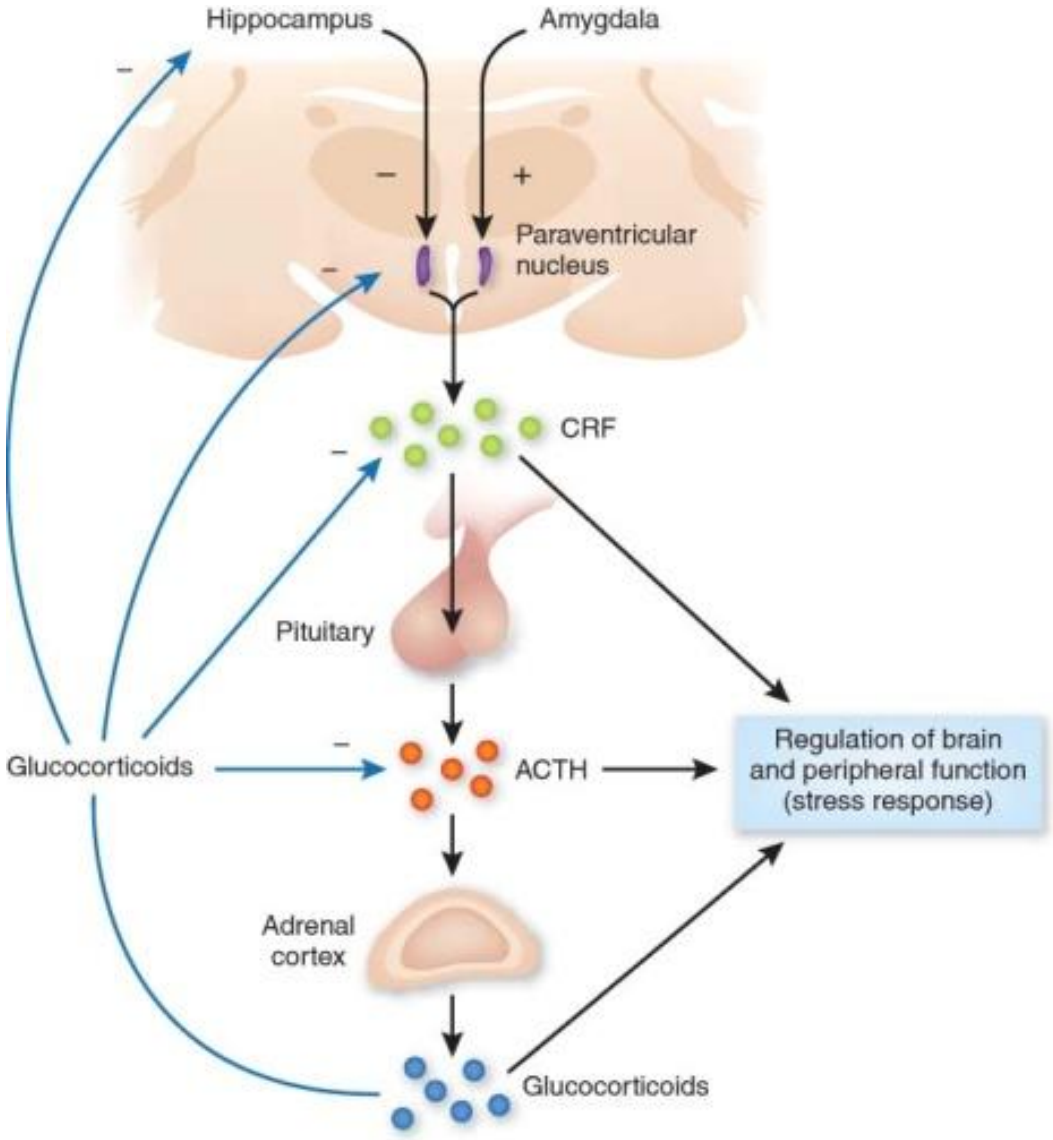

Nature Neuroscience 12, 241 - 243 (2009)

Fig. 1.1 Release of endocrine hormones in response to stress. In the hypothalamus, the paraventricular nucleus releases CRF, which is transported to the anterior pituitary, where it causes the release of ACTH into the blood stream. ACTH stimulates the adrenal cortex to synthesize and release the glucocorticoids cortisol (humans) or corticosterone (rodents). Glucocorticoids feedback at the level of the hippocampus, hypothalamus and pituitary to dampen excess activation of the HPA axis.

2.2 Glucocorticoids stress hormone

Glucocorticoids (GCs) are released during stress, and support homeostasis by assembling energy for emergency responses (Munck et al., 1984). GCs influence at two types of receptors, the high affinity mineralocorticoid receptor (MR or type I receptor) and low-affinity GC receptor (GR or type II receptor), both cytoplasmic receptor (De Kloet et al., 1998). GCs play on many organs and several brain areas through two types of receptor (Reul and de Kloet, 1985). GRs have been found in many brain regions relevant to cognition, i.e., the prefrontal cortex, amygdala and hippocampus. The hippocampus is exceptionally important for spatial memory and the prefrontal cortex is involved in working memory (Swaab et al., 2005). Moreover, other areas are composed of high densities of GR, and positive feedback can be exerted at, prefrontal cortex, amygdala and the brain stem interloping with HPA activity or reactivity and stress effects on memory (Fuchs et al., 2004; Roozendaal, 2002).

GRs have a low affinity for corticosterone and become engaged during stress and levels of glucocorticoids are high. In contrast, MRs has a high affinity for corticosterone and is almost saturated under basal conditions (Reul and de Kloet, 1985). Overexposure to GCs is of cause obvious neuroanatomical alter in neurons. In case the GC concentration is of inefficient amplitude or duration to exert direct neurotoxicity, GCs hazard neurons by enhance the vulnerability of nerve cells to neurotoxic insults (Sapolsky, 1985). Longterm exposure with high doses of corticosterone exerts corrosive effects in the brain and induces (ir) reversible damage to neurons. 3 weeks of repeated restraint stress elicit reversible neuronal atrophy in the CA3 of hippocampus indicated by the imperminent disappearance of apical dendritic branches of pyramidal neurons in CA3 (Luine et al., 1994; Watanabe et al., 1992).

Dexamethasone is used as effective anti-inflammatory protective agents routinely in clinically defined pathological conditions. Dexamethasone exhibit a high affinity on glucocorticoid receptors (GRs or type II) and not mineralocorticoid receptors (MRs or type I) (Roozendaal, 2000). Corticosterone binds MRs with an affinity10-fold higher than that of GRs, while the GRs can be stimulate by the selective agonist dexamethasone (De Kloet et al., 1998). The physiological effects of glucocorticoids on the organism which exposed to stress are more complicated than the

mediation of neuronal cell death. Glucocorticoids have several effects on physiological mechanism in expanding to effects on the brain, but the hormone affect on the modulation of gene expression, reproduction, bone formation and immunity. All effects have a protection on the organism during some situations of stress and the effects of glucocorticoids may be damaging (McEwen et al., 1992).

2.3 Chronic stress response

Chronic stressors stimulate increases in the levels of glucocorticoid (GC) stress hormones and corrosive effects on the structure and function of CNS, especially the hippocampus (Hibberd et al., 2000). Chronic GC elevations reach to abnormally prolonged binding of GRs. The co-incident of binding at GC receptors appears to cause about the greatest vulnerability especially the brain areas with high concentrations of MRs and GRs (Coburn-Litvak et al., 2004). Long-term GCs elevation is found in a various neuropsychiatric disorders (Carroll et al., 1976; Seed et al., 2000; Starkman et al., 1992; Walder et al., 2000). Chronically exposure to glucocorticoids is also associated with several effects on brain morphology, especially in the hippocampus (Reichlin, 1993).

Stress affects on functions of new memory that are mediated by the hippocampus. Exposure to the stress of different environment resulted in deficiency in working memory demonstrative of hippocampal dysfunction (Diamond et al., 1996). Elevation of glucocorticoids perceived with stress was linked with deficits in new learning and damage to the hippocampus (Luine et al., 1994). Long-term treatment of glucocorticoids that mimic the chronic stress condition resulted in deficits in learning and memory behaviors. In addition, the level of deficits new learning and memory behaviors was correlated with the positive neurons in CA3 of the hippocampus (Arbel et al., 1994). Stress affect on long-term potentiation (LTP), which is important for new learning and memory (Diamond et al., 1995) and the effects mediated by glucocorticoids playing through the GR receptor in the hippocampus (Pavlides et al., 1995).

Main mechanisms of GCs impede neuronal functions involve inhibition of the nutrients uptake from the general circulation such as glucose (Doyle et al., 1993), modulation of excitatory (glutamatergic) and inhibitory (GABAergic) neurotransmission (Abraham et al., 1996; Moghaddam et al., 1994) and increasing of intracellular Ca^{2+} signaling (Joels and de Kloet, 1994). Chronic exposure with high GC concentrations was exhibited to enhance the extracellular glutamate level in the hippocampus (Stein-Behrens et al., 1994).

3. Excitotoxicity

3.1 General knowledge of excitotoxicity

Glutamate mediates excitatory synaptic transmission activate the ionotropic glutamate receptors that are NMDA (N-methyl-D-aspartate), AMPA (α-amino-3-hydroxy-5-methyl-4-isoxazolepropionic acid), or kainite receptor and it mediates normal information processing and neuronal plasticity. The interruption with blood supply to the brain causes lake of oxygen and glucose that are applied to produce energy. Impairment of the energy enhances presynaptic glutamate release and case of membrane depolarization through activates the voltage gated Ca^{2+} channel. It is results of the abnormal augmentation of synaptic glutamate. Sustained activation and excess of the glutamate receptors causes neuronal death, particularly glutamate neurotoxicity or excitotoxicity (Won et al., 2002).

Glutamate binds to glutamate receptors in the brain and enhancing intracellular Ca^{2+} signaling along with mobilizing cytosolic free Ca^{2+}. Under physiological condition, Ca^{2+} gathering via glutamate receptors leads to the increasing of synaptic transmission in pre- and postsynaptic component and to the constitution of highly active perforated synaptic communication (Edwards, 1995). Immoderate amounts of cytosolic free Ca^{2+} may influence mitochondrial dysfunction via increases in the formation of reactive oxygen species and diverse activation of Ca^{2+}-dependent proteases and leading potentially to destruction to ultimately all biomolecules (Dugan and Choi, 1994) (Fig. 1.2).

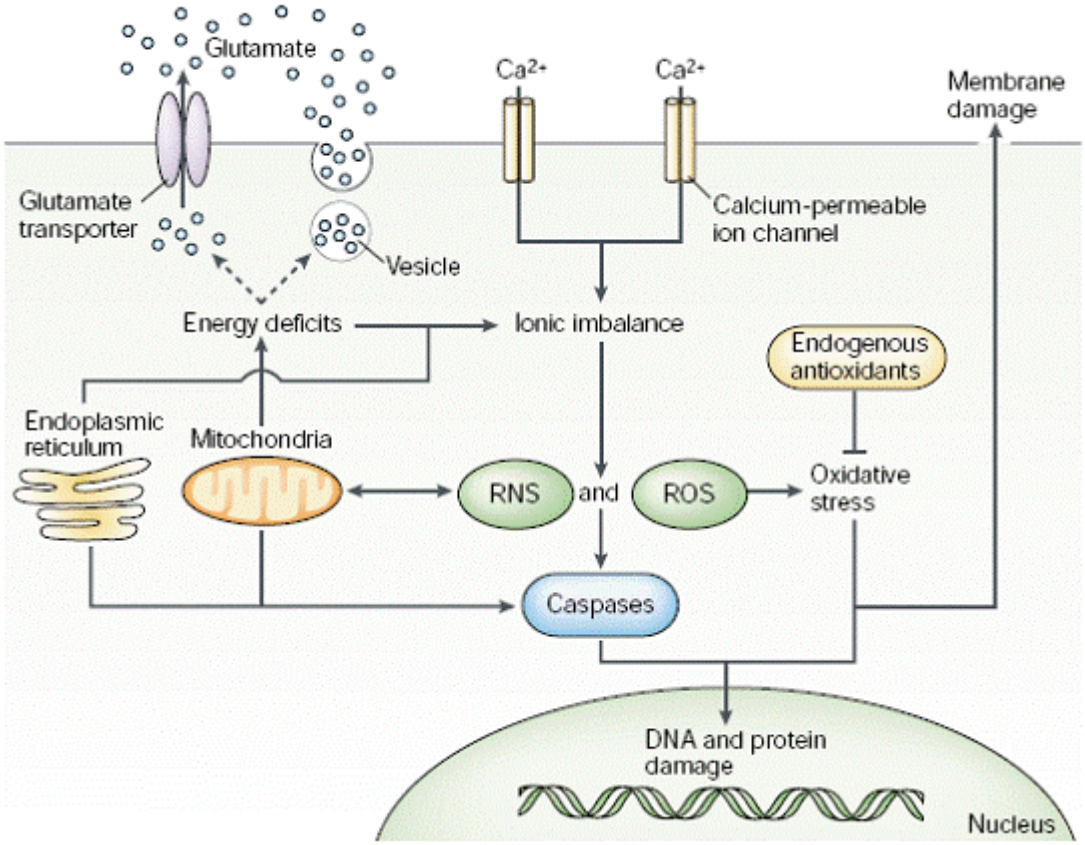

Nature Neuroscience 4, 400 (2003)

Fig. 1.2 The interaction and overlapping between multiple pathways of excitotoxicity that lead to cell death in the brain. RNS, reactive nitrogen species and ROS, reactive oxygen species.

3.2 Kainic acid: glutamate receptor agonist

Kainic acid (KA) is glutamate receptor agonist in kainate subtype. An influence of this KA on neurons fluctuates from depolarization to severe damage (Lothman and Collins, 1981). High dose of KA used as a neurotoxin to produce brain damage such as intracerebral injections of KA cause local destruction of neurons in distant areas (Ben-Ari, 1985). The cortico-limbic neuronal loss models that studied in rats caused by the intraperitoneal (i.p.), subcutaneous (s.c.) or intracerebroventricular (i.c.v.) administration of kainic acid, KA has long been known to destruct neurons and the model have been studied for several years (Montgomery et al., 1999). KA stimulates the Ca^{2+}-kainate receptor or AMPA receptor (A-K receptor) leading to rapid Ca^{2+} entry and the accumulation of Ca^{2+} activate Ca^{2+}-dependent enzymes and generate of ROS. The excess of Ca^{2+} and ROS lead to collapse of mitochondrial membrane potential ($m\Delta\Psi$) and open mitochondrial permeability transition pores (MPT). There is releasing of mitochondrial factors and apoptotic-inducing factor (AIF) and form to apoptosome complex. The apoptosome complexes activate pathway lead to nuclear condensation and DNA fragmentation. Extreme Ca^{2+} overload could directly cause mitochondrial swelling and damage, decrease in ATP, and increase in ROS, which oxidize bio-molecules, causing acute neuronal necrosis (Fig. 1.3).

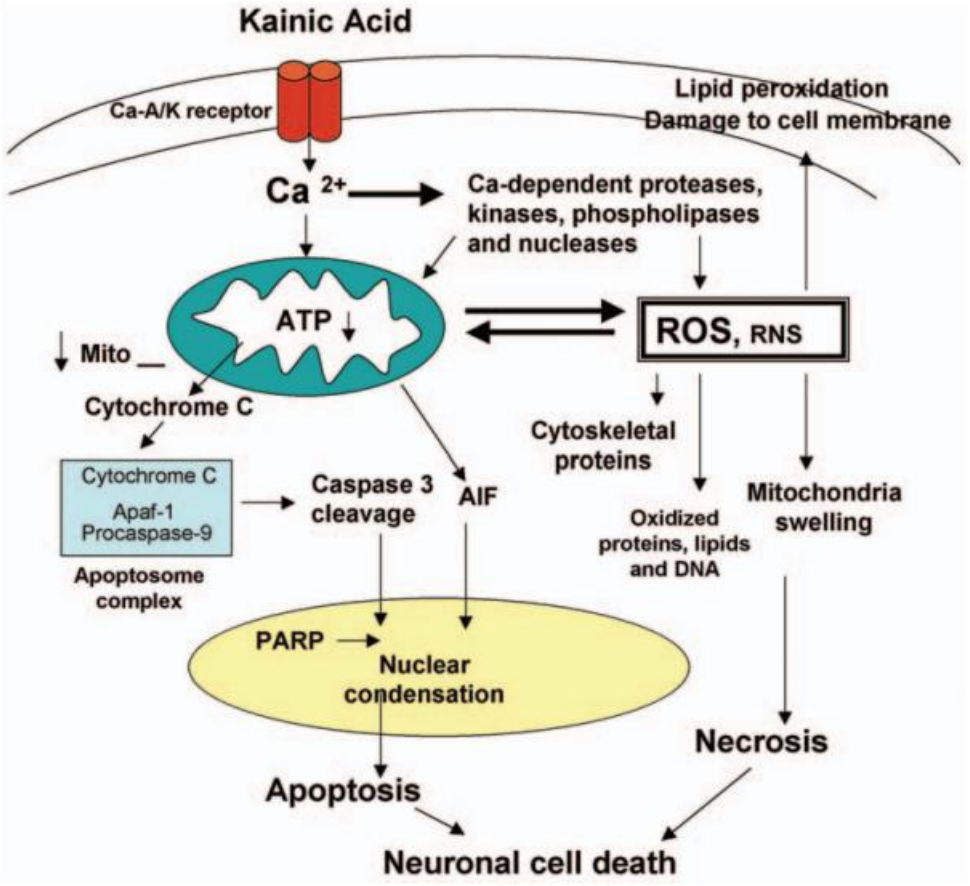

Fig. 1.3 Schematic diagram depicting the neuronal cell death pathway induced by kainic acid (KA)

4. Oxidative stress

Free radicals are chemical species with an unpaired electron and generated via normal metabolites in aerobic biological systems, such as superoxide anion (O_2^-) and nitric oxide (NO) are continuously produced in aerobic cells in mitochondrial membranes and produce ATP for cellular energy needs. Over-production of free radical leads mitochondria to a dysfunctional state lead to apoptosis and tissue aging (Valdez et al., 2000). Reactive oxygen species (ROS) are generated via cell metabolism. ROS are a group of highly reactive molecules that are produced through sequential reductions of O_2 and include superoxide anion (O_2^-), hydrogen peroxide (H_2O_2), and hydroxyl radical (OH^-). Normal levels, ROS play as second messengers in various cellular functions. Concurrently, several mechanisms protect cells against excess ROS. The low chronic explosion of free radicals is presumably not harmful to cell physiology. The chronic and/or sudden increases in ROS levels over a physiological threshold trigger cell death by interfering with normal cellular operations (Finkel, 2003; Romano et al., 2010). Oxidative stress is cause irreversible cellular damage because intracellular defense mechanisms are depleted and consequently cannot protect cells against ROS (Orrenius et al., 2007).

Oxidative stress is induced by an over accumulation of ROS can damage basic components for cell function and cell survival. The brain considers for about 20% of the aerobic metabolism. In normal condition, neuronal cells receive a minimum level of free radicals from exogenous and endogenous sources. The brain has a minimum storage capacity for oxygen and a high possibility of lipid peroxidation and brain cells are especially defenseless to free radical-mediated injury (Won et al., 2002). Two reasons of oxidative stress, (1) they have decreased levels of antioxidant enzymes/ scavengers in their tissue and serum and (2) they fail sufficiently to synthesize/upregulate antioxidant enzymes such as glutathione peroxidase and glutathione (Ikonomidou and Kaindl, 2011).

5. Aging

Brain aging is associated with degrade ability of neurons to maintain ions homeostasis and enhanced ACTH and corticosterone responses to stress, which eventually lead to the increasing of GC-induced neurodegeneration of nerve cells (Landfield et al., 1978; Mattson, 1998 Landfield et al., 1978; Mattson, 1998). The hippocampal dysfunction show down regulates the negative feedback of GC secretion from adrenal gland and enhances corticosteroid secretion and intensify the neurodegenerative process (Abraham et al., 2001). The mechanism of GCs in age-related hippocampal dysfunction demonstrated that adrenal hypertrophy and prolonged hypersecretion of corticosterone absolutely correlate with enhanced neuronal damage and augmentation of reactive astroglia in the hippocampus (Landfield et al., 1978). The observation of age-related impairment of cognitive performance absent a decreasing in hippocampal neurons promotes the primary mechanism of GC-induced hippocampal dysfunction during aging (Geinisman et al., 1995, Rasmussen et al., 1996). The patterns of the age-related cognitive impairment including formerly obtain, the information is rapidly missing, and newly information of learning is vulnerable compared to the information of learning in the past (Driscoll et al., 2006). Age-related changes in LTP are credited to the reduction of perforant pathway synaptic contacts on granule cells and suggested to consider for variety of synaptic plasticity in aging including age-related protein synthesis, calcium regulation, axonal transport and hippocampal synaptic connectivity (Rosenzweig and Barnes, 2003). Age related structural changes that are probably to be pertinent to cognition depend on hippocampus. The hippocampal formation is principally vulnerable to the effects of aging, particularly age-related pathology. Age related structural changes comprise appear of reduce in the number of neuron, change of normal neuronal function.

6. Hippocampus

6.1 The Hippocampal Formation

The hippocampus is a part of the cerebral cortex and the limbic system and reveals a medial temporal lobe structure. The hippocampus is bilateral symmetry and includes the hippocampus (CA1, CA2, CA3 and CA4) and the dentate gyrus (DG, fascia dentate). Each hippocampal region contains a concretely packed sheet of cells including pyramidal and granular that are the principal cell types found in this structure. More over, each region contains a several interneurons that are intermingled with the principal cell types. The hippocampus contains CA1, CA2, CA3, and CA4 region and is primarily contain of pyramidal cells. CA2 and CA4 regions are very small region and not well investigated. However, CA1 and CA3 regions have been more widely explored and studied (Amaral and Witter, 1989) (Fig. 1.5).

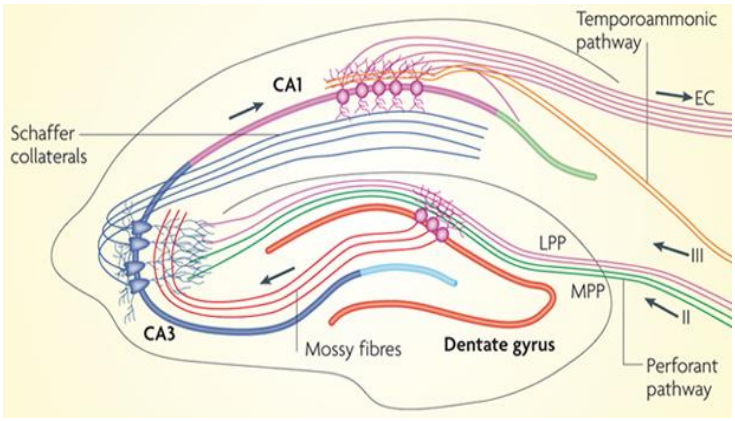

Nature Reviews Neuroscience **11**, 339-350 (2010)

Fig. 1.4 The neural circuitry in the rodent hippocampus.

6.2 The Function of the Hippocampus

The hippocampus has complicated functions that are involved in learning and memory. The hippocampus is necessitating in short-term memory consolidation (Giap et al., 2000). The hippocampus is the main extra-hypothalamic target of corticosterone and several separated populations of hippocampal neurons plentifully express GRs and MRs. Corticosterone has been shown to regulate physiologic, metabolic, and genomic functions of neurons in rats hippocampus (Kim et al., 2001). The long-term potentiation (LTP) is a relatively persisting form of synaptic plasticity that is well represented in the hippocampus. The best candidate for the neural mechanism is underlies information storage in the mammalian brain. It is supposed that the activity-dependent synaptic plasticity is induced at suitable synapses during memory formation and is necessary and adequate for the information storage essential the type of memory mediated by the brain area of the plasticity that are observed (Martin et al., 2000).

7. Sleep

7.1 Sleep definitions

Sleep is instinctively state characterizes by altered awareness and relate with sensory and activity voluntary muscle inhibition. Sleep stage discriminate from waking stage by a decrease capability to respond with all stimulation. Sleep help to preserve energy and decreases metabolism by about 5–10% (Cai, 1991; Franken et al., 2009; Pace-Schott and Spencer, 2011). The stages of sleep were divided by the different electroencephalography (EEG) features of sleep including NREM (non rapid eyes movement) sleep and REM (rapid eyes movement) sleep. NREM sleep exhibit a variably synchronous cortical electroencephalogram, spindles, K complexes, and slow waves associated with low muscle tonus and smallest psychological activity and the REM sleep EEG is desynchronized, muscles are atonic, and dreaming is typical (Barcaro et al., 1998; Dement and Kleitman, 1957).

7.2 Brain stage

7.1.1 Waking

Wakefulness exhibits EEG features mainly with low voltage ($10 - 30\mu V$) and mixed frequencies. Mostly, awake EEG is dominant with alpha activity and relatively high tonic EMG. Variety within waking stage is found to be dependent on arousal levels.

7.1.2 NREM sleep

NREM sleep is separated into 4 stages by the electroencephalogram (EEG) different features. The EEG pattern in NREM sleep is commonly described as synchronous and characteristic of sleep spindles, K complexes, and high voltage slow waves. NREM sleep is normally associated with minimal or fragmentary mental activity. NREM sleep can be defined as a relatively inactive yet actively regulating brain in a movable body.

7.1.3 REM sleep

REM sleep reveals the EEG activation, muscle atonia, and rapid eye movements. In REM sleep, the mental activity is associated with dreaming and approximately 80% of arousals state reported in sleep as clear dream recall. REM sleep can be defined as an activated brain in a paralyzed body (Maquet, 2001; Prinz et al., 1982; Siegel, 2001)

7.4 Hypnogram

A hypnogram is a diagram that represents the stages of sleep as a function of time. It was developed for presentation of the brain wave activity from an electroencephalogram (EEG) and obtained by visually scoring the recordings from EOGs and EMG during a period of sleep including; wakefulness, rapid eye movement sleep (REM) and non-rapid eye movement sleep (NREM). Reliable frequencies EEGs, EOGs and EMGs were displayed and characteristic to determine what stage of sleep or wake the subject is in.

7.4 Physiology of sleep

Sleep-wake cycle is regulated by sleep-wake promoting in the brain. Sleep begins with stimulation of the preoptic area in the anterior hypothalamus and sleep promoting neurons project γ-aminobutyric acid (GABA) to inhibit wake-promoting centers. Then inhibition of wake-promoting neurons works on results in increasing the sleep process. The laterodorsal (LDT) and pedunculopontine (PPT) tegmental in brain stem regulate REM sleep, LDT and PPT project to thalamus, basalforebrain and the cortex, which produce the desynchronized EEG signals. The reticular activating system (RAS) receives collateral inputs from visceral, motor and sensory systems and transmit signal to the forebrain and cortex via thalamic and extrathalamic neural pathways for promoting arousal stage (Halasz et al., 2004; Schwartz and Roth, 2008).

8. Electroencephalography (EEG)

8.1 Neural basis of EEG

The EEG signal is a result of the summation of potentials obtained from the concoction of extracellular currents generated by populations of neurons. The physical sources of the scalp potentials are the pyramidal neurons in cortical layers III and V. Nature of EEG signal is fluctuating wave with different frequencies and amplitudes when considered against time. EEG signals can be analyzed using computer software developed for measurement EEG parameters with high accuracy. EEG is a technique that recorded neuronal cortical activity of the brain and levels of synchronization of neurons are observed in EEG patterns. Moreover, synchronization levels and EEG patterns also differ among different brain states. EEG signal is shown in wave patterns and EEG frequencies ranged from low to high Hz. In classical analysis, total frequency range is classified into delta wave: 0.5~4 Hz, theta wave: 4~8 Hz, alpha wave: 8~12 Hz, beta wave: 12~30 Hz and gamma wave: >30 Hz. EEG is widely used to evaluate brain functions and their abnormalities.

8.2 EEG spectral analysis

The electroencephalogram (EEG; brain waves) recorded by electrodes placed on the scalp. The EEG is an important brain state notice (e.g. waking, sleep, seizure) with specific state dependent patterns. Critical appearances of the signal are recognized by visual inspection of the EEG. The additional quantitative analysis is basic to investigate the EEG in more detail. Spectral analysis is a mathematical access to quantify the EEG. The decomposition of signals is purposed as the EEG, into its constituting frequency components. The fast Fourier transform (FFT) is a widely applied method for obtaining the EEG spectrum. Fast Fourier Transform (FFT) has been generally used in analysis of various types of wave including EEG. Based on the application of the original FFT equation, there are FFT programs that have been developed and improved for EEG analysis. FFT is used to calculated EEG power to reflect amplitude of EEG as a function of frequency in power (μV2) power density (μV2/Hz) or absolute power (dB). However, in this study, only power density of frequency is interested (Schatzman, 1996; Yokoyama, 1992).

8.3 Brain oscillations

Brain oscillations were divided in frequency bands that have been related with different brain states, functions or pathologies (Algimantas Juozapavicius et al., 2011).

(I) ***Delta rhythms*** (1.25-4.5 Hz): they are characteristic of deep sleep stages. Furthermore, delta oscillations with certain specific morphologies, localizations and rhythmicities are correlated with different pathologies.

(II) ***Theta rhythms*** (4.75-6.75 Hz): they are enhanced during sleep and they play an important role in infancy and childhood. In the awake adult, high theta activity is considered abnormal and it is related with different brain disorders.

(III) ***Alpha rhythms*** (7-12.5 Hz): they appear spontaneously in normal adults during wakefulness, under relaxation and mental inactivity conditions. They are best seen with eyes closed and most pronounced in occipital locations.

(VI) ***Beta rhythms*** (12.75-30 Hz): they are best defined in central and frontal locations, they have less amplitude than alpha waves and they are enhanced upon expectancy states or tension.

(V) ***Gamma rhythms*** (30.25-45 Hz): previously not of major interest with regard to the surface EEG, they relate with linking of stimulus features into common perceptual information.

9. Astrocyte

Astrocytes are neuroglial cells and the amount is over fivefold more than that of neurons. Astrocytes exert many essential complex functions in the CNS. One of them is known as reactive astrogliosis which is pathological marker of CNS structural lesions (Cornell-Bell et al., 1990; Nedergaard et al., 2003). Astrocyte is neuroglia that has been divided into two types based on the cellular morphologies and anatomical locations including protoplasmic astrocyte and fibrous astrocyte. Astrocyte is the most abundant glial cells and associated with neuronal synapses. Protoplasmic astrocytes are found in all gray matter and exhibit morphology of various stem branches and fibrous astrocytes are found in all white matter and exhibit morphology of long fiber-like processes (Sofroniew and Vinters, 2010). Astrocyte exhibits many functions such as biochemical support of endothelial cells for blood–brain barrier maintenance, preserving of nutrients to the nervous tissue, controlling extracellular ion balance, and repairing or scarring process of the neural tissue injuries. Moreover, astrocytes produce intercellular calcium ion waves and response to stimulate neurons for release neurotransmitters in a calcium ion dependent manner (Nedergaard et al., 2003; Voutsinos-Porche et al., 2003). Glial fibrillary acidic protein (GFAP) is one of a family of intermediate filament proteins, including vimentin, nestin, and others, that serve largely cyto-architectural functions. GFAP is prototypical marker for immunohisto-chemical identification of astrocytes. GFAP expression is considered as a sensitive and dependable marker that labels reactive astrocytes that are reacting to CNS injuries (Eng et al., 2000; Sofroniew, 2009). The level of GFAP-ir astrocyte determine by immunohistochemistry technique in several neural damage that reveal the change of number in term of up-regulation or down-regulation depend on pathology, violence, timing and brain area. For example, GFAPexpression in the hippocampus and striatum of the adult brain under normal physiological conditions, the postmortem studies of tissue from young patients with depressive disorder exhibit a reduced number of astrocytes in the prefrontal cortex. An increase in GFAP expression by astrocytes in the hippocampus in humans after the age of 65 years is a biomarker of aging (Nichols et al., 2001). The Dexamethasone treatment, model of stress induced neuronal damage, reduced the expression levels of GFAP (Pinto et al., 2013).

Hypotheses

1. Prolonged dexamethasone treatment and intracerebroventricular (i.c.v.) injection of kainic acid affect brain function in terms of neurodegeneration.

2. The neurodegenerative effects of prolonged dexamethasone treatment and i.c.v. injection of kainic acid in rats can be evaluated by using behavioral test and brain histological studies.

3. Specific patterns of electrical brain activity are changed in neurodegenerative rats.

4. There are significant correlations among electrical brain activity, behavioral change and brain histology in neurodegenerative rats

Objectives

1. To investigate effect of prolonged dexamethasone treatment and intracerebroventricular (i.c.v.) injection of kainic acid on learning & memory behavior, brain cells and electrical brain activity in rats.

2. To monitor changes of EEG patterns of prolonged dexamethasone and kainic acid (i.c.v) injected rats.

3. To evaluate relationship among learning & memory behavior, brain structure and electrical brain activity in prolonged dexamethasone and kainic acid (i.c.v) injected rats.

4. To compare among electrical brain activities of chronic dexamethasone treated rats, kainic acid (i.c.v) injected rats and aging rats.

CHAPTER 2

RESEARCH METHODOLOGY

1. Animals

Male Wistar rats with body weight ranging from 300-350 g were used for the whole experiment of this study. They were provided by the Southern Laboratory Animal Facility of Prince of Songkla University, Songkhla, Thailand. They were housed in standard environmental conditions with temperature at 23-25 °C, 50-55% humidity and 12:12 hr. light:dark cycle. Standard commercial food pellets and distilled water were supplied *ad libitum*. The experimental protocols for care and use of experimental animals described in the present study were approved and guided by the Animals Ethical Committee of the PSU. The project license number is MOE 0521.11/1077.

2. Chemical agents and drugs

2.1. Surgery

1. Acrylic resin (Unifasttrad, Japan)
2. Zoletil 100 (Virbac, Thailand)
3. Thiopental sodium
4. 2% Lidocane sulphate
5. Sodium chloride (Ajax Finechem, Australia)
6. 70% alcohol
7. Povidone-iodine (Mundipharma, Thailand)

2.2. Drug treatment

1. Dexamethasone Sodium Phosphate (General Drug House, Thailand)
2. Kainic acid monohydrate (Sigma-Aldrich, USA)
3. Tween 80 (USB Corporation, Japan)

2.3. Tissue preparation

1. 0.1M Phosphate Buffer Saline (PBS) pH 7.4
2. 0.4% Paraformaldehyde in 0.1M PBS (Sigma-Aldrich, USA)
3. Sucrose (Mitr Phol Sugar, Thailand)

2.4. Histology

1. Chloroform
2. Ethanol
3. Triton x-100 (J.T. Baker, USA)
4. Cresyl violet (acetate) (Merck, Germany)
5. Gelatin mounting medium
6. Anti-Mouse Glial Fibrillary Acidic Protein (GFAP) monoclonal antibody (Chemicon, USA)
7. Anti-Mouse Texas Red IgG (H+L) antibody (Vector Laboratories, USA)
8. Normal horse serum (Vector Laboratories, USA)
9. Vectashield Mounting Medium (Vector Laboratories, USA)

3. Equipment

1. Animal surgical apparatus sets
2. Stereotaxic apparatus (Narishige Scientific Instrument Lab., Japan)
3. Electric micro motor dental handpiece (drill) (Marathon, Korea)
4. Stainless steel screws
5. Wire electrodes (Narishige Scientific Instrument Lab., Japan)
6. 6–channel sockets
7. Bio Amp cable (AD Instrument Pty Ltd, Australia)
8. EEG Bio Amp cable (AD Instrument Pty Ltd, Australia)
9. PC computer
10. PowerLab (AD Instrument Pty Ltd, Australia)
11. Recording chamber
12. Webcam video camera
13. Y-maze apparatus
14. Balance, Model CC023D10ADBAAA (Avery Barkel, UK)
15. pH meter
16. TESPA-coated slide
17. Cryostat, Model LEICA CM 1850
18. DP50 digital camera (Olympus, Japan)
19. Light microscope (Olympus, Japan)
20. Fluorescence microscope (Olympus, Japan)

4. Methods

4.1. Electroencephalography study

4.1.1. Animal surgery for EEG electrodes and cannula implantation

Animals were anesthetized with Zoletil 100 (50 mg/kg i.m.). Anesthetic depth was monitored using a gentle toe pinch to stimulate withdraw reflex. Individual rat was monitored as deep anesthetized when the flexion of the limb did not occur and withdrawal reflex was absent. The surgery for electrodes and cannula implantation was performed when animal was deeply anesthetized and unconscious. Anesthetic depth was also intensively monitored during the surgery process. Any reaction of too light anesthesia from the animal was responded with additional anesthetic top-ups. Fur of animal's head was shaved off with electric razor. Then, animal was placed onto the stereotaxic apparatus and rat's head was clamped with the apparatus. Ear bar of the apparatus was inserted into each side of ear canal then checked for tightening between ear bar and ear canal by gentle pressing and shaking animal's head. Proper fixation was confirmed when rat's head could not wobble. Rat's incisor was attached to incisor bar and animal's tongue was pulled out of the mouth to prevent chocking during surgery. Otherwise, a nose clamp was held to cover rat's nose properly. Both incisor bar and nose clamp were used to secure animal's head with apparatus and the position of head on stereotaxic apparatus was fixed in the standard position for the electrode and cannula implantation on the skull (Fig 2.1). The scalp was cleaned with 70 % ethanol and followed by iodide before the skin was incised for 2 cm long from the lambda to just in-between the eyes. After that the head skin was pulled apart using sterile hemostats for splitting the incision. The connective tissues were cleared out and the skull surface was exposed for drying.

The EEG electrodes and cannula were implanted on the skull at the following positions (Fig. 2.2).

1. Frontal cortex with the co-ordinates: 3 mm lateral to the left, 3 mm anterior to bregma and
2. Right or left parietal cortex with the co-ordinates: 4 mm lateral to the right or left, 4 mm posterior to bregma.
3. Midline cerebellum with the co-ordinates: 12 mm posterior to bregma was used as reference and ground electrode.
4. The cannula was implanted to right lateral ventricle for intracerebroventricular (i.c.v.) injection with the co-ordinates: 1.3 mm lateral to the right, 0.8 mm anterior to bregma and 3.3 mm skull to brain.

Two EMG wire electrodes were inserted into the dorsal neck muscles bilaterally. The screw anchors were implanted symmetrically on the opposite hemisphere to recording electrodes. All electrodes were secured in place by mounting with dental acrylic. After surgery, animals were allowed to recover for 14 days (Fig 2.3).

Stainless steel screws were made up as EEG electrodes, coated wire electrode was used as EMG electrodes and sterile hypodermic needle was used as cannula. All of these were made up in the department laboratory (Fig 2.4).

Fig. 2.1 Fixation of rat's head with stereotaxic apparatus for surgery.

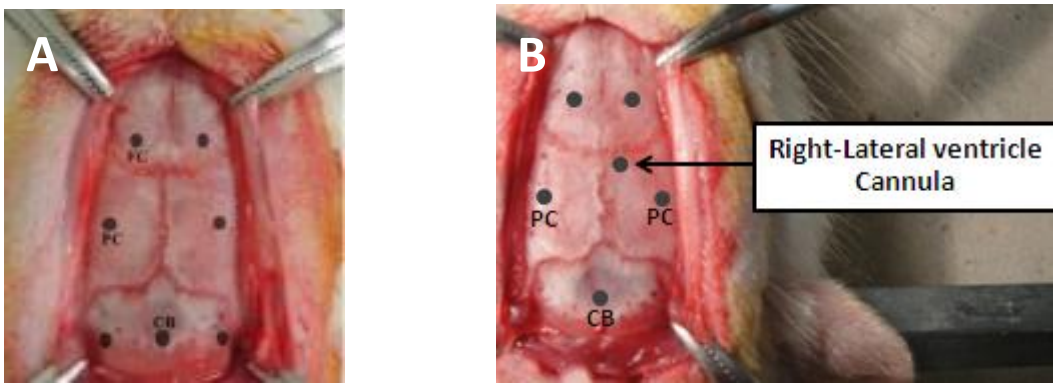

Fig. 2.2 Coordination for electrodes and cannula implantation. Electrode implantation for **(A)** dexamethasone-induced neurodegeneration, aging models and **(B)** kainic acid-induced neurodegeneration.

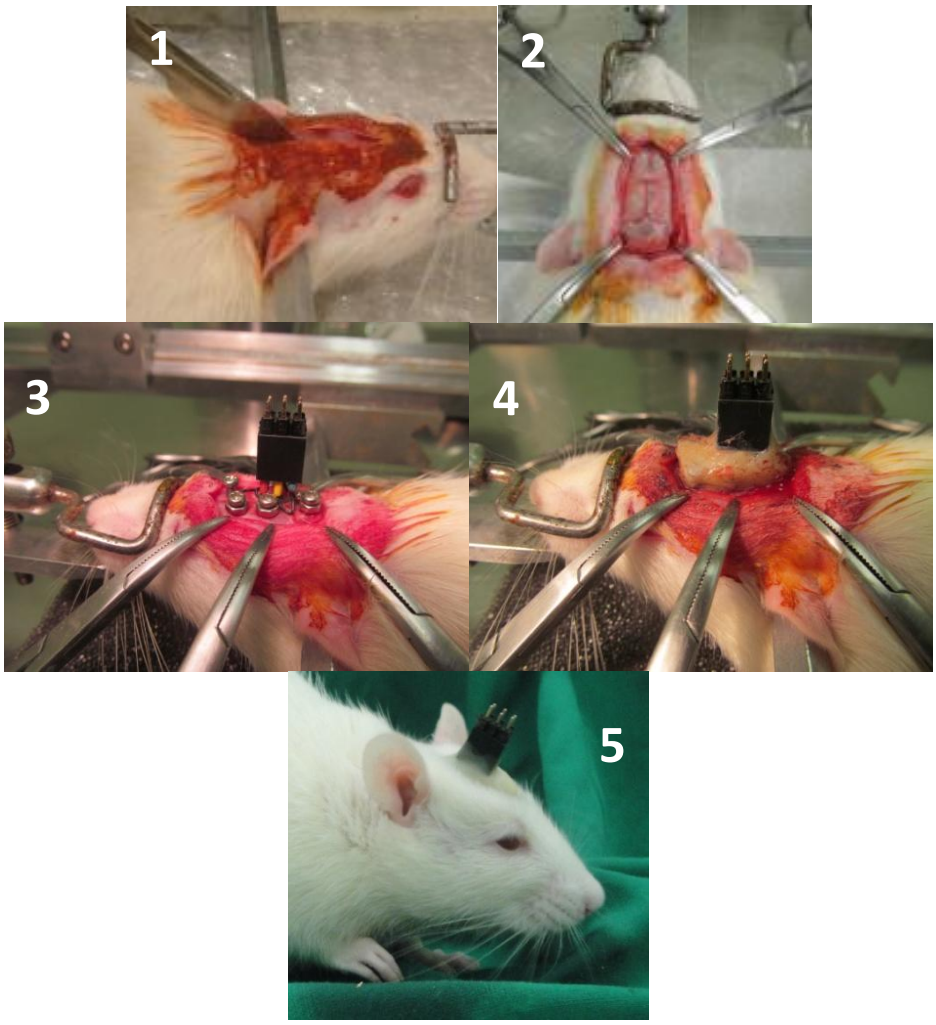

Fig. 2.3 Electrode and cannula implantation processes.

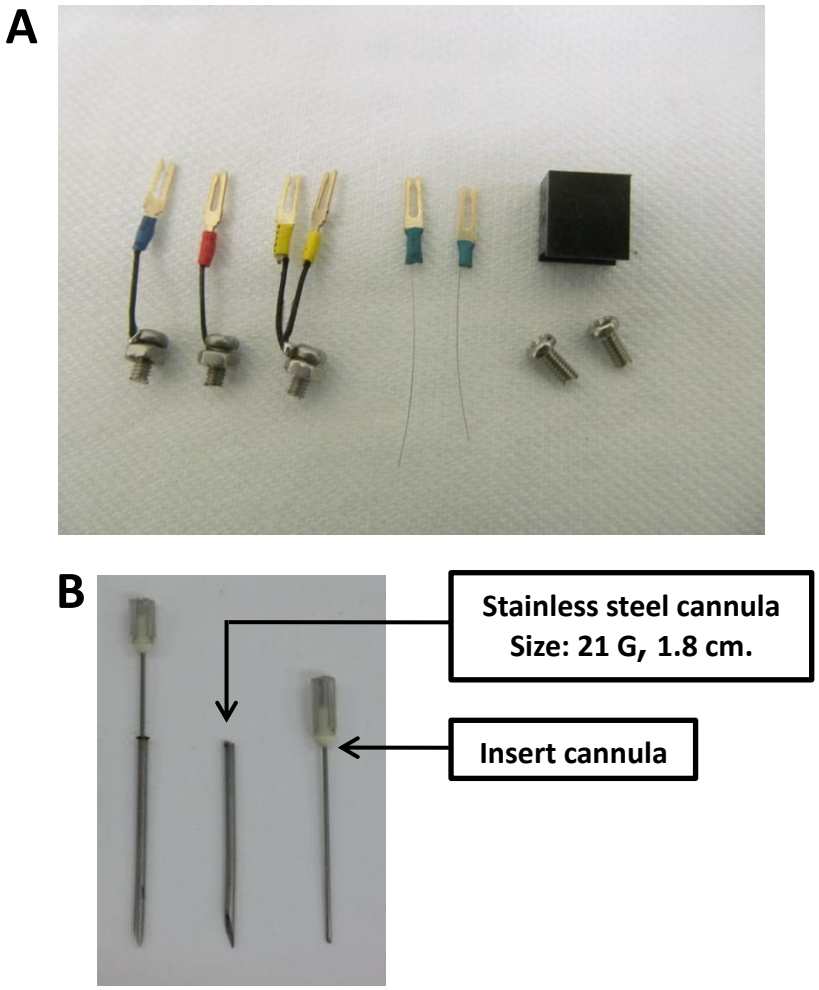

Fig. 2.4 (A) Electrodes for EEG recording and **(B)** Cannula set up for i.c.v. injection.

4.1.2. Signal recording and data acquisition

EEG recording system consists of recording chamber, recording cable, Bio-Amp set, Power Lab, a PC computer and a monitor (Fig 2.5). EEG recording started with connecting electrodes on rat's skull with recording cables via 6-channel socket. After that, animals were individually put into the recording chamber. Then, recording cables were connected with Bio-Amp sets and from Bio-Amp sets to PowerLab. Signal from rat's brain was amplified, filtered and digitized by Bio-Amp sets and PowerLab. Eventually, signal from rat's brain were shown on monitor and data were stored in PC computer for analysis. Lab Chart program was used to record EEG signal from rat's brain. For recording operation, input setting of Bio-Amp was assigned with 400/s of sample rate, 500 μV of range. The low-pass and high-pass filter were provided between 0.1 and 100 Hz. Furthermore, 50 Hz notch and main filter were selected for signal recording

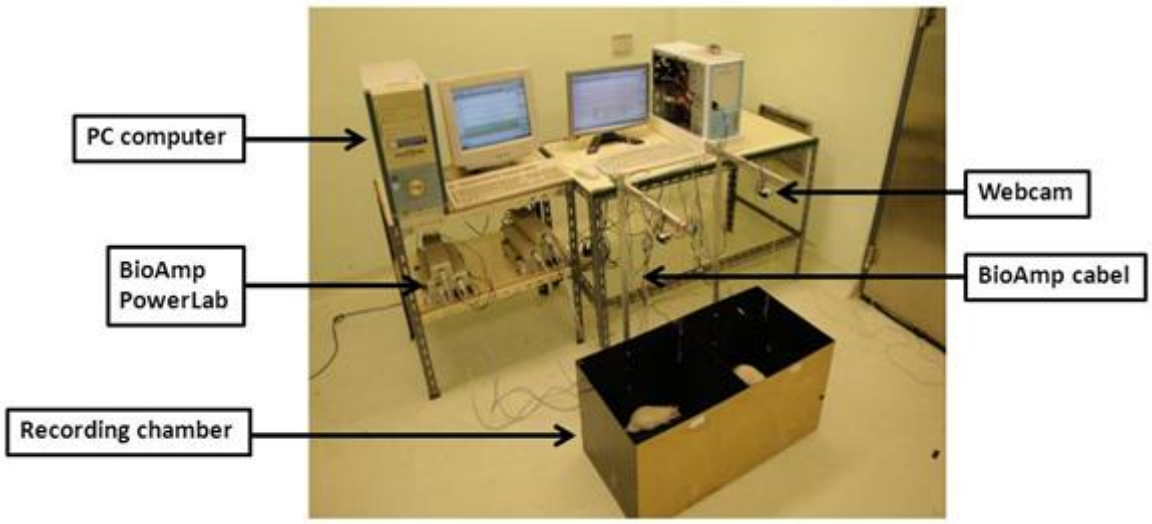

Fig. 2.5 The set up for EEG recording

4.1.3. Offline signal analysis

All data collected from EEG recording were filtered from 1.25-45 Hz using band pass filter. Moreover, raw EMG signals were filtered from 10-100 Hz. For EEG analysis, the signals were segmented into 1024 point (50% overlap) and Fast Fourier transform (FFT) algorithm was used to convert data from time domain to frequency domain and the data were shown in power spectra (μV2) and power density (μV2/Hz) . Then, the power spectra of 2.56-sec sweeps in selected time period was calculated and displayed as percent of baseline of EEG activity. The percent of EEG power from baseline was calculated by using the following equation.

$$\textbf{Power density (\%baseline)} = \textbf{Power density of post treatment x} \frac{\mathbf{100}}{\boldsymbol{Power\ density\ of\ base\ line}}$$

Broad frequency range was roughly divided into 2 major categories. First category is slow wave and the other is fast wave. Slow wave includes 3 frequency bands:

1. Delta (1.25-4.5 Hz)
2. Theta (4.75-6.75 Hz)
3. Alpha (7-12.5 Hz)

Fast wave was divided into 2 frequency bands:

1. Beta (12.75-30 Hz)
2. Gamma (30.25-45 Hz)

Then power of each band was analyzed independently. Mainly, changes of amplitude in each frequency bands were analyzed in terms of power. To make it clearer for presentation, percent change based on baseline activity were calculated to expand the change of dominant brain activity in particular. The base line values were set as 100%. The percentage changes of either control or treatment groups were the calculated from the base line values. Thus, the percentage change of EEG power and EEG power density in control group was compared with treated groups. The data of control group was normally fluctuated (more or less than 100%).

4.1.4. Classification brain states

EEG signals were classified to 3 brain stages.

1. Active awake period was identified with fast wave, low amplitude EEG and high EMG activity.
2. Inactive awake period had similar signal to that of active awake period except the absence of EMG activity.
3. Slow wave sleeps (SWS) or non-rapid eye movement sleep (non-REM sleep) was identified with slow wave and high amplitude EEG. REM sleeps were detected with fast wave, low amplitude EEG and absent EMG activity.

Vigilance states were also confirmed through visual inspection by using spectrogram (Fig 2.6). Spectral power of continuous signal was represent by coded color spectrum. With representative colors, levels of power were conveniently investigated. In each duration, distribution of frequencies with specific levels of power indicated by coded color to make it clear for the identification of wakefulness, slow wave sleep and REM sleep. Therefore, duration of each vigilance state of experimental animals were simply evaluated. This confirmation suggested the acceptable data quality.

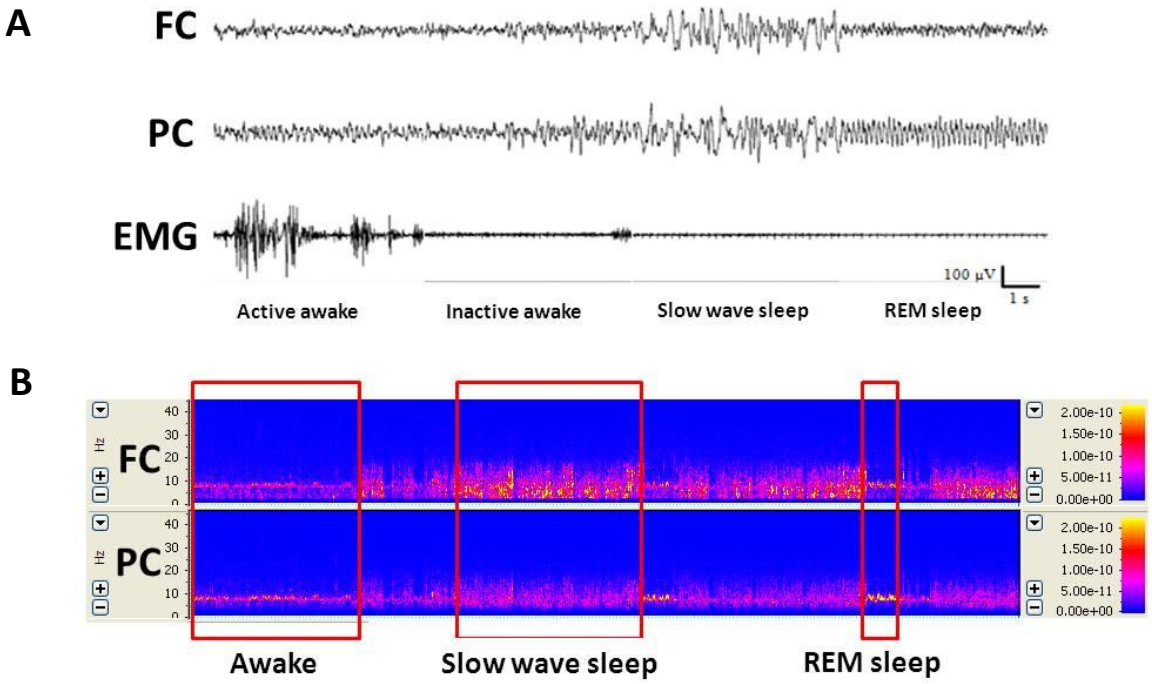

Fig. 2.6 (A) Raw EEG signals of each brain stage; active awake, inactive awake, slow wave sleep and REM sleep periods. **(B)** The spectrograms displaying spectral power and values are expressed as a coded color of frequency against time.

3.5. Data representation for EEG signal

Powers of frontal and parietal EEG during baseline and post-treatment were calculated. EEG baseline was set as 100% and values of post-treatment were calculated as percent change of baseline. All data were averaged and expressed as mean ± S.E.M.

4.2. Behavioral study

4.2.1 Spatial memory evaluation

The maze was made of grey plastic, with each arm 40 cm length, 12 cm height, 3 cm width at the bottom. The 3 arms were connected at an angle of 120^{o} (Fig 2.7). Rats were individually placed at the end of an arm and allowed to explore arms freely for 5 min. Spontaneous alternation percentage (SA%) was defined as a ratio of the arm choices that differed from the previous two choices ("successful choices") to total choices during the run ("total entry minus two" because the first two entries could not be evaluated). For example, if a mouse made 10 entries, such as 1-2-3-2-3-1-2-3-2-1, there are 5 successful choices in 8 total choices (10 entries minus 2). Therefore, SA% in this case is 62.5%.

4.2.2 Data analysis and statistic analysis for behavioral test

Spontaneous alternation percentage (SA%) and total of entries were averaged and expressed as mean ± S.E.M. Differences between treatments were considered using one-way ANOVA, followed by Student-Newman-Keuls method. p <0.05 was considered statistically significant.

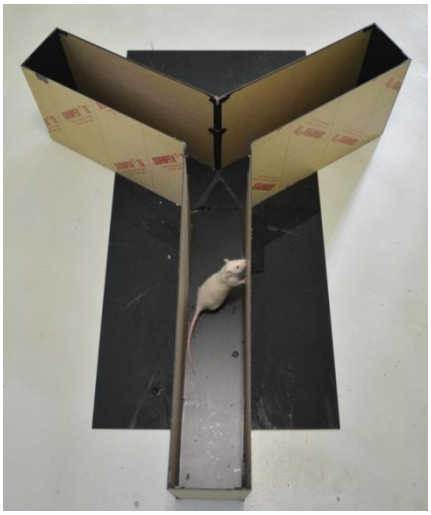

Fig. 2.7 Y-maze apparatus.

4.3. Histological study

4.3.1 Tissue preparation (Transcardial perfusion fixation)

1. Rats were deeply anesthetized by intraperitoneal injection of 100 mg/kg Thiopental sodium.
2. The thoracic cavity was opened to expose the heart and the pericardium was removed.
3. Cannula was inserted into the left ventricle and the right atrium was cut to remove the blood.
4. The rats were perfused transcardially with 0.1M PBS (pH 7.4) followed by 4% paraformaldehyde in 0.1M PBS.
5. The brains were removed and post-fixed with 4% paraformaldehyde in 0.1M PBS $4^{o}C$ (72 hrs).
6. Subsequently, the brains were cryoprotected by equilibration with 30% sucrose in 0.1M PBS until they sank and were rapidly frozen.
7. Coronal serial sections (20 µm thick for Nissl staining and and 40 µm thick for GFAP immuno-histochemistry staining, respectively) were obtained using cryostat.

4.3.2 Nissl staining method

1. The frozen sections were mounted on TESPA-coated slide and air dry at room temperature for 30 minutes.
2. The sections were processed for background fat staining reduction (de-fat) with 1:1 alcohol/chloroform and followed by rehydration process through 100% and 95% alcohol to distilled water.
3. The sections were soaked in 0.1% cresyl violet solution (warm up in 40 ^{o}C).
4. The sections were rinsed with distilled water and coverslipped with gelatin mounting medium.
5. The morphology of cresyl violet positive neurons was studied with light microscope.

4.3.3 GFAP immuno-histochemistry stains (Indirect immunofluorescence method)

1. Free-floating sections were incubated for 1 hr. at room temperature in blocking serum (0.1M PBS pH7.4 containing 2% normal horse serum and 0.3% Triton X-100)
2. Primary antibodies (anti-mouse Glial Fibrillary Acidic Protein (GFAP) monoclonal antibody) were diluted in blocking serum (1:200). The sections were incubated for 24 hrs. at 40^0 C in the primary antibodies.
3. The sections were rinsed with 0.1M PBS.
4. Secondary antibodies (anti-mouse Texas Red IgG antibody) were diluted in blocking serum (1:200). The sections were incubated for 1 hr. at room temperature in the secondary antibodies.
5. The sections were rinsed with 0.1M PBS.
6. The sections were placed on the TESPA-coated slide and coverslipped with vectashield mounting medium. And sealed with nail paste
7. Control sections, omitting the primary antibody, were routinely processed to ensure that any observed staining as due to GFAP.
8. The morphology of GFAP-ir astrocytes were studied with BX50 fluorescence microscope.

4.3.4 Quantification of neurons and GFAP-immunoreactive (ir) cells

Each area of the hippocampus (CA1, CA2, CA3 and dentate gyrus) (Fig 2.8) was identified using the rat brain atlas (Paxinos and Watson, 2007). The sections were systemic randomly selected and coded such that all subsequent analyses were carried out blind. About 8 sections from each rat of each study were collected in this study. There micrographs from selected sections were captured by a digital camera (DP71, Olympus, Japan). The number of cresyl violet positive neurons and GFAP-ir in each micrograph were counted and the area of each section examine was measured using image analysis software (Olympus, Japan).

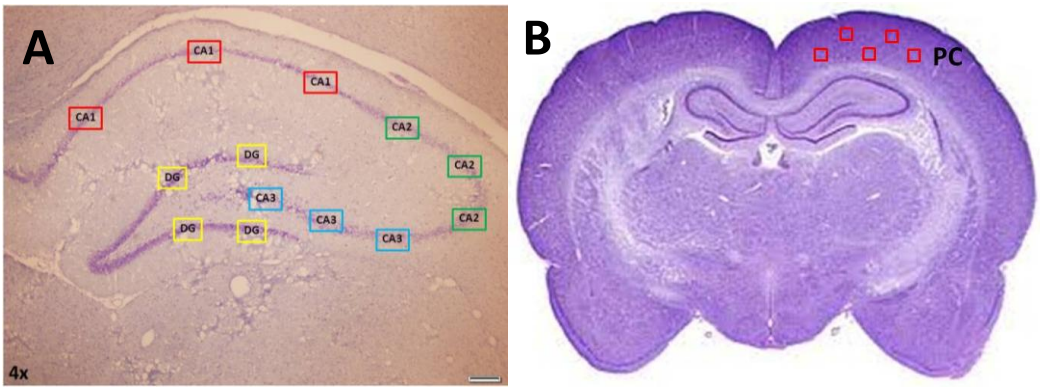

Fig. 2.8 Micrographs areas from selected sections of **(A)** the hippocampus and **(B)** parietal cortex.

4.3.5 Data analysis

Number of neurons in the hippocampus and parietal cortex were shown in positive neurons/mm^2 and number of GFAP-ir astrocytes shown in GFAP-ir/mm^2. All data were averaged and expressed as mean ± S.E.M.

CHAPTER 3

THE EFFECTS OF DEXAMETHASONE INDUCED NEURODEGENERATION ON EEG PATTERNS, SPATIAL MEMORY BEHAVIOR AND BRAIN STRUCTURE

\

3.1 Experimental protocol

The animals were randomly divided into for 2 groups with 8 rats in each group. In group I or control group, rats were treated with 0.9% saline (i.p.) once a day for 21 consecutive days. In group II or treated group, rats were treated with dexamethasone 0.5 mg/kg (i.p.) in a similar schedule. After a full recovery period of 14 days, rats were habituated with recording chamber and EEG recording system simultaneously for 3 days. On the testing day or baseline day, animals were set up similarly to the habituation days but EEG recording instrument was turned on to record electrical signal. EEG recording was carried on for 2 hrs. After 1 hr. of recording, rats were given 0.9% saline and dexamethasone for control and treated group, respectively. On the last testing day (day 21), rat's spatial memory behavior was examined by using Y-maze apparatus and their brains were collected for histological study (Fig 3.1).

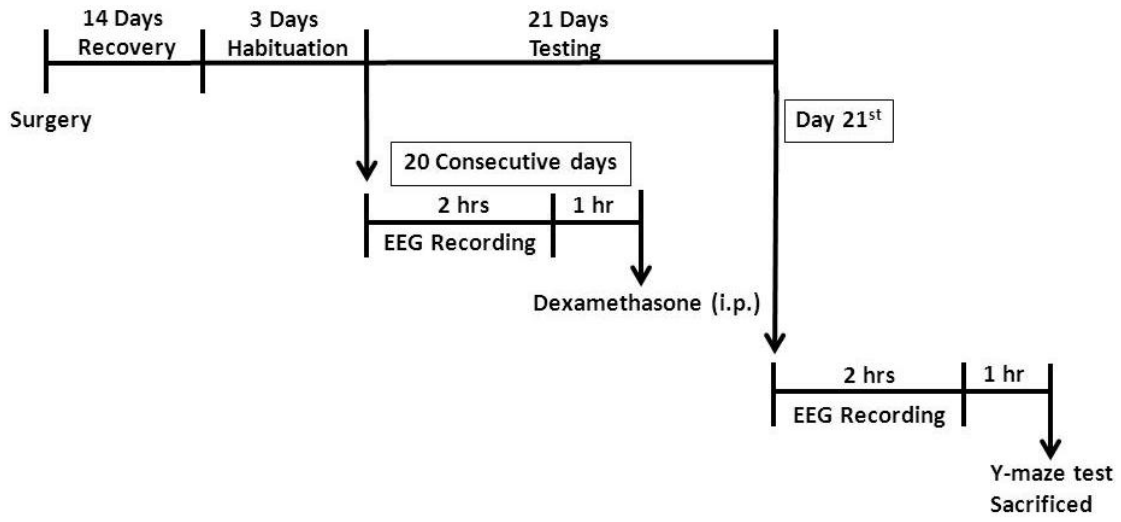

Fig. 3.1 Schematic diagram of protocol for examination of dexamethasone induced neurodegeneration.

3.2 Data analysis

3.2.1 For EEG analysis, powers of frontal and parietal EEG during baseline and post-treatment were calculated. EEG baseline was set to 100% and values of post-treatment were calculated as percent change of baseline. All data were averaged and expressed as mean ± S.E.M. Effects of treatment were determined by using t-test and statistical significance was considered at $p < 0.05$

3.2.2 Y-maze test, Spontaneous alternation percentage or SA% and total of entries were averaged and expressed as mean ± S.E.M. Effects of treatment were determined by using t-test and statistical significance was considered at $p < 0.05$

3.2.3 Number of neurons in the hippocampus and parietal cortex were shown in positive neurons/mm^2 and number of GFAP-ir astrocytes shown in GFAP-ir/mm^2. All data were averaged and expressed as mean ± S.E.M. Effects of treatment were determined by using t-test and statistical significance was considered at $p < 0.05$

3.2.4 The relationships among EEG patterns, spatial memory behavior and brain structure were exhibited in regression analysis and data were expressed as R-square. The significant correlation was considered at $p < 0.05$.

3.3 Results

3.3.1. Chronic effects of dexamethasone on EEG power.

EEG powers of animals were analyzed with no regard for brain state on day 1, 6, 11, 16 and 21 following the start of dexamethasone treatment. Broad spectrum of EEG power was divided and expressed in 5 frequency bands: delta, theta, alpha, beta and gamma. All data were normalized with values obtained before the start of dexamethasone treatment to express as baseline percentage (% baseline). Data were shown in comparison to that of control using t-test.

Frontal EEG analysis revealed no significant change induced by the dexamethasone in any duration and any frequency band (Fig. 3.2 A). However, the analysis of parietal EEG signal (Fig. 3.2 B) indicated that dexamethasone significantly increased powers of slow waves including Delta (Dx=165.07±10.18 and control=96.41±9.95, $p<0.001$), Theta (Dx=196.86±19.71 and control=92.19±18.75, $p=0.002$) and Alpha (Dx=199.73±9.86 and control=105.03±19.58, $p<0.001$) bands. Multiple comparisons indicated that significant changes were observed only on day 21 for delta band. In theta band, significant changes were confirmed as early as day 11 and until day 21. Alpha powers were also significantly increased from day 16 until day 21.

Therefore, EEG power was separately analyzed with regard for specific brain vigilance including awake state (AW) and slow wave sleep stage (SWS). Signals were taken from the first 5 min recording of the first appearance of each state) on day 21 after dexamethasone treatment, EEG power analysis was classified bases on 5 frequency bands. Awake EEG analysis confirmed that dexamethasone significantly induced increases in power of slow frequency bands including Delta (Dx=166.44±17.86 and control=94.37±13.08, $p=0.06$), Theta (Dx=152.08±14.10 and control=107.16±12.62, $p=0.032$) and Alpha (Dx=158.82±15.04 and control=102.04±13.41, $p=0.014$) activity for parietal EEG and only Alpha activity for frontal EEG (Dx=156.40±18.33 and control 96.42±13.48, $p=0.019$). However, the analysis of EEG signals during slow wave sleep found significant change only within Beta band of both frontal and parietal EEG (FC: Dx=138.58±11.70 and control 106.48±9.13, $p=0.048$ and PC: Dx=149.65±11.13 and control 112.26±7.38, $p=0.014$) (Fig. 3.3).

Altogether, significant effects of dexamethasone were particularly observed within slow wave activities ranging from delta to alpha wave of parietal EEG in awake stage (Fig 3.4). Activity of this frequency range remained unchanged when signals during slow wave sleep were analyzed.

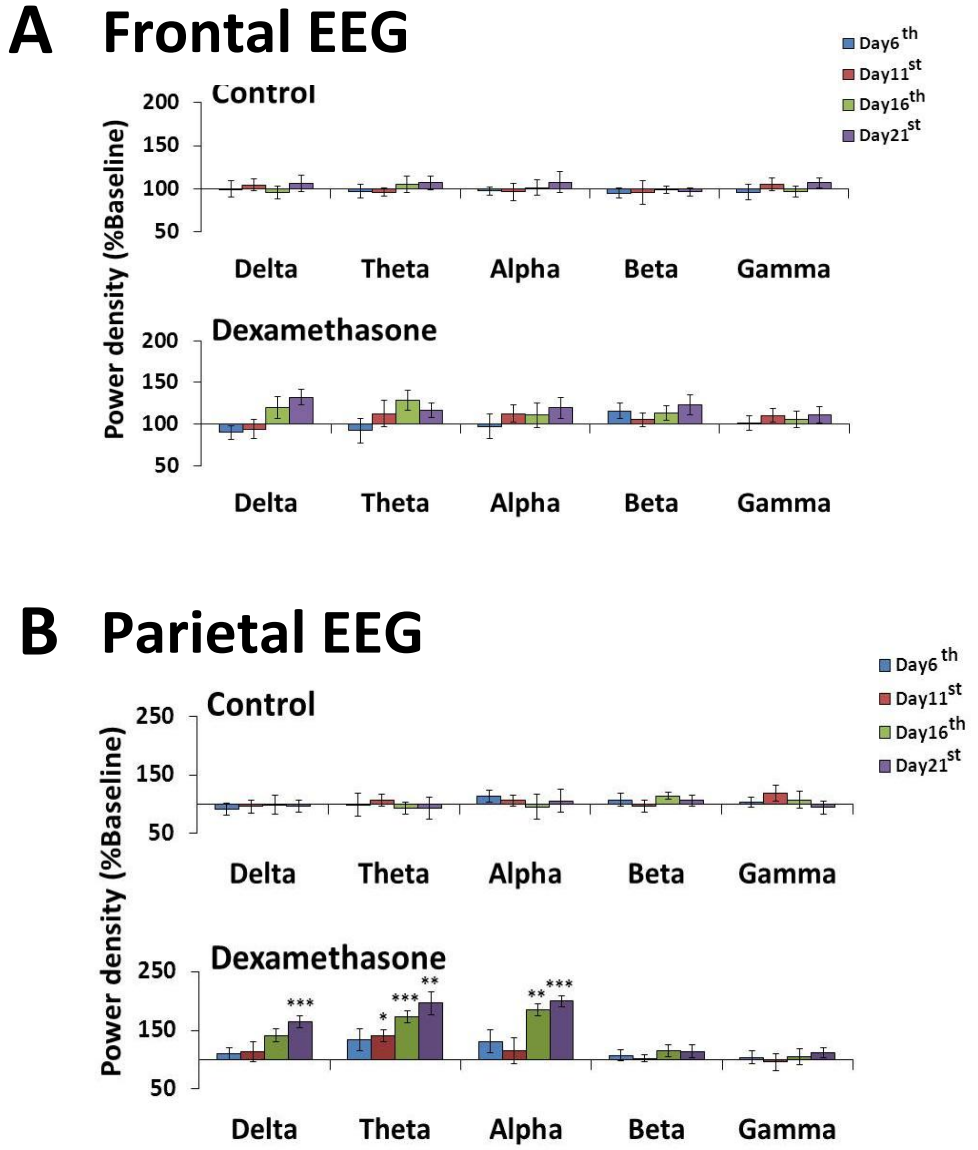

Fig. 3.2 Chronic effects of dexamethasone on EEG power, **(A)** frontal and **(B)** parietal EEG power from dexamethasone induced neurodegenerative group is shown in comparison to control group. Baseline activities were evaluated from 2 hrs. on first day recording before drug administration. After the administration, EEG was recorded for 2 hrs. in each day. Data analysis was classified base on 5 frequency bands: delta, theta, alpha, beta and gamma. Data are expressed as mean ± S.E.M. of power density (%baseline). Effects of treatment were determined by using t-test,* $p<0.05$, **$p<0.01$, ***$p<0.001$ compare with control group.

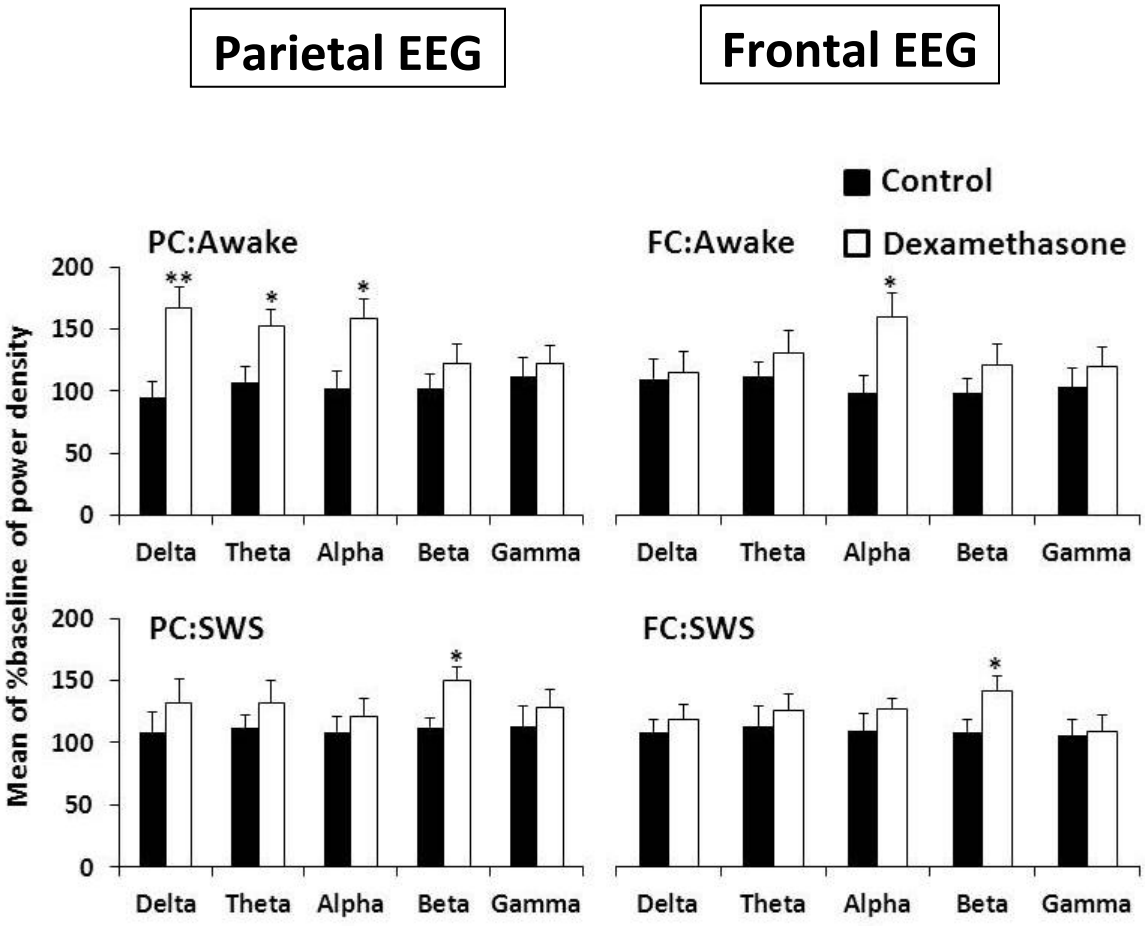

Fig. 3.3 Histogram shown mean of %baseline of power density in each band wave (delta, theta, alpha, beta and gamma) of awake stage and slow wave sleep stage (SWS), the data were evaluated from frontal and parietal EEG. Data are expressed as mean ± S.E.M. of power density (% baseline). Effects of treatment were determined by using t-test, *p<0.05, **p<0.01 compare with control group.

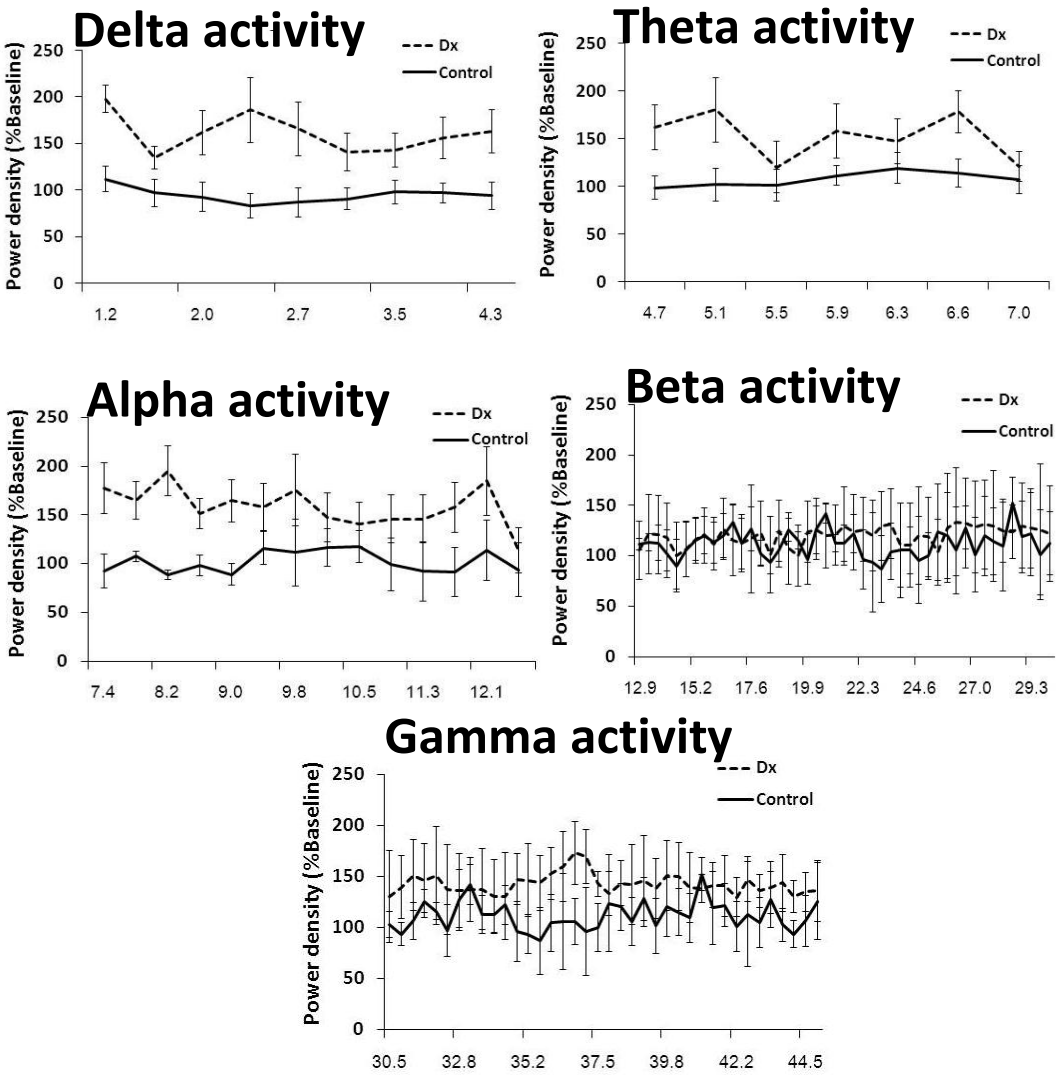

Fig 3.4 Chronic effect of dexamethasone induced neurodegeneration on parietal EEG activity on day 21st after treated with dexamethasone in induced neurodegenerative group (Dx) and normal saline in control group. EEG analyses were evaluated on awake stage. Data are expressed as mean ± S.E.M. of power density (% baseline).

3.3.2. Chronic effect of dexamethasone on sleep patterns.

Effects of chronic dexamethasone on sleep-wake patterns were analyzed from EEG signals recorded following 21 days of dexamethasone treatment. Hypnograms provide means to display a visual presentation of basic sleep-wake cycles (Fig. 3.5). Spectral differentiation of stage-specific EEGs provides more accurate and quantitative measures. Fast Fourier Transform (FFT) power spectra indicate that the awake periods (AW) had peaks at theta wave for frontal and parietal EEG. On the other hand, peaks were specifically found within delta range during slow wave sleep (SWS) for both frontal and parietal EEG. The most unique characteristic was detected during rapid eyes movement (REM) sleep when parietal EEG exhibited dominant theta peak whereas frontal EEG had relatively overall low power. In this study, 2 parameters of sleep were particularly analyzed which include sleep latency and percentage of each brain stages during 2-hrs period recording.

The results showed that chronic dexamethasone exposure significantly decreased percentage of REM sleep (Dx=1.22±2.04 and control=6.42±0.59, p=0.005) (Fig. 3.6). No significant change in percentage was found for AW or SWS stages. The analysis of sleep latency also revealed no significant change induced by dexamethasone.

The distribution of spindles was observed from frontal and parietal raw EEG signals. Types of EEG spindle were characterized by power spectrum analysis of frontal EEG signals using Fast Fourier Transform (FFT) (Fig. 3.7 A). Raw EEG signals were filtered for 6-10 Hz oscillation to extract EEG spindles and inspect their structures. Two main types of spindles were characterized. Sleep spindles were recognized from frontal EEG with relatively low powers when filtered for 6-10 Hz activity. On the other hand, non sleep spindles exhibited high amplitude loop when filtered for 6-10 Hz activity with peak frequency in the range. Therefore, numbers of both types of EEG spindles were counted from 2-hrs period of EEG recording on day 21 (Fig. 3.7 B). The results showed that chronic dexamethasone exposure significantly increased number of non sleep spindle in AW and SWS stage (AW: Dx=3.88±0.72 and control=1.63±0.50, p=0.022 and SWS: Dx=8.25±1.23 and control=2.88±0.72, p=0.002) No significant change was observed for sleep spindles.

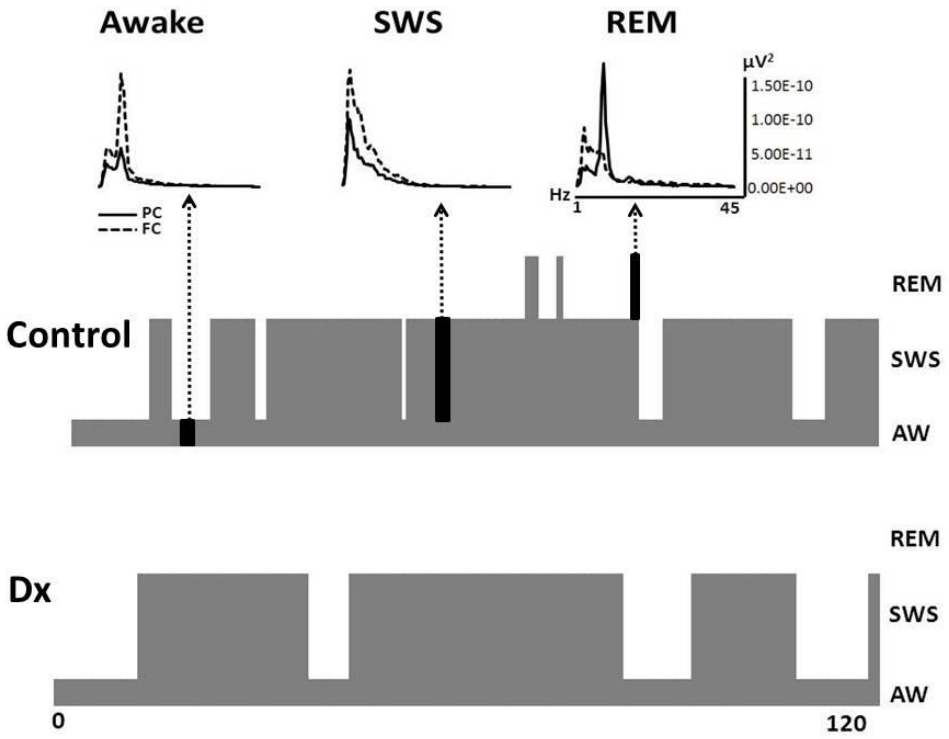

Fig. 3.5 Hypnograms and EEG spectra of representative rats. Hypnograms provide a visual impression of sleep-wake period over 2 hrs. of EEG recording from normal rat and dexamethasone induced neurodegenerative rat from day 21st after treatment. Brain stages were classified to 3 stages: awake stage (AW), slow wave sleep stage (SWS) and rapid eyes movements sleep stage (REM).

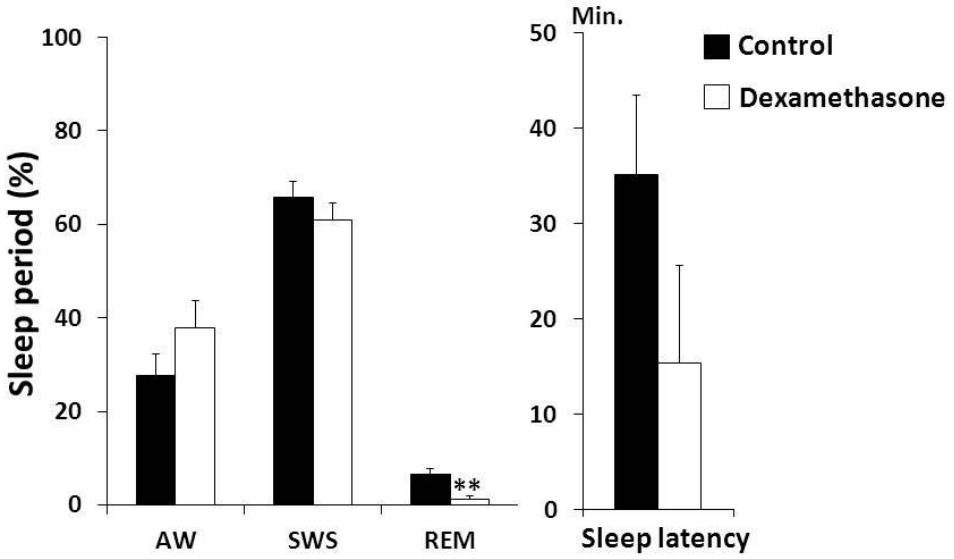

Fig. 3.6 Chronic effects of dexamethasone induced neurodegeneration on sleep period and sleep latency. Percentage of sleep period and sleep latency from EEG recording 2 hrs. on day 21st after treatment with dexamethasone in induced neurodegenerative group (Dx) and normal saline in control group. Sleep stages were divided into 3 stages: awake stage (AW), slow wave sleep stage (SWS) and rapid eye movement sleep stage (REM). Data are expressed as mean ± S.E.M. of sleep period (%) and sleep latency (minutes). Effects of treatment were determined by using t-test, $^{**}p<0.01$ compare with control group.

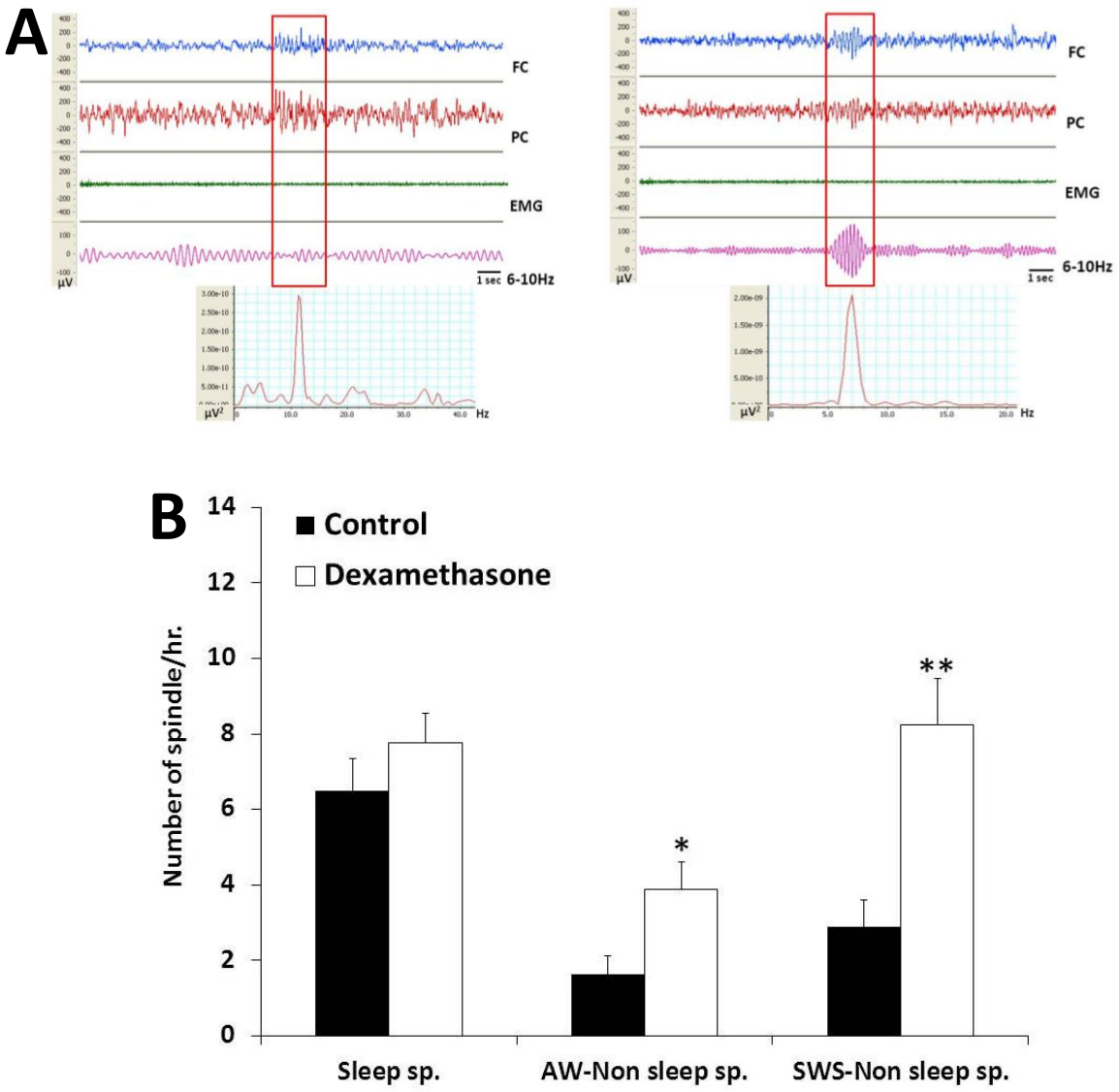

Fig. 3.7 Chronic effect of dexamethasone induced neurodegeneration on EEG spindle. Number of EEG spindle from EEG recording 2 hrs. at day 21st after treated with dexamethasone in induced neurodegenerative group (Dx) and normal saline in control group. **(A)** EEG spindle was divided into 2 types from EEG spectrogram, non sleep spindle (6-10 Hz) and sleep spindle (10-14 Hz). **(B)** Non sleep spindle analysis were separated into 2 stage, awake stage (AW) and slow wave sleep stage (SWS). Data are expressed as mean ± S.E.M. of number of spindle (times/hr.). Effects of treatment were determined by using t-test, *p<0.05, **p<0.01 compare with control group.

3.3.3. Chronic effects of dexamethasone on spatial memory behavior.

Y-maze test showed that control level of spontaneous alternation percentage (SA%) was 81.63±7.84 while that of dexamethasone injected rats was 57.86±6.96. This clearly indicated that long term exposure of dexamethasone significantly decreased SA% in Y-maze test (p = 0.04). No statistically significant difference between groups was detected in total arm entries. It means that both groups had the same levels of spontaneous locomotor activity (Fig. 3.8).

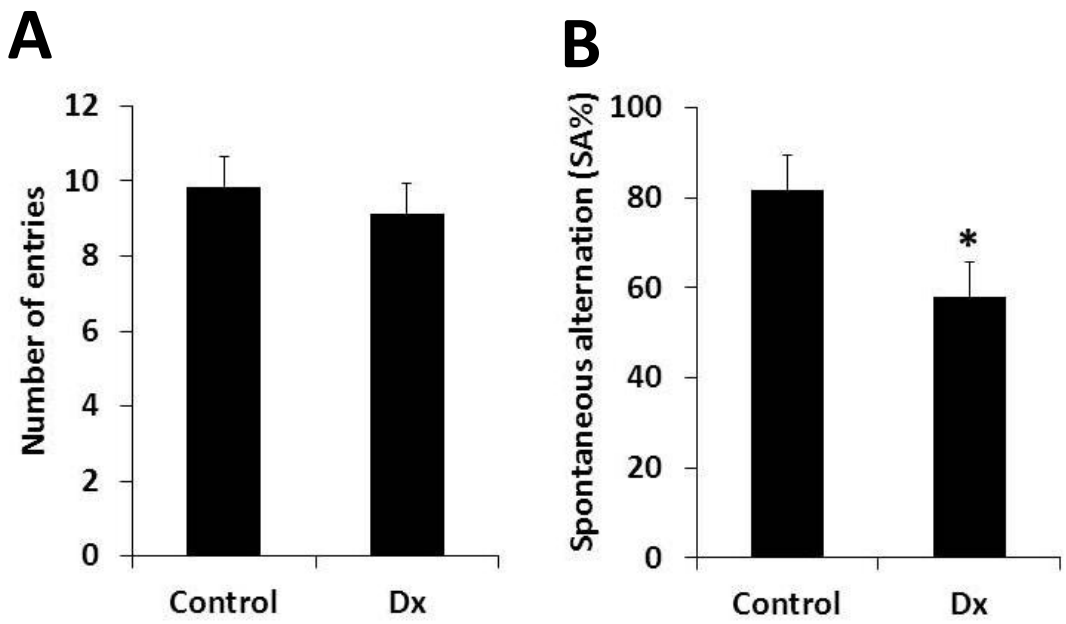

Fig. 3.8 Chronic effect of dexamethasone induced neurodegeneration on spatial memory behavior. Spatial memory behavior were measured on day 21st after treated with dexamethasone in induced neurodegenerative group (Dx) and normal saline in control group with Y-maze apparatus. Data analysis in terms of **(A)** number of entries and **(B)** spontaneous alteration percentage or SA%, data are expressed as mean ± S.E.M. Effects of treatment were determined by using t-test, *p<0.05 compare with control group.

3.3.4. Chronic effects of dexamethasone on brain histology.

Cresyl violet positive neurons were identified in selected areas of the hippocampus; CA1, CA2, CA3 and dentate gyrus (DG) (Fig. 3.9) and parietal cortex (PC). High magnification of micrographs were illustrated to visualize morphology of cells in CA1 (Fig. 10 A), CA2 (Fig. 10 B), CA3 (Fig. 3.10 C), DG (Fig. 3.10 D) and the parietal cortex (Fig. 3.11). It was found that number of neurons in CA1, CA3 and DG of the hippocampus and parietal cortex were significantly reduced by dexamethasone (565.85±45.16 cell/mm^2, 823.43±37.62 cell/mm^2, 1,323.93±84.53 cell/mm^2 and 918.35±78.46 cell/mm^2, respectively) compared to that of control group (963.37±35.09 cell/mm^2, 1,074.48±68.98 cell/mm^2, 1,948.72±27.80 cell/mm^2 and 1,394.06±120.07 cell/mm^2, respectively) ($p < 0.05$) (Fig. 3.12).

For the study of dexamethasone effects on astrocyte density, specificity of GFAP-ir cells was confirmed in immuno-histochemical method by omitting the primary antibody. This is a routine process to ensure that any observed staining was due to the existence of GFAP antigen. This type of controls did not show any labeling (Fig 3.13). For the standard staining protocol, GFAP-ir astrocytes were identified in all area of the hippocampus; CA1 (Fig. 3.14 A), CA2 (Fig. 3.14 B), CA3 (Fig. 3.14 C), DG (Fig. 3.14 D) and the parietal cortex (Fig. 3.15). The densities of GFAP-ir astrocytes in CA1, CA3 and DG of hippocampus and the parietal cortex were significantly reduced in the dexamethasone groups (481.56±92.81 cell/mm^2, 317.78±47.93 cell/mm^2, 331.23±61.06 cell/mm^2 and 527.73±81.15 cell/mm^2, respectively) compared to that of control group (645.61±66.50 cell/mm^2, 575.21±71.51 cell/mm^2, 851.26±93.13 cell/mm^2 and 845.97±124.55 cell/mm^2, respectively) ($p < 0.05$) (Fig. 3.16).

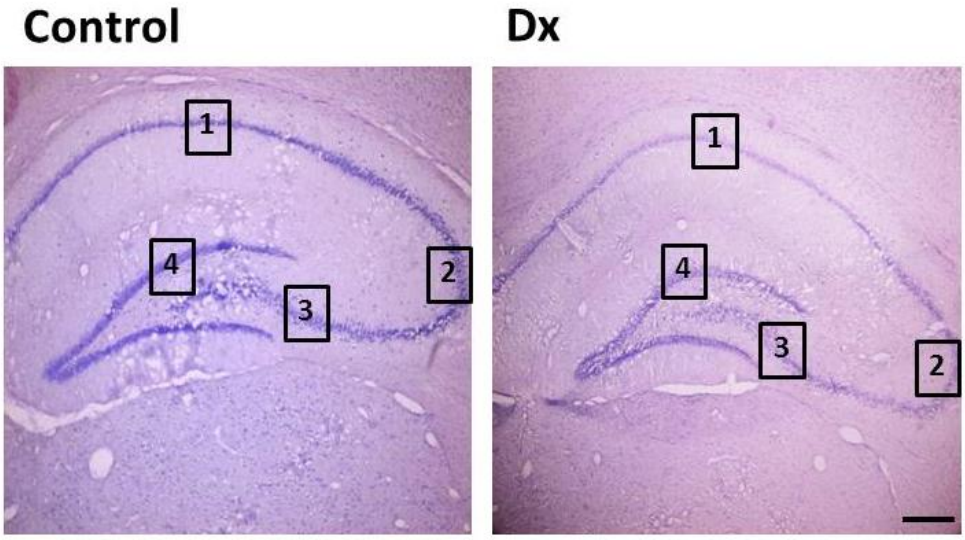

Fig. 3.9 Micrographs of a coronal section of the hippocampus showing CA1 (1), CA2 (2), CA3 (3) and dentate gyrus (DG) (4) of control and dexamethasone (Dx)**,** Bar= 40 µm**.**

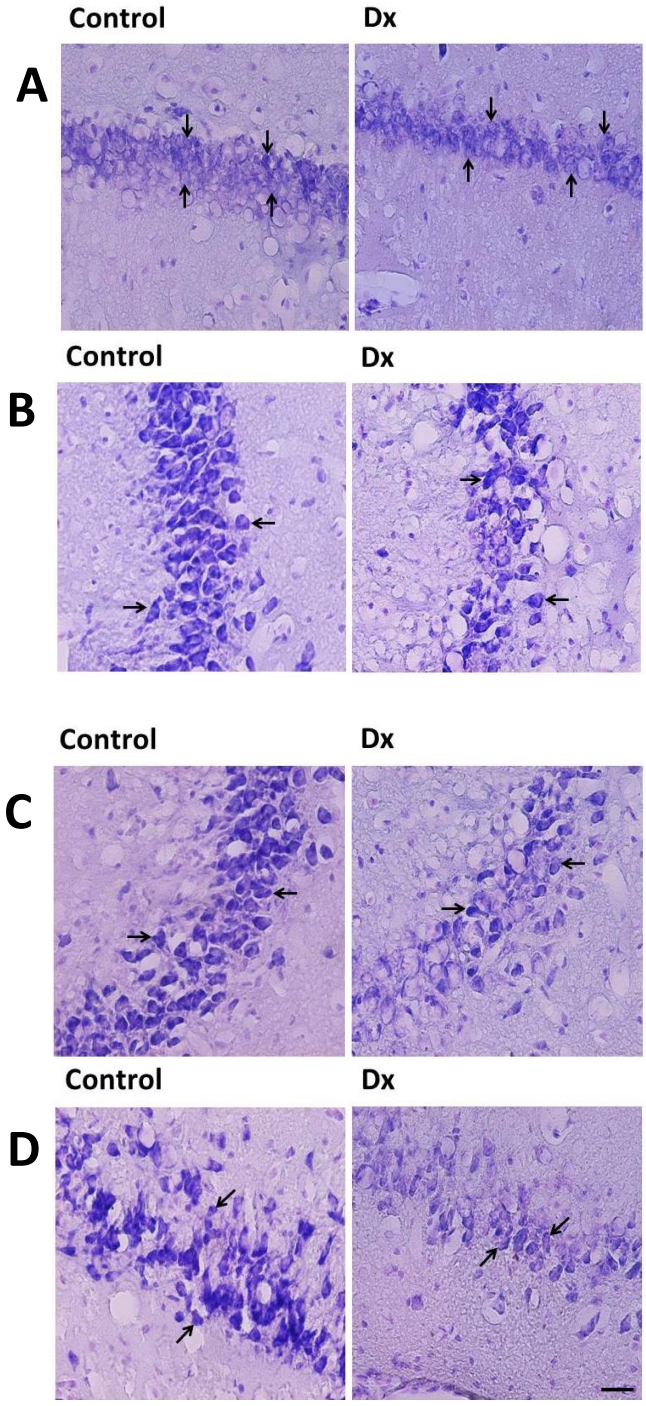

Fig. 3.10 Micrographs of **(A)** CA1, **(B)** CA2, **(C)** CA3 and **(D)** DG in hippocampus magnified from the framed area in Fig 3.9 showing the cresyl violet positive neurons (arrows) in different treatment groups, Bar= 400 µm.

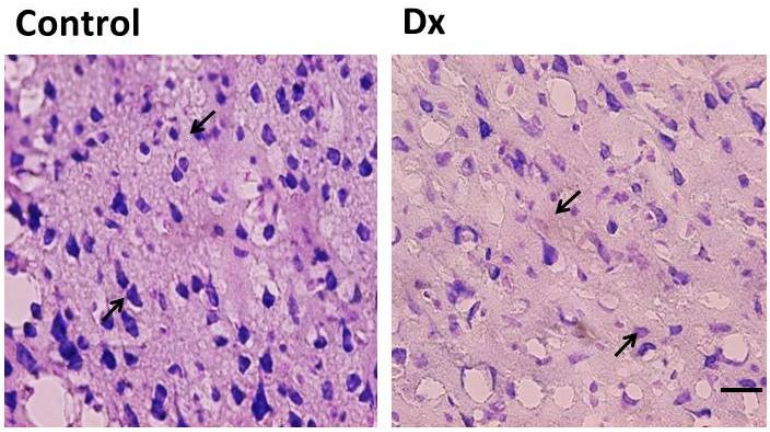

Fig. 3.11 Micrographs of cresyl violet positive neurons (arrows) in parietal cortex in different treatment groups, Bar= 400 µm.

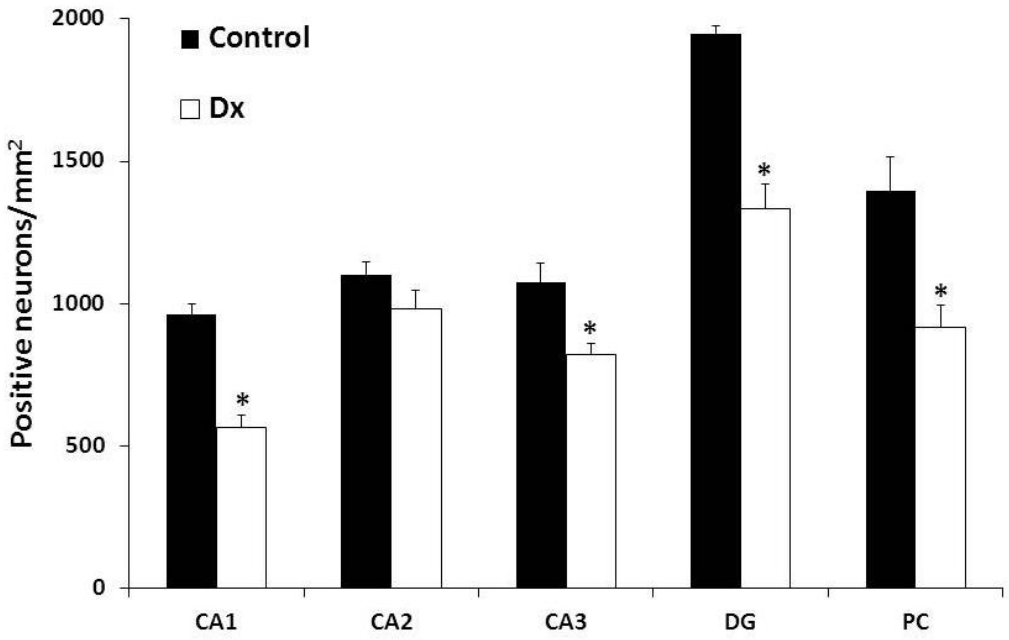

Fig. 3.12 Chronic effects of dexamethasone induced neurodegeneration on hippocampal and cortical neurons. The number of positive neurons in the CA1, CA2, CA3 and dentate gyrus (DG) of hippocampus and parietal cortex (PC) were measured at day 21st after treated with dexamethasone in induced neurodegenerative group (Dx) and normal saline in control group with Nissl staining method. Data are expressed as mean ± S.E.M. Effects of treatment were determined by using t-test, *p<0.05 compare with control group.

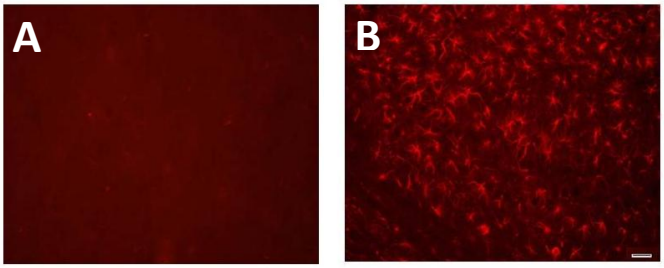

Fig. 3.13 Micrographs of **(A)** negative control and **(B)** positive control of GFAP-ir astrocytes

Bar= 200 µm

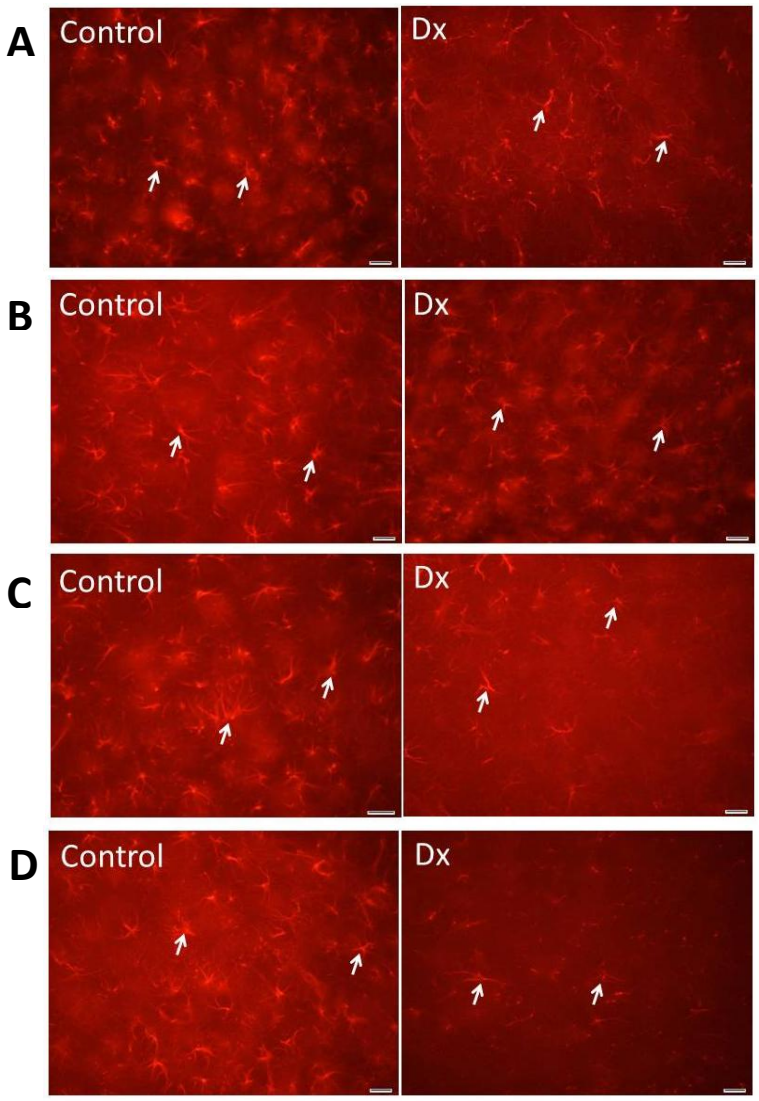

Fig. 3.14 Micrographs of GFAP-ir astrocytes (arrows) in **(A)** CA1, **(B)** CA2, **(C)** CA3 and **(D)** DG in hippocampus in different treatment groups, Bar= 400 µm.

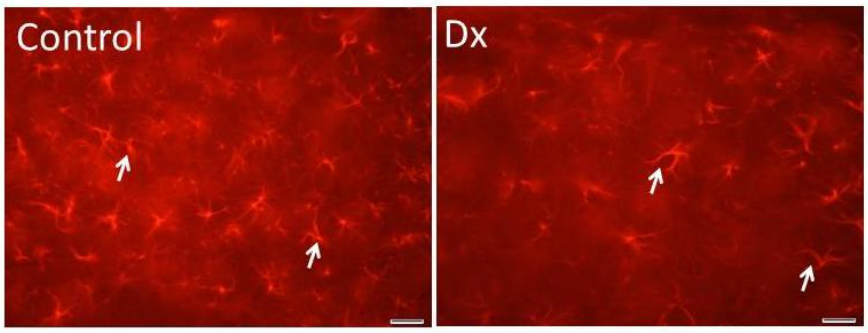

Fig. 3.15 Micrographs of GFAP-ir astrocytes (arrows) in parietal cortex in different treatment groups, Bar= 400 µm.

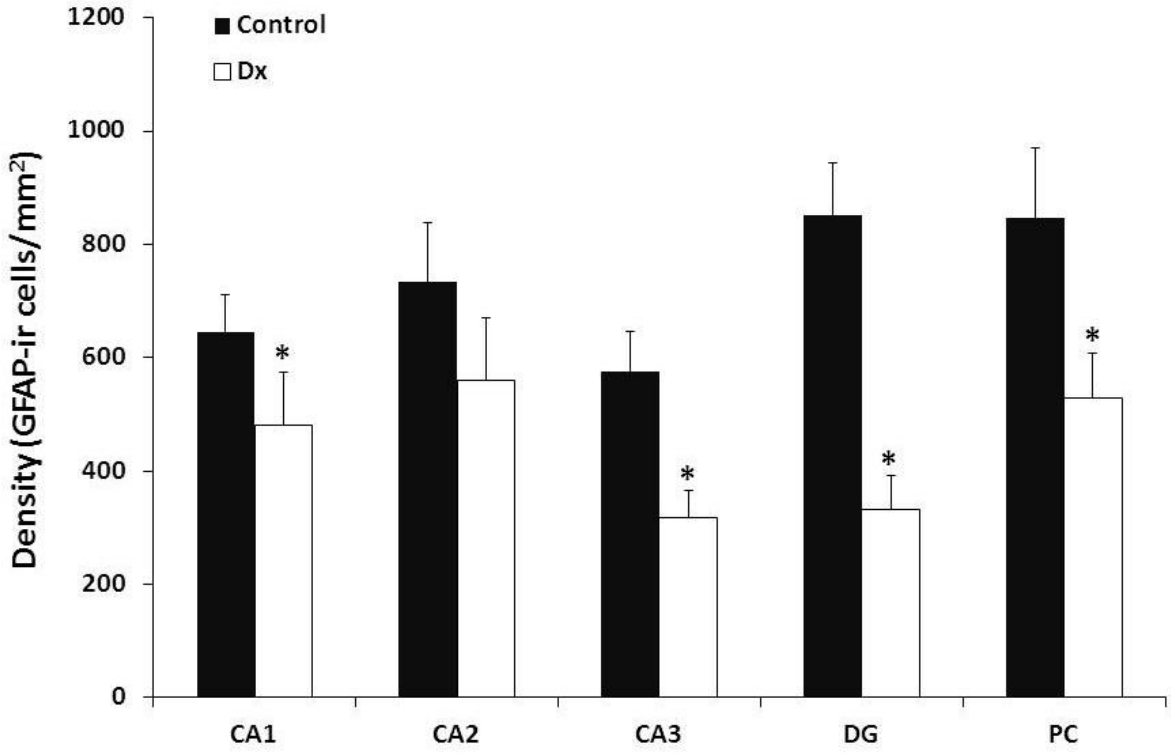

Fig. 3.16 Chronic effects of dexamethasone induced neurodegeneration on hippocampal and cortical astrocytes. The GFAP-ir density in the CA1, CA2, CA3 and dentate gyrus (DG) of hippocampus and parietal cortex (PC) were measured at day 21st after treated with dexamethasone in induced neurodegenerative group (Dx) and normal saline in control group with GFAP immunofluorescence staining method. Data are expressed as mean ± S.E.M. Effects of treatment were determined by using t-test,*p<0.05 compare with control group.

3.3.5 The Correlations between spatial memory behavior and factors of either electrical activity or brain histology in dexamethasone induced neurodegenerative rats.

The correlation between spatial memory behavior and factors of either electrical brain activity or brain histology in dexamethasone-induced neurodegenerative rats and control rats were evaluated using linear regression analysis. The data were shown with R-square score and considered statistically significant at $p<0.05$. A total of 18 significant changes analyzed from EEG patterns and brain structures were evaluated for correlation scores against spontaneous alternation percentage or SA%. The lists of factors are shown as follows.

(1) number of positive neurons in CA1,
(2) number of positive neurons in CA3,
(3) number of positive neurons in dentate gyrus or DG,
(4) number of positive neurons in parietal cortex or PC,
(5) number of GFAP-ir in CA1,
(6) number of GFAP-ir in CA3,
(7) number of GFAP-ir in dentate gyrus and
(8) number of GFAP-ir in parietal cortex
(9) power activity from parietal cortex of delta in awake stage,
(10) power activity from parietal cortex of theta in awake stage,
(11) power activity from frontal cortex of alpha in awake stage,
(12) power activity from parietal cortex of alpha in awake stage,
(13) power activity from frontal cortex of beta in slow wave sleep stage,
(14) power activity from parietal cortex of beta in slow wave sleep stage,
(15) rapid eyes movement sleep period percentage or REM%,
(16) number of non-sleep spindle in awake stage,
(17) number of non-sleep spindle in slow wave sleep stage,

The results showed that SA% had significant correlation with some of these parameters (Table 1).

The most interesting and strong correlations between the impairment of spatial memory behavior and electrical brain activity were demonstrated with high correlation scores. In particular, Delta and Alpha activity were correlated with SA% with R-square 0.460 and 0.408 respectively (Fig. 3.17). In terms of histological changes, densities of either cresyl positive cells or GFRP-ir cells were used for the analysis. Significant correlations were also observed between SA& and number of positive cells in the area CA1, CA3 and DG with R-square 0.296, 0.307 and 0.270 respectively (Fig.3.18 A). Similarly, densities of GFRP-ir cells in the area CA1 and DG were found to have clear rcorrelation with the SA% (Fig.3.18 B).

Table 1 R-square data of correlation among EEG patterns, spatial memory behavior and brain histology in dexamethasone induced neurodegenerative rats, * $p<0.05$.

Correlation with SA %		**R^2**	***p*- value**
Brain histology	Positive neuron CA1	0.296*	0.029
	Positive neuron CA3	0.307*	0.009
	Positive neuron DG	0.270*	0.039
	Positive neuron PC	0.126	0.176
	GFAP-ir CA1	0.550*	0.001
	GFAP-ir CA3	0.083	0.277
	GFAP-ir DG	0.389*	0.010
	GFAP-ir PC	0.189	0.092
EEG activity	Delta activity PC : AW	0.460*	0.004
	Theta activity PC : AW	0.256	0.065
	Alpha activity FC : AW	0.264	0.051
	Alpha activity PC : AW	0.408*	0.010
	Beta activity FC : SWS	0.203	0.080
	Beta activity PC : SWS	0.008	0.073
Sleep patterns	REM sleep period%	0.233	0.058
	Non-sleep spindle AW	0.211	0.073
	Non-sleep spindle SWS	0.193	0.241

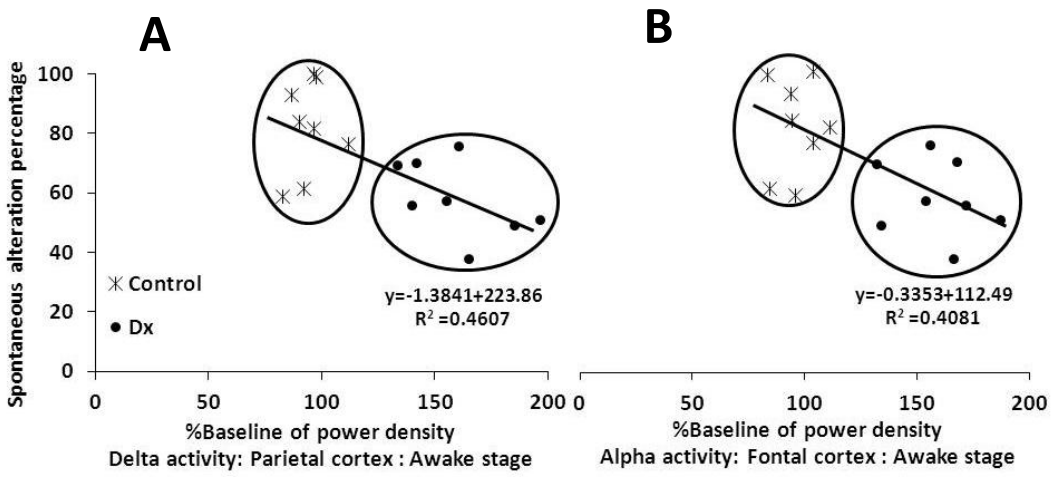

Fig. 3.17 Linear regression analysis between **(A)** spontaneous alteration percentage (SA%) and delta activity from parietal EEG in awake stage **(B)** spontaneous alteration percentage (SA%) and alpha activity from frontal EEG in awake stage. Data were evaluated form normal rats (control) and dexamethasone treated rats (Dx). Each correlation was expressed as R-square (R^2) and linear equation.

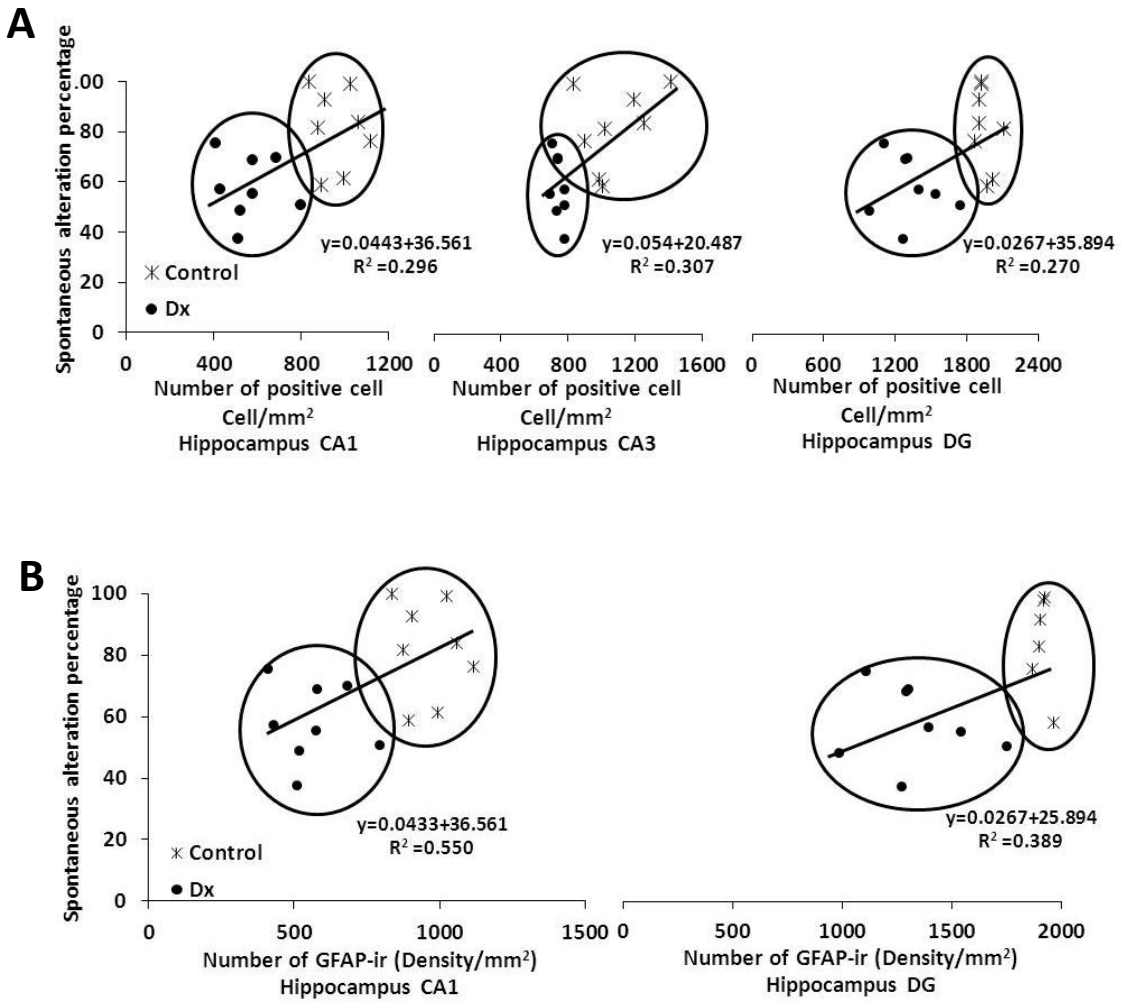

Fig. 3.18 Linear regression analysis between **(A)** spontaneous alteration percentage (SA%) and number of positive neurons in hippocampus area CA1, CA3 and dentate gyrus (DG) **(B)** spontaneous alteration percentage (SA%) and number of GFAP-ir in hippocampus area CA1 and dentate gyrus (DG). Data were evaluated form normal rats (control) and dexamethasone treated rats (Dx). Each correlation was expressed as R-square (R^2) and linear equation.

3.4 Discussions

3.4.1 Chronic effects of dexamethasone on EEG power.

Some aspects of cerebral functioning can be overviewed and surveyed from electrical brain activity. Recently, visual electroencephalography (EEG) interpretation has been applied to understand brain function (Micanovic and Pal, 2013). The present study demonstrated that**,** from the analysis of parietal and frontal EEG signal, dexamethasone increased powers activity of slow wave frequency (delta, theta and alpha) on day 21 of the treatment. The increase in EEG power implied that dexamethasone increased the amplitude of electrical field potential. Previously, steroid-mediated increase in depolarization-induced Ca^{2+} influx was evidenced (Sze and Yu, 1995). The high-dose glucocorticoids can induce a rapid prolongation of NMDA receptor-mediated Ca^{2+} elevation in hippocampal slices (Takahashi et al., 2002). However, high levels of glucocorticoids (GCs) are possible to produce hyperexcitability and finally neuronal loss. GCs have also been shown to intensify neuronal damage through mechanisms that modulate synaptic glutamate concentrations suggests that GC-induced neuronal death in all these physiological and pathophysiological settings occurs by apoptosis (Reagan and McEwen, 1997). A relationship between slow-wave activity in the spectral analysis of EEG and dementia has also been detected in Alzheimer's disease (AD) such as the increase in theta activity is a typical finding in mild AD (Coben et al., 1983; Kwak, 2006). Global cortical dysfunction was also associated with increased theta activity in the EEG spectra (Helkala et al., 1996). Significant increase of delta power was observed in later stages of AD (Prichep et al., 1994). Consistently, EEG changes across physiological aging were found with increases in EEG power of the slower delta (2–4 Hz) and theta (4–8 Hz) frequency ranges (Dujardin et al., 1995). The processes of degeneration of neurons in AD led to disturbances in cholinergic transmission which are cleared in a slower frequency of alpha cortical rhythm and the presence of slow wave (Ellis, 2005; Soininen and Riekkinen, Sr., 1992).

In addition, chronic dexamethasone exposure particularly targeted on slow wave frequency in the parietal cortex and alpha activity of the frontal EEG in wake stage. In general, the EEG activity during wakefulness depends considerably on the behavioral state, electrode location and animal species. On average, cortical EEG during wakefulness consists of low-voltage, called desynchronized or activated EEG (Lancel, 1993). Wakefulness and EEG desynchronization require excitatory innervation mainly from the forebrain. Being awake depends on various systems which release glutamate, acetylcholine (ACh), or the monoamines (serotonin and norepinephrine) in particular. These are absolutely necessary for the expression of wakefulness (Jones, 2005). Administering the anti-cholinergic scopolamine and the monoamine depletor reserpine led to amplitude increases of frequency ranging between 0.5–20 Hz, with the delta (0.5–4 Hz) and theta (4–8 Hz) bands mainly. However, during SWS, dexamethasone increased beta power activity from the parietal and frontal cortex. Beta activity reflects arousal level during sleep and its power is higher in the lighter parts of SWS sleep (Perlis et al., 2001; Uchida et al., 1992). Beta activity is also elevated in individuals with primary insomnia and in association with symptoms of stress (Hall et al., 2007).

3.4.2 Chronic effects of dexamethasone on sleep patterns.

The present data demonstrated that dexamethasone decreased percentage of REM sleep. In general, corticosteroids appear to have direct neural effects as the HPA axis plays a key role in modulating sleep patterns (Hall et al., 2007). Exogenous GCs administration reduces REM sleep (Moser et al., 1996). Excess of GCs alters dendritic morphology of hippocampal neurons (Sapolsky, 1996). Prolonged exposure to corticosterone accelerates the process of cell loss in the hippocampus of rats and analysis of size distribution of hippocampal cell bodies shows a loss of certain types of neurons (Sapolsky et al., 1985). REM sleep has been thought to reflect the overnight learning by establishing information in the hippocampal and cortical regions of the brain (Walker et al., 2005). REM sleep is involved in the memory consolidation process. The mechanism which allows this type of memory consolidation to occur during REM sleep may be found in the hippocampus, a region of the brain with a well-established link to declarative memory (Bodizs et al., 2001; Grosmark et al., 2012; Smith, 1995).

3.4.3 Chronic effects of dexamethasone on EEG spindles.

Chronic dexamethasone exposure increased numbers of non sleep spindle in wake stage and slow wave sleep stage. This study used spectral analysis to identify 2 types EEG spindle. First category includes physiological spindles or sleep spindles, sleep spindles in SWS and sleep spindles during barbiturate anaesthesia or barbiturate spindles (10-14 Hz) which are recognized as relatively normal events. The second ones are non-sleep spindles, spindles induced by picrotoxin and naturally occurring spindles in a rat model of absence epilepsy or absence spindles (6-10 Hz). Non sleep spindle exhibited higher voltage signals than sleep spindle indicating that more cells are related in the epileptiform phenomena (Mackenzie et al., 2004). SWS and spindle frequency activity (SFA) are thought to be generated by a common thalamo-cortical mechanism, which depends on the degree of hyperpolarization of thalamo-cortical neurons (McCormick and Bal, 1997; Steriade et al., 1993). In animal models of human generalized non-convulsive seizures, the seizures are generated in a circuitry involving both the cerebral cortex and the thalamus. The dysfunction of cortex, a cortical hyper-excitability, not affected thalamic, but a thalamic hypersynchronisation imposed upon the cortex (Mackenzie et al., 2010; Steriade et al., 1985; Steriade and Deschenes, 1984). The thalamic structures have been shown to be generally involved in the generation of sleep, barbiturate and absence spindles (Coenen and Van Luijtelaar, 1987; Inoue et al., 1990). In addition, the hippocampal neurons have to oscillate at the frequencies associated with spindling; these structures generated the theta rhythm with a frequency of around 7 Hz related to that of spindles (Tesche and Karhu, 2000). Furthermore, the changes in beta and gamma power associated with some spindles are likely to relate with the brain states during which the spindling phenomenon occurs (Mackenzie et al., 2004).

3.4.3 Chronic effects of dexamethasone on spatial memory behavior.

The spontaneous alternation percentage (SA%) is the score that reflects spatial memory behavior performance. The Y-maze apparatus were used for evaluation of spatial working memory behavior. This study showed that long term exposure of dexamethasone significantly decreased SA% scores compared to control condition. Rats with impaired spatial memory would be likely to explore the previous arms not the other arms. The results suggested that glucocorticoid exposure, including endogenous glucocorticoids associated with stress, decreases memory and learning function and hippocampal atrophy. An impaired hippocampus could lead to problems in retaining spatial memory, because hippocampus plays a particularly important role in finding shortcuts and new routes between familiar places (Alhassan et al., 2009; Heffelfinger and Newcomer, 2001; Reus and Wolkowitz, 2001).

3.4.5 Chronic effects of dexamethasone on brain histology.

In the present study, histological examination showed that, chronic administration of dexamethasone resulted in reduced levels of hippocampal pyramidal cells in the area CA1 and CA3, dentate granular cell and cortical neurons in the parietal cortex. In dexamethasone treated rats, the number of positive neurons was decreased. Moreover, the number of GFAP-ir astrocytes in the area CA1, CA3 and DG of hippocampus were significantly reduced in the dexamethasone treated rats. Altogether, dexamethasone treatment appeared to induce neuronal cell death and astrocyte damage in almost all hippocampal regions studied. This study demonstrated that 21 days of progressively increasing exposure to stress levels of GCs accelerated neurodegeneration. In previous studies, evaluated levels or prolonged exposure to high level of GCs could induce similarly damage to hippocampus and cortical neurons (Conrad et al., 2007; Haynes et al., 2001; Hibberd et al., 2000; Reagan and McEwen, 1997; Sapolsky et al., 1985b; Woolley et al., 1990).

Previously, dexamethasone-induced neuronal apoptosis is mediated via a type II glucocorticoid receptor-dependent mechanism (Haynes et al., 2001). It has been hypothesized that GCs could impair energy metabolism by inhibiting glucose transport (Virgin, Jr. et al., 1991) and elevated levels of glutamate neurotransmitter (Moghaddam et al., 1994). Overstimulation of glutamate receptors results in excessive calcium influx and disturbance of the postsynaptic calcium homeostasis leading to production of free radicals via Ca^{2+}-dependent enzyme. Reactive oxygen species or ROS is the cause of degradation of intracellular components and mitochondrial damage that would lead to degeneration of cytoskeletal proteins, so oxidative stress contributes to neuronal damage (Abraham et al., 2001; Sapolsky, 1996). Moreover, GCs could provide to neuronal damage by diminishing the antioxidant enzyme capacity in the brain that in turn, make neurons more vulnerable to free radical (McIntosh and Sapolsky, 1996). Several studies have shown consistent results indicating that GCs exposure caused reducing of astrocyte through inhibition of astrocyte proliferation *in vivo* (Unemura et al., 2012) and induced reductions in GFAP expression both in terms of RNA or protein levels, as well as in the number of GFAP positive cells (Claessens et al., 2012; Czeh et al., 2006; Nichols et al., 1990). In addition, GCs have been reported to affect the number of GFAP positive astrocytes (Czeh et al., 2006), the differentiation of GFAP (Bohn et al., 1991) and the production of GFAP in astrocytes (O'Callaghan et al., 1989). GCs cause astrocytic growth inhibition by inducing exit from the cell cycle and contribute to the functional remodeling of astrocytes (Yu et al., 2008). In addition, chronic stress interferes with glial cell metabolism, through glutamatergic mechanisms (Banasr et al., 2010).

3.4.6 The Correlations among EEG patterns, spatial memory behavior and brain histology.

Strong correlations between spatial memory performance and patterns of change in electrical brain activity or densities of brain cells were established in dexamethasone induced neurodegenerative rats. These data mean both phenomena are associated with the decline of cognitive performance. It would be practical to predict cognitive decline with either EEG biomarkers or degenerations of brain cells. The most important thing is that EEG recording is a non-invasive technique that would be practical to detect the early sign of neurodegeneration and its progression, thus, it is possible to detect biomarkers of neurodegenerative disease in early stage of the disease by EEG monitoring.

3.5 Conclusion

In general, consequences of chronic stress can be assessed from brain histology such as loss of neuronal or glial cells in the brain. These changes clearly impact patterns of behavior including spatial memory impairment in particular. To evaluate brain changes during degenerative process in animals, they have to be sacrificed for histological studies. This type of examination allows to obtain data only once at selected time point. It is insufficient to monitor brain function in longitudinal study.

The present findings obtained from EEG study suggest the options of how to follow the changes of brain oscillation from the beginning before and during the induction of neurodegeneration. The most interesting point is that unique patterns of electrical brain activity are detected in each brain stage. EEG records can be used for sleep pattern analysis to check the occurrence of non-sleep spindle density that would reflect some levels of brain degeneration. Taken together, these obvious parameters needed for evaluation can be analyzed in EEG study.

The translation of this into a routine test for neurodegenerative diseases in the clinic is possible. The technique is nonexpensive and non-invasive. So, it is practical to monitor brain oscillation in longitudinal studies. The ideal research should better start with control subjects with intact physical and cognitive performances. In animal studies, it is possible to record spontaneous electrical brain activity before the induction of neurodegeneration. Therefore, regular record can be performed during a period of neurodegenerative induction in order to capture gradual changes.

CHAPTER 4

THE EFFECTS OF KAINIC ACID INDUCED NEURODEGENERATION ON EEG PATTERNS, SPATIAL MEMORY BEHAVIOR AND BRAIN STRUCTURE

4.1 Experimental protocol

The animals were randomly divided into 2 groups, with 6 rats in each group. In group I or control group, rats were treated with 0.9% saline (i.c.v.) once daily. In group II or treated group, rats were treated with kainic acid 1 nmol/µl (i.c.v.) also once daily. After a full recovery period of 14 days, animals were habituated with recording chamber and EEG recording system simultaneously for 3 days. On the testing day or baseline day, the process was setup similarly to that of the habituation days but EEG recording instrument was turned on to record electrical signal. EEG recording was carried on for 2 hrs. After 1 hr of recording, rats were given 0.9% saline and kainic acid for control and treated group, respectively. On day 7 of treatment, rats were used for EEG recording, tested for spatial memory behavior with Y-maze apparatus and sacrificed for brain collection for histological study (Fig. 4.1).

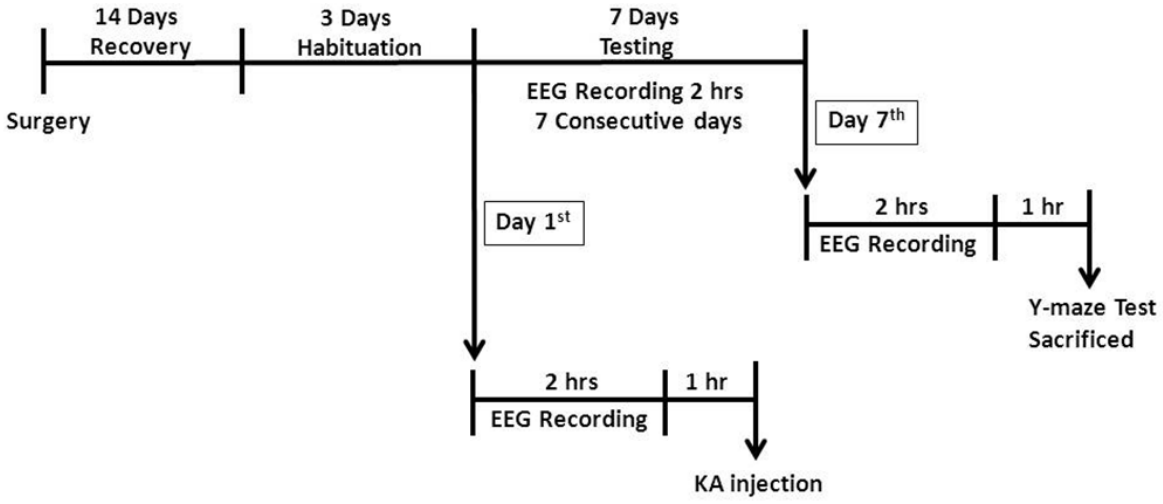

Fig. 4.1 Schematic diagram of protocol for examination of kainic acid induced neurodegeneration.

4.2 Data analysis

4.2.1 For EEG analysis, powers of parietal EEG during baseline and post-treatment were calculated. All data were normalized with values obtained from the start of the experiment to express as % baseline. Values of post-treatment were calculated as percent change of baseline. All data were averaged and expressed as mean ± S.E.M. Effects of treatment were determined by using t-test and statistical significance was considered at $p < 0.05$

4.2.2 In Y-maze test, spontaneous alternation percentage (SA%) and total entries were averaged and expressed as mean ± S.E.M. Effects of treatment were determined by using t-test and statistical significance was considered at $p < 0.05$

4.2.3 Number of neurons in the hippocampus and parietal cortex were shown in positive neurons/mm2 and number of GFAP-ir astrocytes in GFAP-ir/mm2. All data were averaged and expressed as mean ± S.E.M. Effects of treatment were determined by using t-test and statistical significance was considered at $p < 0.05$

4.2.4 The relationship among EEG patterns, spatial memory behavior and brain structure were performed in regression analysis and data were expressed as R-square. The significant correlation was considered at $p < 0.05$.

4.3 Results

4.3.1. Acute effects of kainic acid on EEG powers.

EEG powers of animals were analyzed on day 7 after kainic acid (i.c.v.) injection. EEG power spectrum was expressed in 5 frequency bands: delta, theta, alpha, beta and gamma. First, continuous signals were analyzed without selection of specific brain state. T-test performance revealed that kainic acid treatment significantly increased powers of delta band (KA=215.91±46.80 and control=106.02±9.62, p=0.044) and decreased that of theta (KA=55.81±18.98 and control=106.93±8.35, p=0.033), alpha (KA=79.58±10.22 and control=107.76±6.98, p=0.046), beta (KA=70.41±9.15 and control=96.41±4.45, p=-0.029) and gamma KA=66.00±15.98 and control=106.83±5.45, p=0.036) bands (Fig. 4.2).

Therefore, EEG power of awake state (AW) and slow wave sleep stages (SWS) were separately analyzed. Signals of each stage (first 5 min recording of the first appearance of each state) were collected. The results showed that slow frequency range appeared to be sensitive to kainic acid both during awake and slow wave sleep periods (Fig. 4.3). Therefore statistical analysis indicated that kainic acid significantly increased delta activity (KA=213.77±40.34 and control=104.95±24.32, p=0.043) and decreased theta activity (KA=61.06±17.51and control=107.75±11.39, p=0.049) during awake period. During slow wave sleep, the increase in delta power is the only significant change (KA=162.75±10.22 and control=92.40±10.55, p=0.033) (Fig. 4.4). Taken together, acute administration of kainic acid specifically affected delta and theta activity mainly during awake stage and only delta activity in SWS stage.

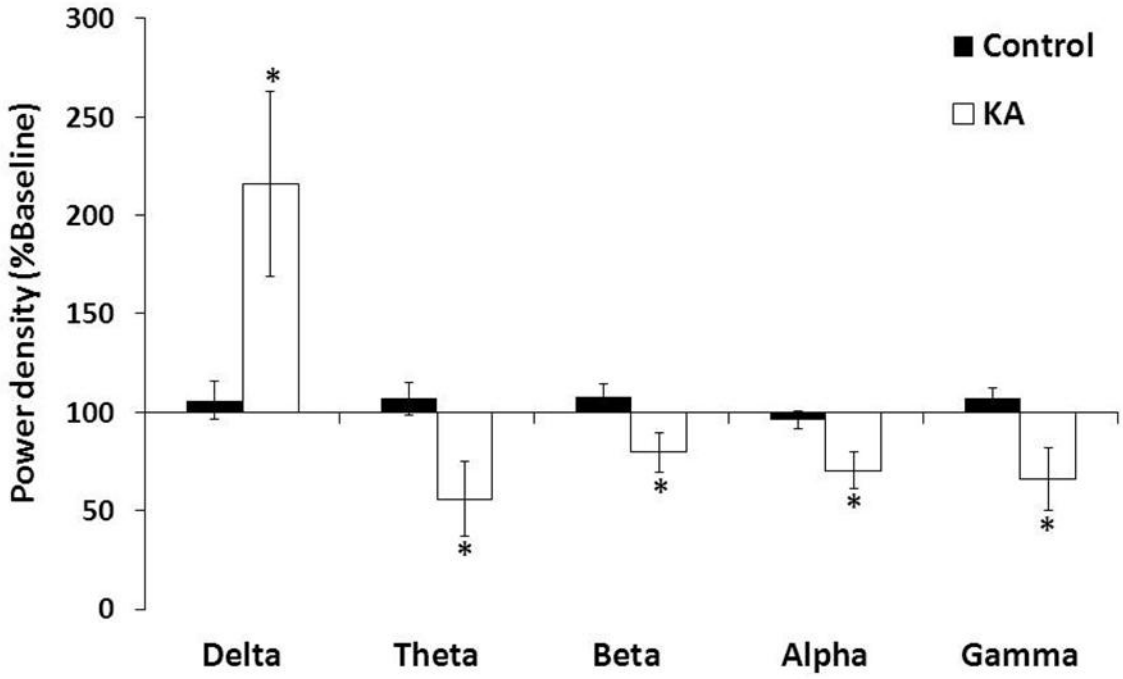

Fig. 4.2 Effects of kainic acid on EEG power activity. Parietal EEG powers from kainic acid induced neurodegenerative group (KA) are shown in comparison to control data. Baseline activities were evaluated for 2 hrs. on first day recording before drug administration. After the administration of KA, EEG was recorded for 2 hrs. in each day. Data analysis was classified base on 5 frequency bands: delta, theta, alpha, beta and gamma. Data are expressed as mean ± S.E.M. of power density (% baseline). Effects of treatment were determined by using t-test, $p<0.05$ compare with control group.

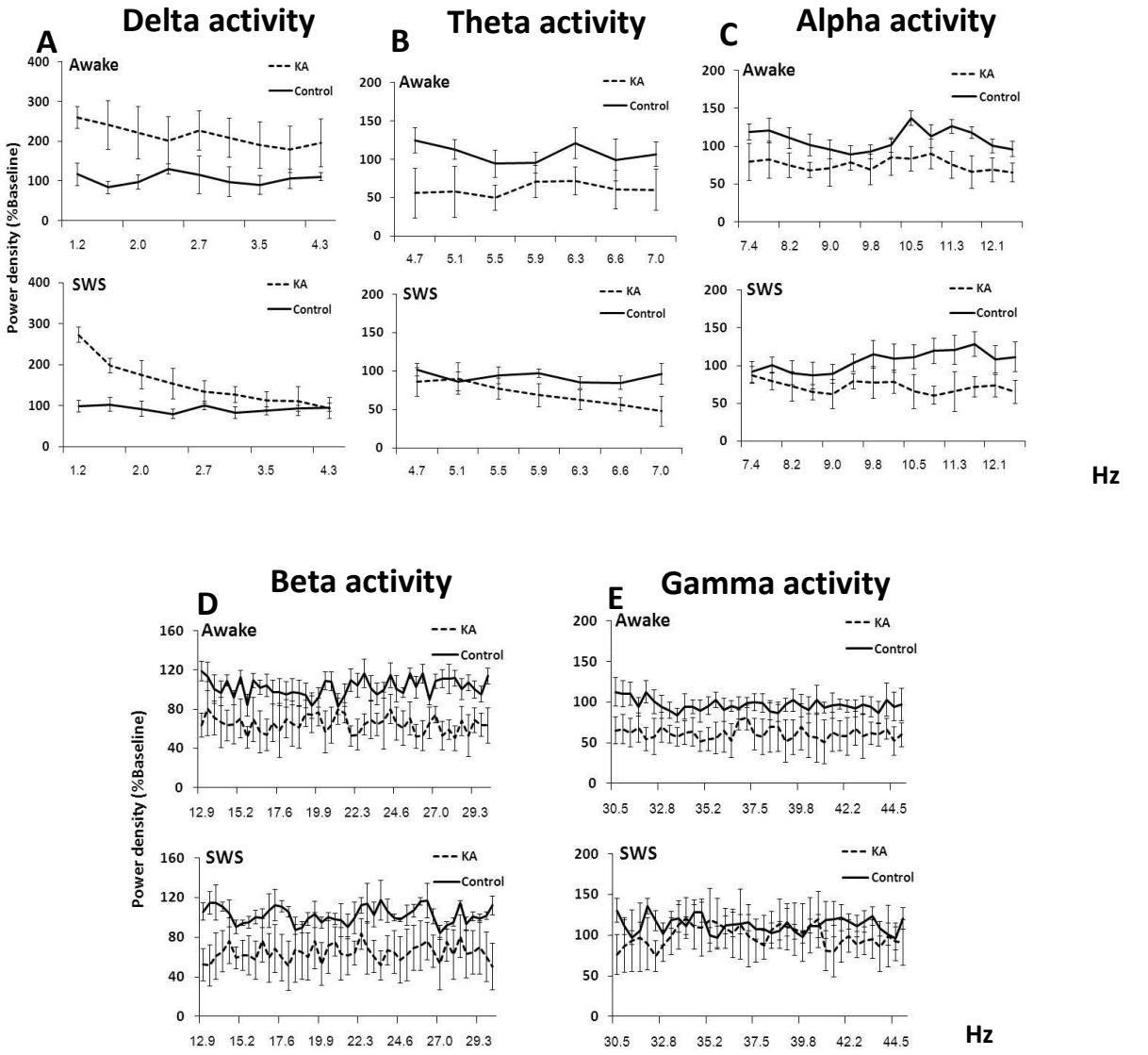

Fig. 4.3 Effects of kainic acid induced neurodegeneration on **(A)** delta, **(B)** theta, **(C)** beta, **(D)** alpha and **(E)** gamma power activity. Power activity from parietal EEG on day 7th after treated with kainic acid in induced neurodegenerative group (KA) and normal saline in control group. EEG analysis were separated into 2 stages: awake stage and slow wave sleep stage (SWS) (continuous 5 minutes). Data are expressed as mean ± S.E.M. of power density (%baseline).

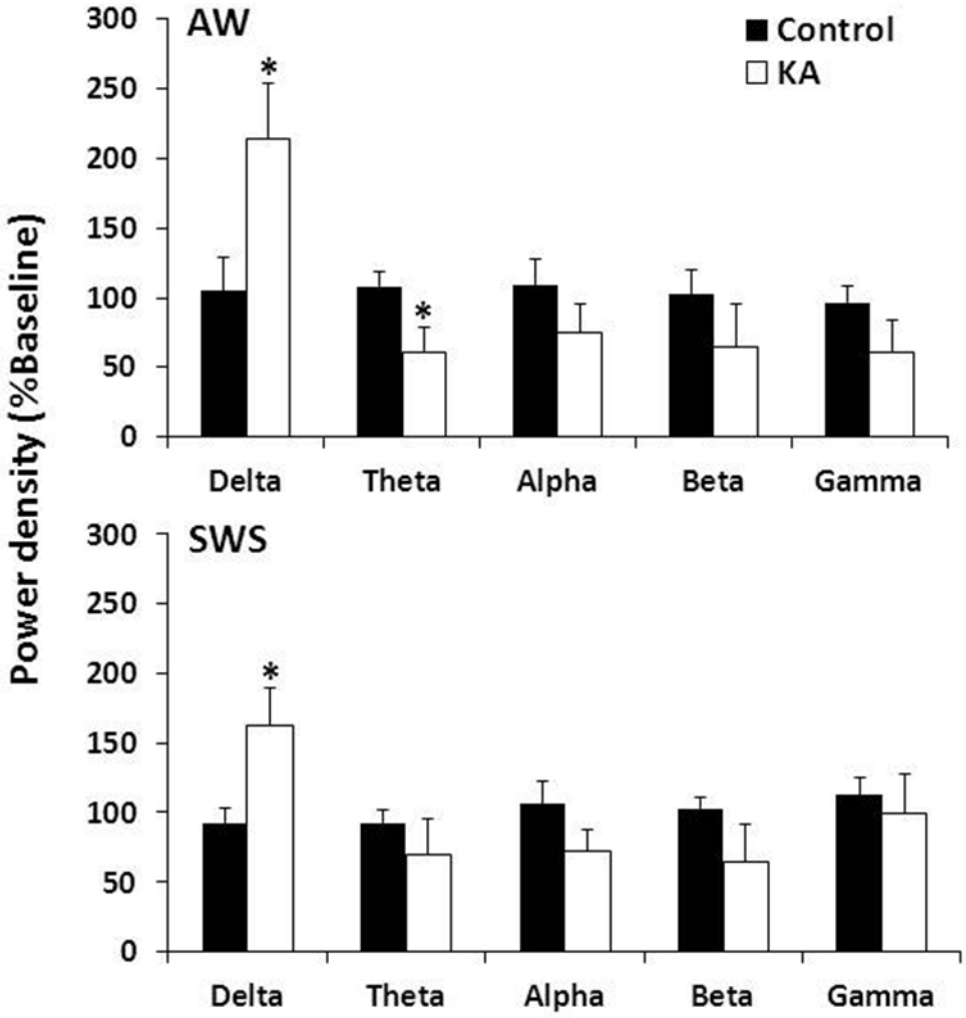

Fig. 4.4 Histogram shows mean of %baseline of power density in each band wave (delta, theta, alpha, beta and gamma) of awake stage and SWS stage. Data were evaluated from right parietal EEG. Data are expressed as mean ± S.E.M. of power density (%baseline). Effects of treatment were determined by using t-test, *p<0.05 compared with control data.

4.3.2. Acute effects of kainic acid on sleep patterns.

Hypnograms provide means to display a visual image of basic sleep-wake cycles (Fig. 4.5A). In this study, 2 parameters of sleep were particularly analyzed which included sleep latency and percentage of awake stage (AW), slow wave sleep stage (SWS) and rapid eyes movement sleep stage (REM) during 2-hr period recording (Fig. 4.5 B). The results showed that kainic acid exposure significantly decreased percentage of AW and REM stage and increased percentage of SWS stage; AW (KA=11.88±6.67 and control=29.56±3.49, p=0.039), REM (KA=1.49±1.67 and control=7.53±2.12, p=0.049) and SWS (KA=86.63±9.08 and control=62.91±4.89, p=0.044). The analysis of sleep latency show that kainic acid exposure significantly decreased latent period (KA=5.83±3.21 and control=38.91±13.24, p=0.036). Altogether, kainic acid exposure led to reduction of time spent on desynchronization but increase synchronization of brain wave. The enhancement of slow wave sleep was also observed in shortening of time spent before entering the first episode of sleep.

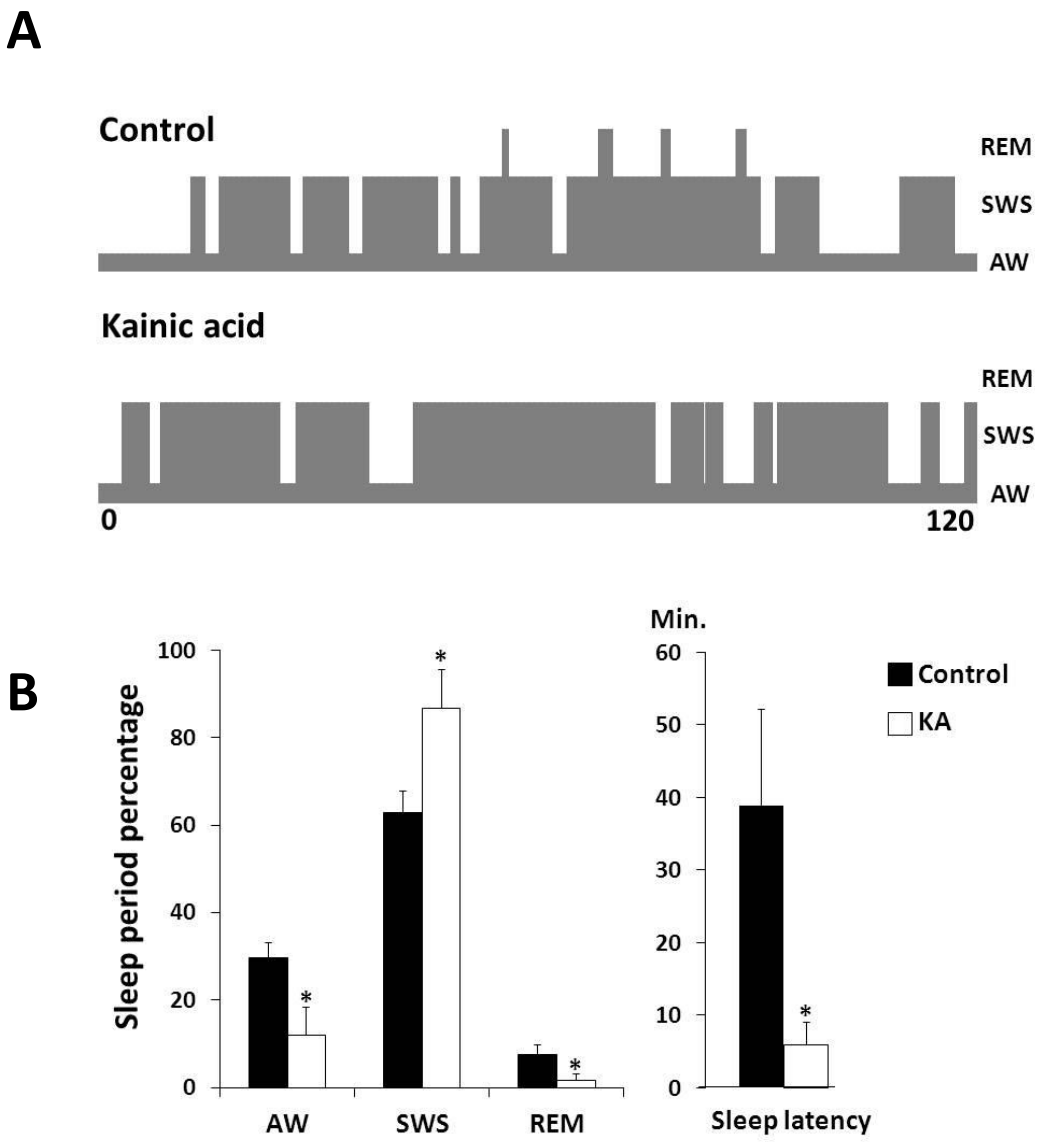

Fig. 4.5 (A) Hypnograms of example data from representative rat and provide a visual impression of sleep-wake period over 2 hrs. of EEG recording from normal rat and kainic acid induced neurodegenerative rats from day 7th after treatment. (B) Effect of kainic acid induced neurodegeneration on sleep period and sleep latency. Percentage of sleep period and sleep latency from EEG recording 2 hrs. on day 7 after treatment with kainic acid in induced neurodegenerative group (KA) and normal saline in control group. Mental stages were divided into 3 stages: awake stage (AW), slow wave sleep stage (SWS) and rapid eye movement sleep stage (REM). Data are expressed as mean ± S.E.M. of sleep period (%) and sleep latency (minutes). Effects of treatment were determined by using t-test, $p<0.05$.

4.3.3. Effects of kainic acid on spatial memory behavior.

Locomotors activities of kainic acid injected rats was significantly decreased, compared to that of normal rats (KA = 1.14±0.43 and control = 9.43±0.84, $p<0.001$) (Fig. 4.6). The number of entries of kainic acid group was lower than the criteria (more than 7 times in 5 min.) for Y-maze test. Therefore, Y-maze test showed that spontaneous alternation percentage (SA %) of the control rats was 84.49±9.94 while that of kainic acid injected rats not evaluated.

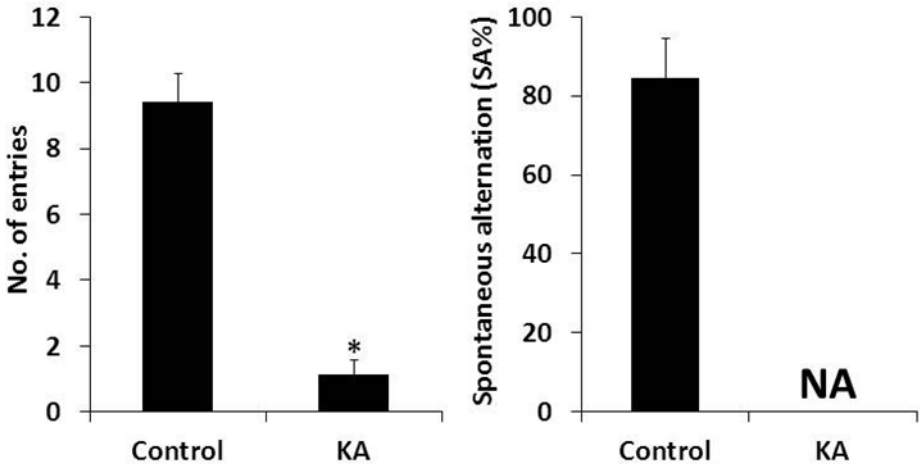

Fig. 4.6 Effects of kainic acid induced neurodegeneration on spatial memory behavior. Spatial memory behavior was measured on day 7 after treated with kainic acid in induced neurodegenerative group (KA) and normal saline in control group with Y-maze apparatus. Data analysis in terms of number of entries and spontaneous alteration percentage (SA%). Data are expressed as mean ± S.E.M. Effects of treatment were determined by using t-test, $p<0.05$.

4.3.4. Acute effects of kainic acid on brain structure.

The neurons were identified in selected areas of the hippocampus: CA1, CA2, CA3 and dentate gyrus (DG) (Fig. 4.7) and parietal cortex (PC). The results showed that density of neurons appeared to reduce in CA1 (Fig. 4.8 A), CA2 (Fig. 4.8 B), CA3 (Fig. 4.8 C) and DG (Fig. 4.8 D) and not changed in parietal cortex (Fig. 4.9). Statistical analysis revealed that number of neurons in CA1, CA3 and DG of hippocampus were significantly reduced in the kainic acid group (338.78±91.20 cell/mm2, 705.61±80.30 cell/mm^2, 507.05±138.57 cell/mm^2 and 1,107.69±144.87 cell/mm^2, respectively) compared to those of control group (1,103.93±122.02 cell/mm^2, 1,056.82±66.01 cell/mm^2, 1,295.02±92.98 cell/mm^2 and 1,703.18±139.30 cell/mm^2, respectively) ($p < 0.05$) (Fig. 4.10).

GFAP-ir astrocytes were also counted in these brain areas (Fig. 4.11 to 4.12). However, no significant change was found (Fig. 4.13).

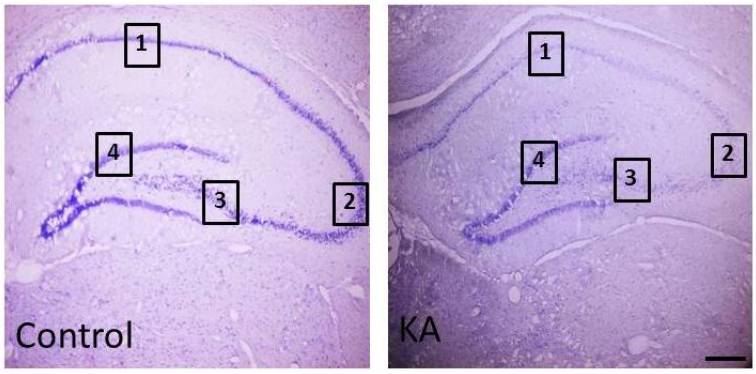

Fig. 4.7 Micrographs of a coronal section of hippocampus showing CA1 (1), CA2 (2), CA3 (3) and dentate gyrus (DG) (4) of control and kainic acid (KA), Bar= 40 µm.

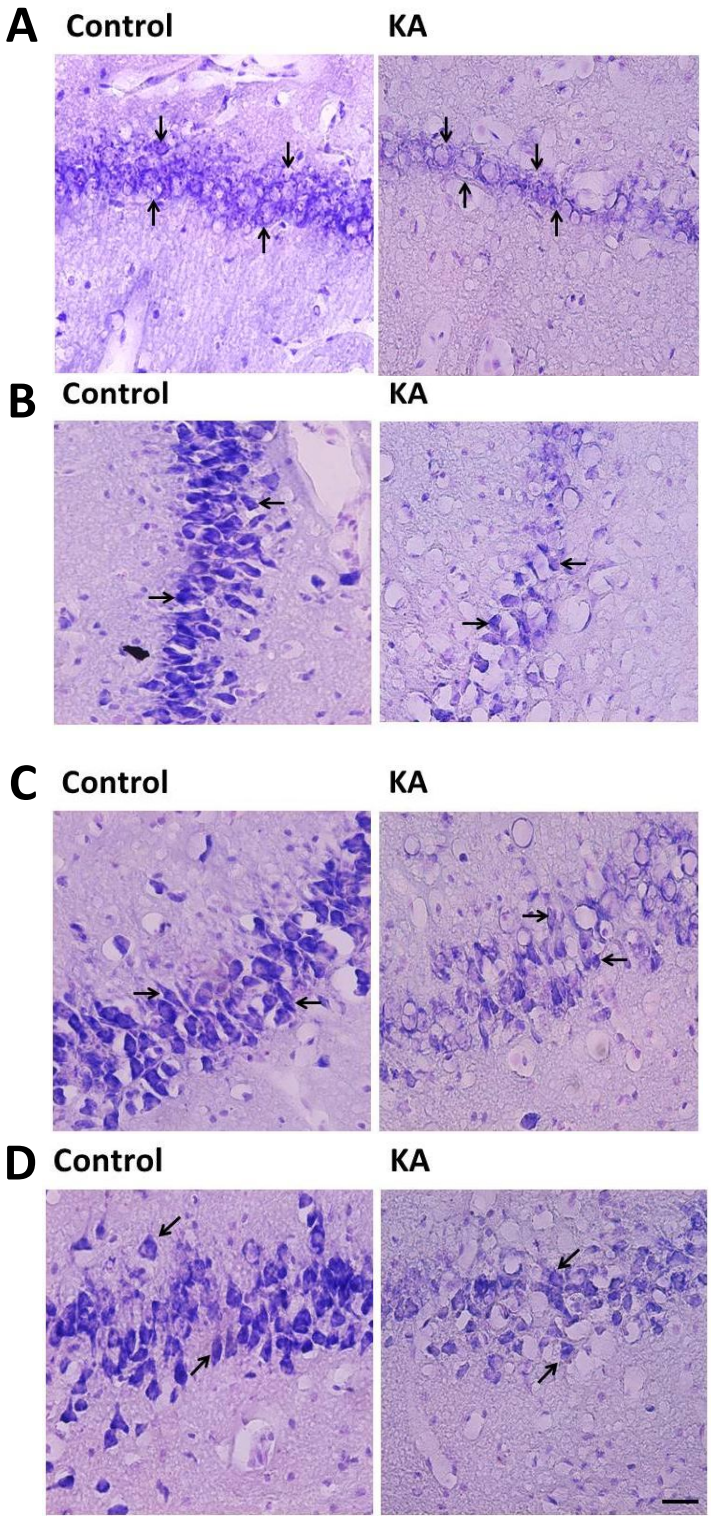

Fig. 4.8 Micrographs of (A) CA1, (B) CA2, (C) CA3 and (D) DG in hippocampus magnified from the framed area in figure 4.7 showing the cresyl violet positive neurons (arrows) in different treatment groups, Bar= 400 µm.

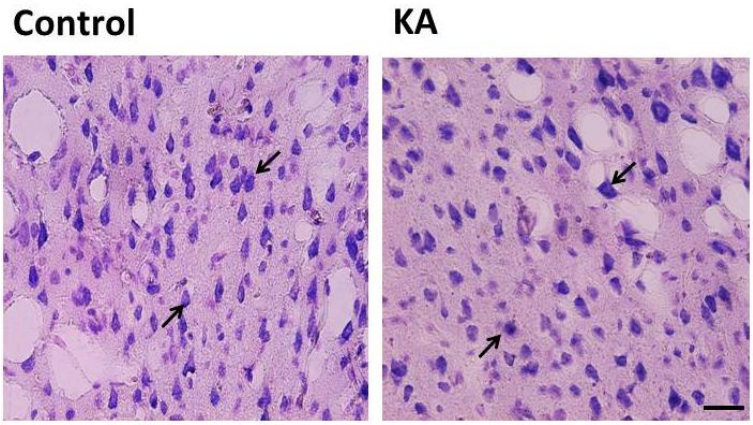

Fig. 4.9 Micrographs of cresyl violet positive neurons (arrows) in the parietal cortex in different treatment groups, Bar= 400 µm.

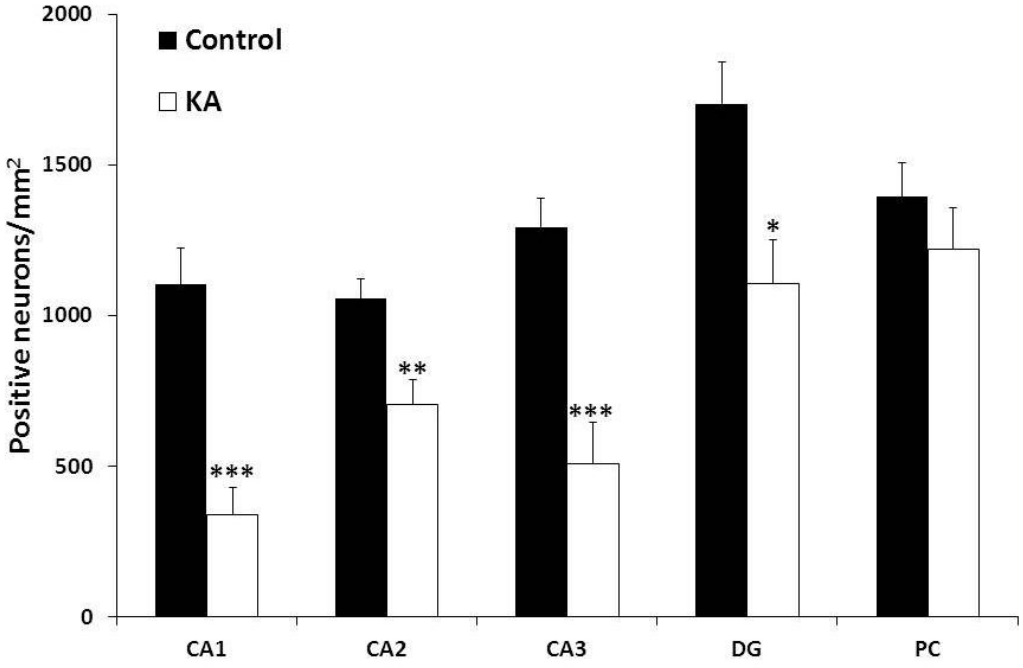

Fig. 4.10 Acute effects of kainic acid induced neurodegeneration on hippocampal and cortical neurons. The number of positive neurons in the CA1, CA2, CA3 and dentate gyrus (DG) of hippocampus and parietal cortex (PC) were measured on day 7 after treated with kainic acid in induced neurodegenerative group (KA) and normal saline in control group with nissl staining method. Data are expressed as mean ± S.E.M. Effects of treatment were determined by using t-test, *p<0.05, **p<0.01, ***p<0.001 compare with control group.

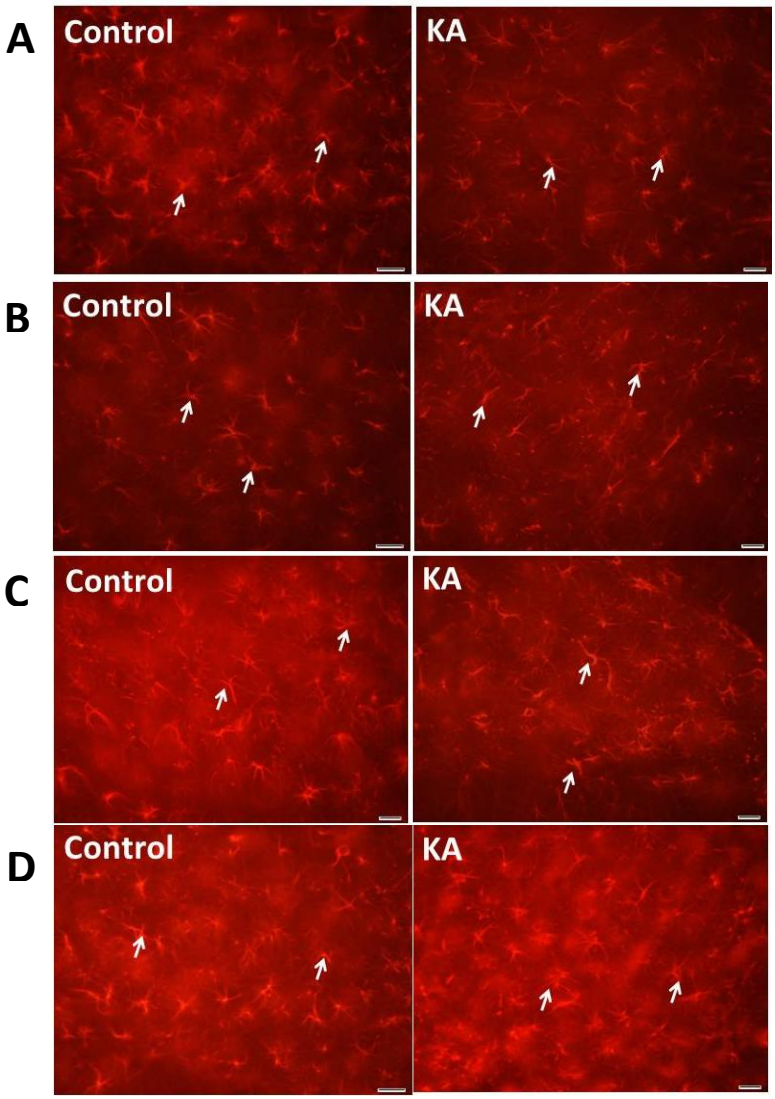

Fig. 4.11 Micrographs of GFAP-ir astrocytes (arrows) in **(A)** CA1, **(B)** CA2, **(C)** CA3 and **(D)** DG in hippocampus in different treatment groups, Bar= 400 µm.

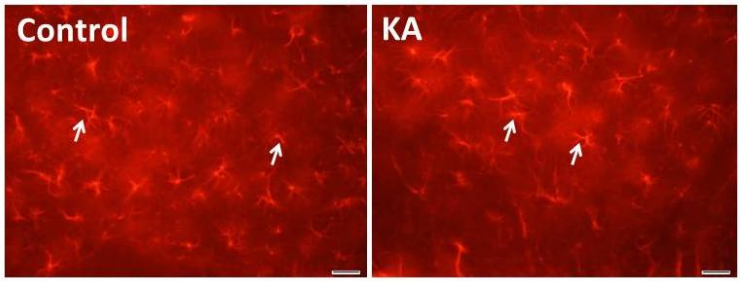

Fig. 4.12 Micrographs of GFAP-ir astrocytes (arrows) in parietal cortex in different treatment groups, Bar= 400 µm.

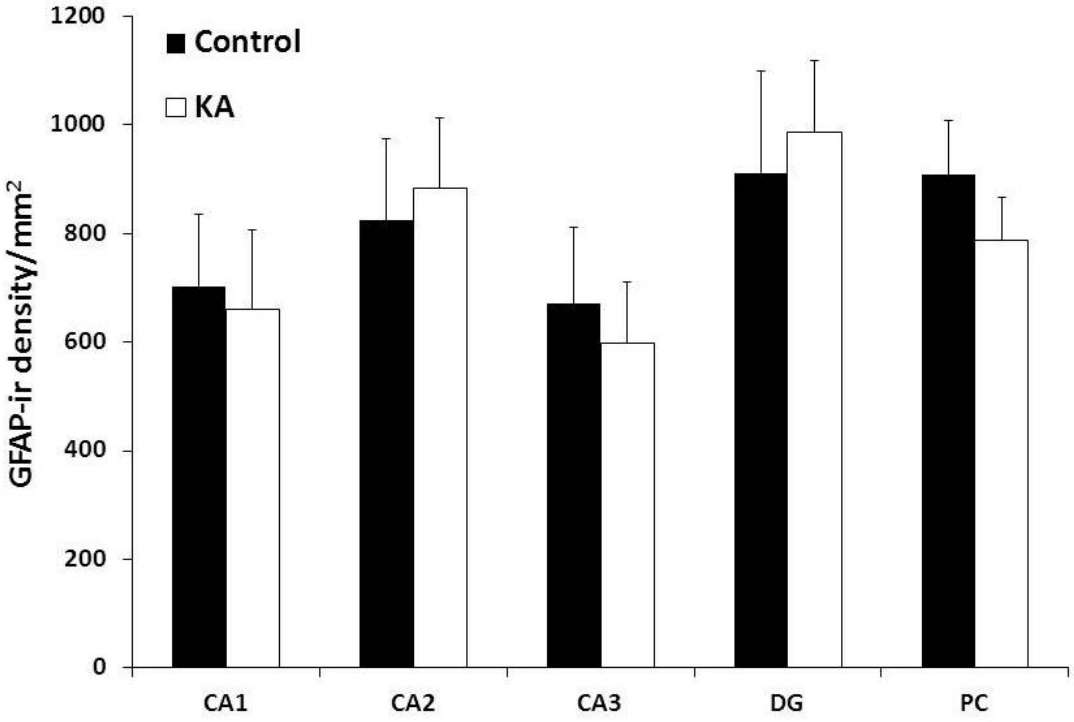

Fig. 4.13 Acute effects of kainic acid induced neurodegeneration on hippocampal and cortical astrocyes. The GFAP-ir density in the CA1, CA2, CA3 and dentate gyrus (DG) of hippocampus and parietal cortex (PC) were measured on day 7 after treated with kainic acid in induced neurodegenerative group (KA) and normal saline in control group with GFAP immunofluorescence staining method. Data are expressed as mean ± S.E.M. Effects of treatment were determined by using t-test,* $p<0.05$ compare with control group.

4.3.5 The Correlations among EEG patterns, spatial memory behavior and brain structures in kainic acid induced neurodegenerative rats

To have an overview of kainic acid effects on neurodegeneration, correlations between score of spatial memory behavior and factors of brain histology or electrical brain activity were evaluated by using linear regression analysis. However, numbers of entries were used instead of SA% as Y-maze test was not performed due to minimal movement of animals produced by kainic acid. The data were shown in R-square score and considered statistically significant at $p<0.05$. From the previous data, EEG patterns, spatial memory behavior and brain histology exhibit significant change of 12 factors and all of factors were evaluated the correlation. Among EEG frequencies, Delta activity during awake period was found to have significant correlation with number of entries (Table 2). When analyzed in terms of time spent in each specific brain state, significant correlations with number of entries were observed for total awake and SWS percentages but not that of REM. Sleep latency also exhibited strong correlation with number of entries. The regression also revealed strong correlations between numbers of entries and density of neurons in the areas CA1 and DG but not CA2 and CA3. The correlations are particularly shown with R-square values for Delta activity (Fig. 4.14) brain state parameters (Fig. 4.15) and densities of neuronal cells (Fig. 4.16).

Table 2 R-square data of correlation among EEG patterns, spatial memory behavior and brain histology in kainic acid induced neurodegenerative rats, * $p<0.05$.

Correlation with Number of entries		**R^2**	***p*-value**
Brain histology	Positive neuron CA1	0.529*	0.007
	Positive neuron CA2	0.117	0.276
	Positive neuron CA3	0.316	0.057
	Positive neuron DG	0.463*	0.015
EEG activity	Delta activity AW	0.340*	0.033
	Theta activity AW	0.300	0.059
	Delta activity SWS	0.259	0.063
Sleep patterns	AW period%	0.570*	0.005
	SWS period%	0.599*	0.003
	REM period%	0.220	0.123
	Sleep Latency	0.409*	0.025

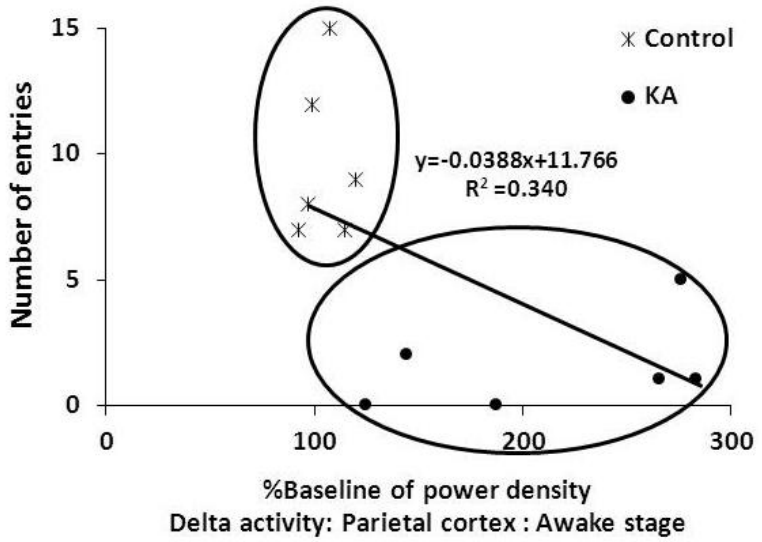

Fig. 4.14 Linear regression analysis between number of entries and delta activity from parietal EEG in awake stage, data were evaluated form normal rats (control) and kainic acid treated rats (KA). Each correlation was expressed as R-square (R^2) and linear equation.

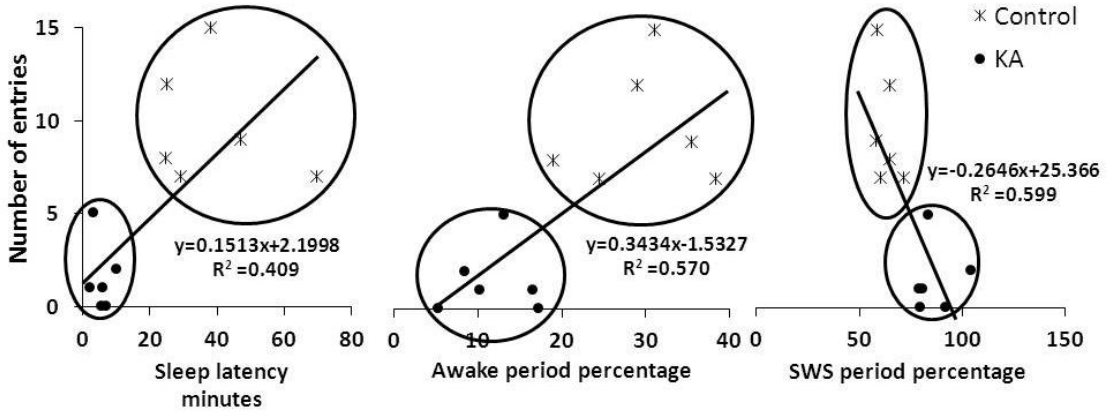

Fig. 4.15 Linear regression analysis between number of entries and sleep index; sleep latency, awake period percentage and slow wave sleep period (SWS) percentage. Data were evaluated form normal rats (control) and kainic acid treated rats (KA). Each correlation was expressed as R-square (R^2) and linear equation.

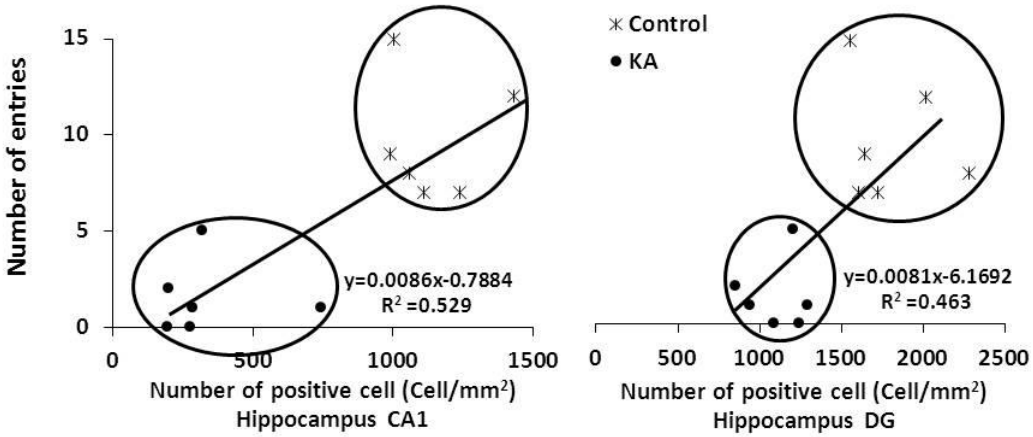

Fig. 4.16 Linear regression analysis between number of entries and positive neurons in hippocampus CA1 and dentate gyrus (DG) area, data were evaluated from normal rats (control) and kainic acid treated rats (KA). Each correlation was expressed as R-square (R^2) and linear equation.

4.4 Discussions

4.4.1 Effects of kainic acid on EEG power.

Kainic acid (KA) was commonly used to induce neurodegenertion in epilepsy model of previous studies. Activation of postsynaptic kainate receptors by kainic acid generates an excitatory postsynaptic current that leads to the cumulative depolarization of the postsynaptic membrane. The over activation of kainate receptors by kainic acid leads to excessive calcium ion influx inside the neuronal cell resulting in neuronal damage defined excitotoxicity (Routbort et al., 1999). Kainate receptors are involved in KA-induced neuronal damage in several cell types in cortical and hippocampal neurons by changing intracellular calcium concentration (Verdaguer et al., 2002). The result of over activation is neuronal loss especially in the hippocampus (Kim et al., 2011). In this study, the resting EEG of kainic acid-induced rats showed an increase of delta activity in awake and slow wave sleep stage, compared to that of control animals. This may be linked with mechanisms involved in epilepsy-associated tissue damage. Alteration of delta activity have been described as a consequence of numerous cerebral pathology of brain damage and the increase in delta activity is concurrent with underlying development of brain lesion (Carpentier et al., 2001). In addition, the analysis of parietal EEG showed that kainic acid significantly decreased theta oscillation in awake stage. The hippocampus generates some of the largest EEG signals of any brain structure and the EEG signal is dominated by regular waves at 4–10 Hz. This EEG pattern is known as the hippocampal theta rhythm (Grunwald et al., 2007). Thus, the reduction of hippocampal neurons may interfere on theta activity. Moreover, the EEG signal analysis in rats shows that hippocampal theta appears when a rat is engaged in active motor behavior such as walking or exploratory sniffing, and also during REM sleep (Vyazovskiy and Tobler, 2005).

4.4.2. Effects of kainic acid on sleep patterns.

In dementia, the sleep disruptions (e.g., increased number of nighttime awakenings after falling asleep, lower sleep efficiency, increased daytime napping, changes in the amount of rapid eye movement (REM) and non-rapid eye movement (NREM) sleep increase as the dementia progresses in severity (Cole and Richards, 2006; Jan et al., 2010). In this study, kainic acid exposure decreased percentages REM sleep. In general, the reduction of REM sleep related with the decrease of neurons in the locus coeruleus and in cingulate cortex and hippocampus. The decreases in cell proliferation or neuronal dysfunction are related to a reduction in REM sleep, whereas a reduction in the number of cells that subsequently develop into adult neurons may be related to a reduction of REM sleep (Lu et al., 2000; Meerlo et al., 2009). In addition, kainic acid treated rats showed the increase of slow wave sleep period (SWS), the decrease of awake period (AW) and latent period. The period of SWS, AW and sleep latency are related. The present data demonstrated that kainic acid treated rat exhibited the increase of delta power activity. The increase of delta activity is related with stage 3 of NREM sleep or SWS (Darchia et al., 2007). Synchronization of the EEG during SWS depends on thalamic as well as intrinsic cortical oscillators and the firing rate of cortical neurons has generally been reported to be reduced during NREM relative to wakefulness and REM. On the other hand, low activity of these neurons either neuronal loss or dysfunction would in a retain brain stage mostly in SWS not switch over to wakefulness and REM (Binder et al., 2014; Morairty et al., 2013).

4.4.3. Effects of kainic acid on spatial memory behavior.

Numbers of entries to each arm of Y-maze apparatus refer to the exploration and locomotor activity. The exploration performance, depend on locomotor activity, is the first parameter used to evaluate spatial memory behavior. In the results of this study, 7-day i.c.v. injection of kainic acid (KA) was found to decrease number of entries. The major target of KA is hippocampal neurons which exhibit high density of glutamate receptor (Chen et al., 2004). Hippocampus is necessary for the display of normal exploratory movements. The absence of exploration in hippocampal lesion rats was discussed in relation to severe hippocampal dysfunction (Clark et al., 2005). In addition, the previous study reported that intrahippocampal administration of KA significantly impaired locomotor activity and memory performance (Kumar et al., 2011). However, the first day after kainic acid injection, rats exhibited the seizure-like activity such as increase signs of aggression and high locomotor activity. KA, as a nondegradable analog of glutamate, is 30-fold more potent in neurotoxicity than glutamate as it binds and stimulate kainate receptor with a very long period (Wang et al., 2005; Wolter et al., 2014). The rats repeated the experience of seizures by strongly administration with KA in a dose sufficient to trigger a seizure-related brain damage. The severity of seizures is a major cause of severity in neuronal damage and neuronal loss through extreme excitotoxicity. The strongly neurodegenerative induction have an effect on abnormal locomotor performance.

4.4.4. Effects of kainic acid on brain histology.

The densities of neuron were reduced in CA1, CA2, CA3 and DG of the hippocampus. KA administered in rats through systemic or i.c.v. routes has long been known to produce hippocampal neuronal loss (Bardgett et al., 1995; Montgomery et al., 1999). It has been shown to increase production of reactive oxygen species, mitochondrial dysfunction, and apoptosis in neurons in many regions of the brain, particularly in the hippocampal subregions of CA1 and CA3, and in the hilus of dentate gyrus (DG) (Wang et al., 2005). Moreover, activation of kinate receptor by KA has been shown to elicit a number of cellular events, including the increase in intracellular Ca^{2+}, production of ROS, and other biochemical events leading to neuronal cell death or excitotoxicity induce cell death (Sun et al., 1992).

4.3.5 The correlations among EEG patterns, spatial memory behavior and brain histology.

Within the model of kainic acid-induced neurodegeneration, the relationship between increase of delta power activity and the change of sleep pattern is sensible. Delta power activity particularly maintains the brain activity in slow wave sleep (SWS). Thus, the increase of delta power activity is directly related with increase of SWS period percentage. In addition, theta power activity is a predominant oscillation in rapid eye movement (REM) sleep, so that the reduction of theta signal correlates with the loss of REM period. Thus, the increase of SWS period rightfully correlates with the decrease of awake period and sleep latency. The reduction of number of entries correlated with the increase of delta power activity which promote the brain stage maintain in SWS, indicating that rats are in non-active brain stage and showed the low exploration and locomotor behavior.

4.5 Conclusion

Basically, the intracerebroventricular injection of kainic acid to induce neurodegeneration has been extensively used for epilepsy induction. In this study, even higher concentration of kainic acid than that for epilepsy study was used in order to ensure brain damage through excitotoxicity. In particular, the impact was rather direct to the hippocampus through glutamate receptors which were present in relatively high density on hippocampal neurons. The present data were consistent to previous reports in that loss of hippocampal neurons was dramatically obvious. Moreover, these histological findings were positively correlated to behavioral results. Animal's locomotor activity and exploratory behaviors were severely affected. They are essential components of learning and memory processes.

The analysis of electrical brain wave highlighted that hippocampus-specific frequency range which is theta band wave was clearly reduced. This is specific to kainic acid treatment whereas other types of induction usually increase slow wave activity following degeneration of many types of neurons in the brain.

It means that the method used in this study had the hippocampus as a major target. Brain wave oscillations obtained from rats treated with kainic acid were likely to reflect changes related to hippocampal damage. Thus, these specific brains oscillatory might be recognized as EEG biomarkers of neurodegeneration.

CHAPTER 5

THE COMPARISON EEG PATTERNS

AMONG

DEXAMETHASONE INDUCED RATS,

KAINIC ACID INDUCED RATS

AND AGING RATS

5.1 Experimental protocol

Animals were randomly divided into 2 groups, with 6-8 rats in each group. The control group was normal rats (3-4 months old) without any drug treatment. The aging group had aging rats (21-22 months old) also without any drug treatment. At some points, data of these two groups were compared to that of chronic dexamethasone (Dx) and kainic acid (KA) induced neurodegeneration group previously described.

In Aging group, rats were implanted with electrodes for EEG recording. After recovery period, they were habituated with recording chamber and EEG recording system for 3 days before recording. EEG recording was performed for 2 hrs. on the last testing day. After 18 months, rat's EEG was recorded and they were tested for spatial memory behavior with Y-maze apparatus (Fig 5.1).

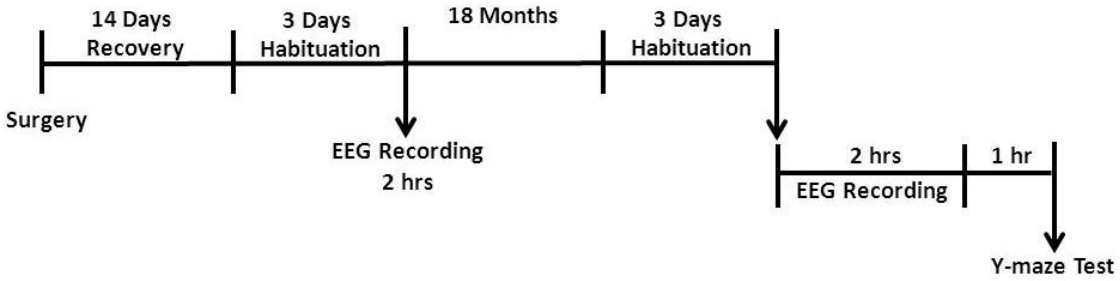

Fig. 5.1 Schematic diagram of protocol for examination of the effect of aging on neurodegenration.

5.2 Data analysis

For EEG analysis, powers of frontal and parietal EEG of control and aging rats were calculated and converted into percentages of total power of each power band for individual rat. Therefore, all data in each group were averaged and expressed as mean ± S.E.M. Differences between groups were considered using one-way ANOVA, followed by Student-Newman-Keuls method and $p < 0.05$ was considered statistically significant.

5.3 Results

5.3.1 The comparisons among EEG powers of dexamethasone induced rats, kainic acid induced rats and aging rats

The electrical brain oscillations were analyzed EEG powers from 2 hrs recording. EEG power spectrum was expressed in 5 frequency bands. One-way ANOVA of frontal EEG power revealed significant difference among control, aging and Dx group in delta frequency [$F(21,2)=11.015$, $p<0.001$] (Fig. 5.2). Parietal EEG analysis revealed significant differences in delta frequency [$F(27,3)=24.044$, $p<0.001$] with the specific comparison between control and KA groups and also in theta frequency [$F(27,3)=19.276$, $p<0.001$] with the specific comparison among control, Dx and KA groups (Fig. 5.3).

The EEG powers of awake state (AW) and slow wave sleep stage (SWS) was separately analyzed. Each stage was selected for 5-min continuous recording when they first appeared. From frontal EEG analysis, significant difference was found only in Delta frequency for both awake stage and slow wave sleep stage in aging AW=[$F(21,2)=4.120$, $p=0.033$]and SWS=[$F(21,2)=4.271$, $p=0.029$] (Fig. 5.4).

Parietal EEG analysis confirmed only significant changes in KA group on comparison to control group for both awake and SWS stages. During both stages, KA was found to elevate Delta AW=[$F(27,3)=4.938$, $p=0.008$] but suppress Theta power AW=[$F(27,3)=4.076$, $p=0.018$] and SWS=[$F(27,3)=4.497$, $p=0.012$]. No significant change was detected in aging and Dx groups (Fig. 5.5).

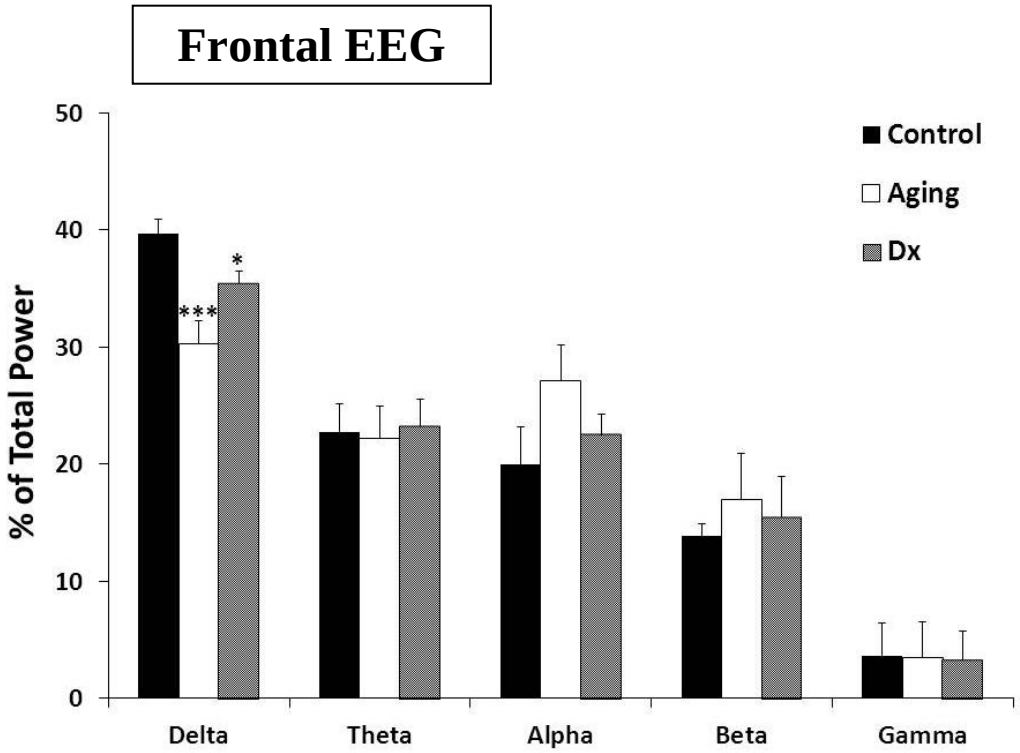

Fig. 5.2 Frontal EEG powers are shown in percentage of total power and comparison with control group. The power activities were evaluated from 2 hrs. Data analysis was classified base on 5 frequency bands: delta, theta, alpha, beta and gamma. Data are expressed as mean ± S.E.M. and differences between groups were considered using one-way ANOVA, followed by Student-Newman-Keuls method, *p<0.05 and ***p<0.001 compare with control group.

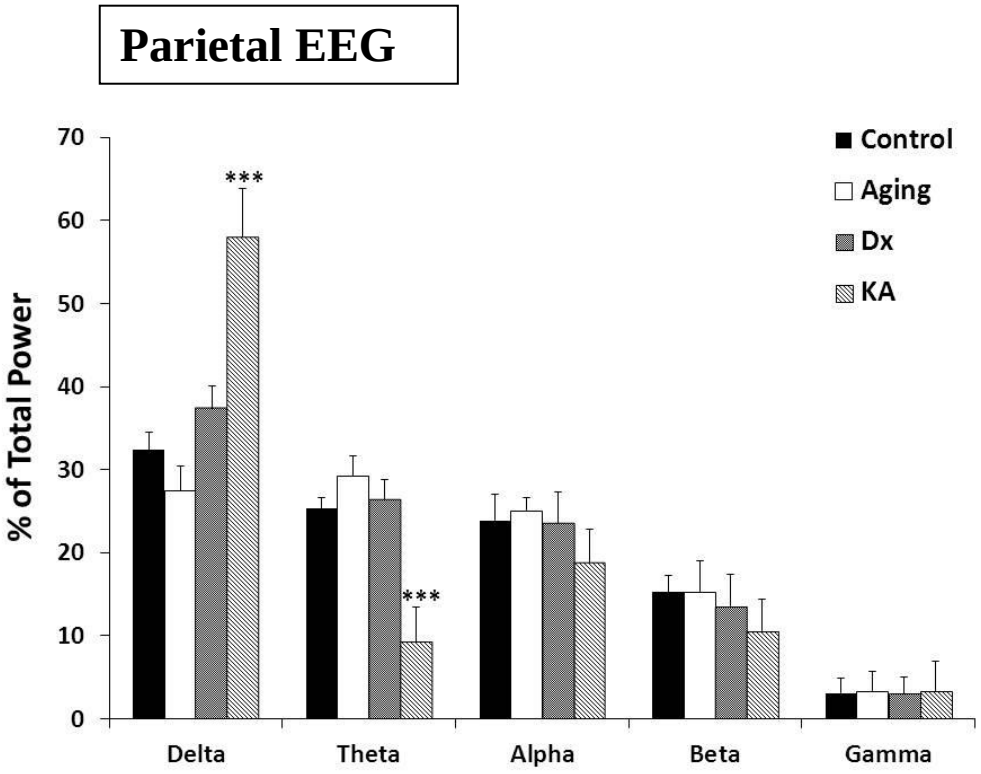

Fig. 5.3 Parietal EEG powers are shown in percentage of total power and comparison with control group. The power activities were evaluated from 2 hrs. Data analysis was classified base on 5 frequency bands: delta, theta, alpha, beta and gamma. Data are expressed as mean ± S.E.M. and differences between groups were considered using one-way ANOVA, followed by Student-Newman-Keuls method, $^{**}p<0.01$ and $^{***}p<0.001$ compare with control group.

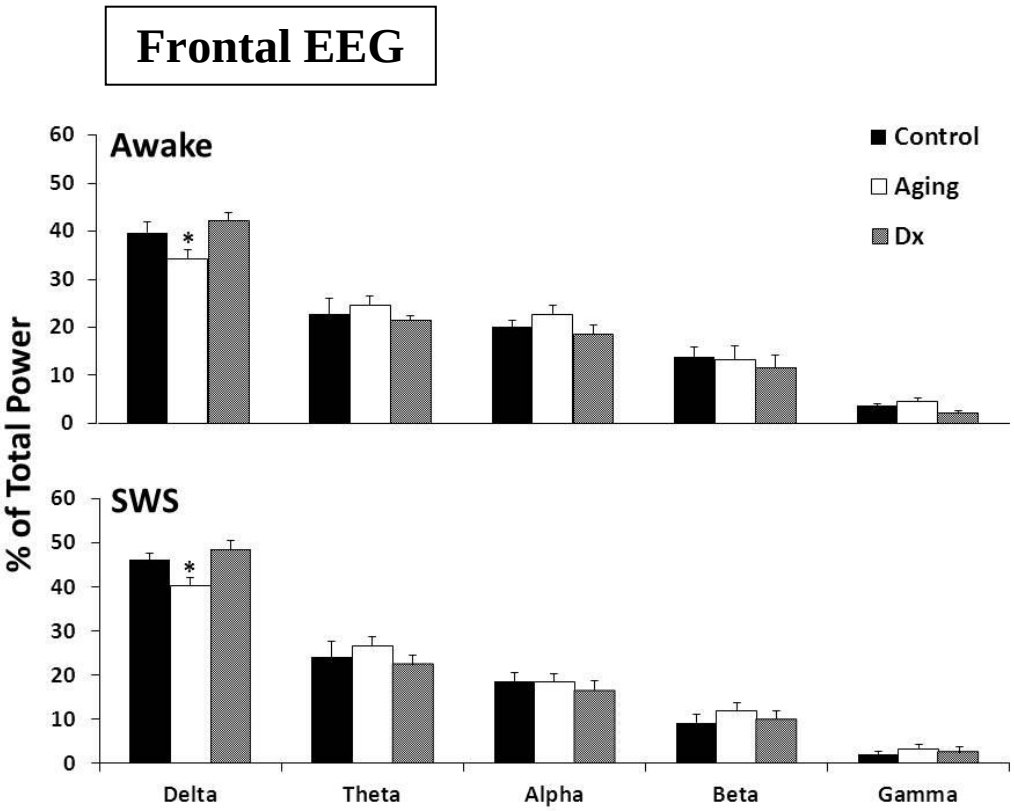

Fig. 5.4 Histogram shows mean of total power percentage in each band wave (delta, theta, alpha, beta and gamma) of awake (AW) stage and slow wave sleep (SWS) stage, the data were evaluated from frontal EEG. Data are expressed as mean ± S.E.M. and differences between groups were considered using one-way ANOVA, followed by Student-Newman-Keuls method, *p<0.05 compare with control group.

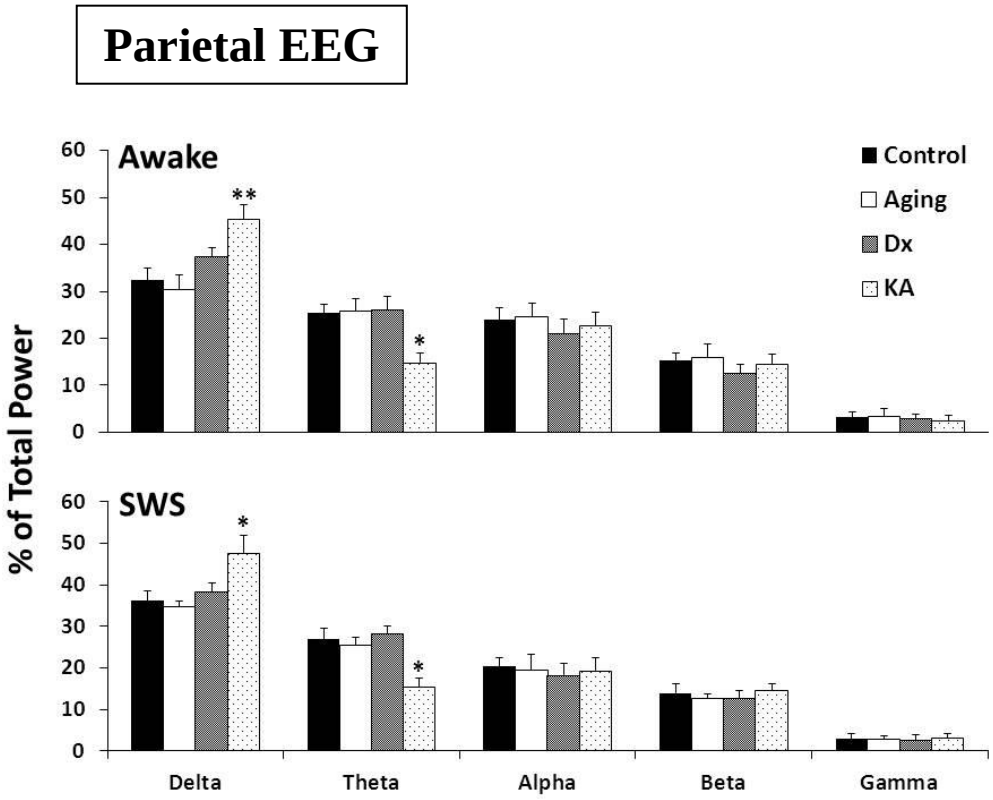

Fig. 5.5 Histogram shows mean of total power percentage in each band wave (delta, theta, alpha, beta and gamma) of awake (AW) stage and slow wave sleep (SWS) stage, the data were evaluated from parietal EEG. Data are expressed as mean ± S.E.M. and differences between groups were considered using one-way ANOVA, followed by Student-Newman-Keuls method, *p<0.05 and **p<0.01 compare with control group.

5.3.2 Comparisons among sleep patterns of dexamethasone induced rats, kainic acid induced rats and aging rats

Two parameters of sleep were particularly analyzed which included sleep latency and percentage of each brain stages during 2-hr period recording. It was found that kainic acid significantly reduced sleep latency when compared to the control values (control=38.91±13.24 and KA=5.83±3.21, p=0.036) (Fig. 5.6 A). No change was observed in aging and Dx groups. When each stage was separately analyzed, kainic acid significantly increased percentage of SWS stage (control=62.91±4.89 and KA=86.63±9.08, p=0.044) and decreased percentage REM sleep stage (control=6.42±0.59 and Dx=1.22±2.04, p=0.005). Altogether, aging had no effect on percentage of sleep period in all brain stages (Fig. 5.6 B).

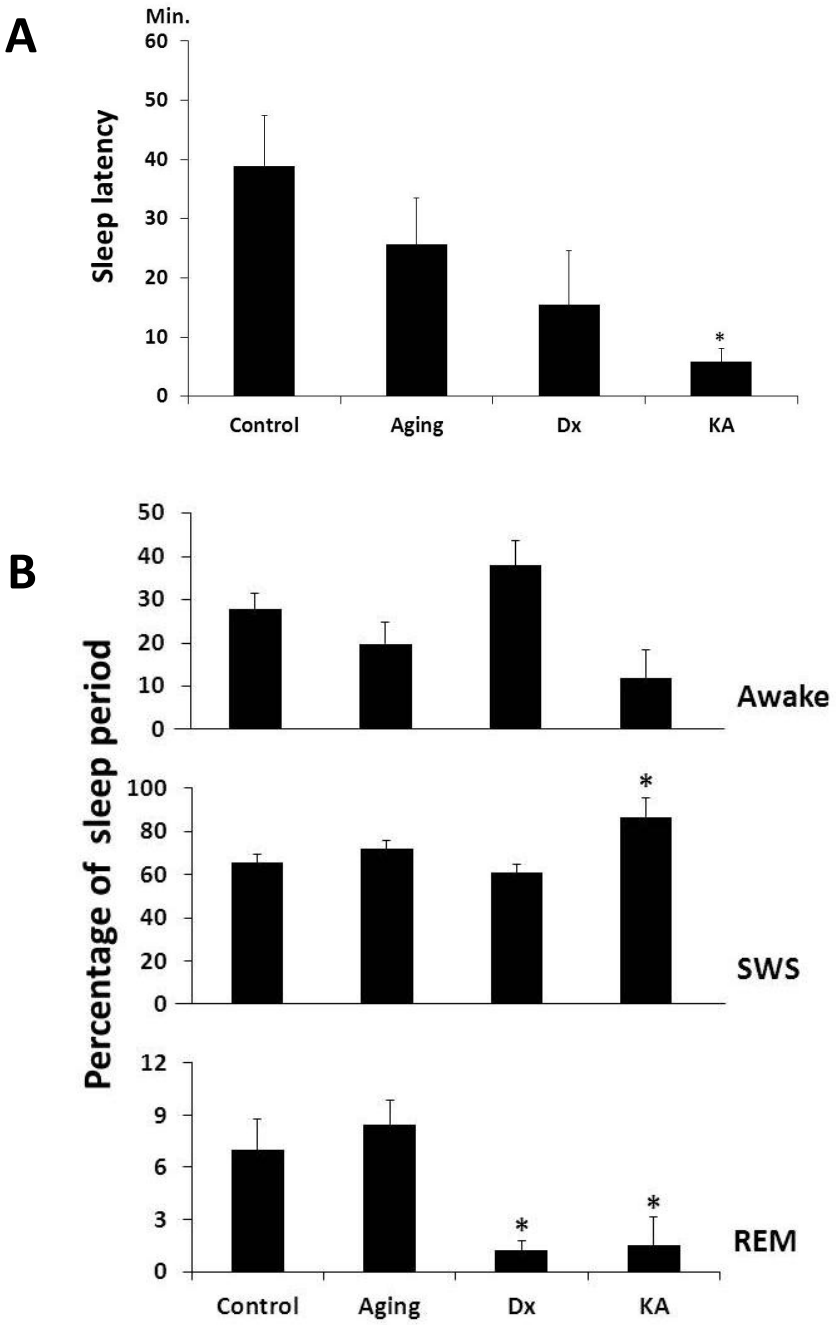

Fig. 5.6 The effects of neurodegeneration models on sleep patterns. Data were analyzed in terms of **(A)** sleep latency **(B)** percentage of sleep period. Data are expressed as mean ± S.E.M. and differences between control group and treated group in each model were determined by using t-test, p <0.05 and differences between groups of all model were considered using one-way ANOVA, followed by Student-Newman-Keuls method,*p<0.05 compare with control group.

5.3.3 Comparisons of EEG spindles between dexamethasone induced rats and aging rats

Two main types of spindles were characterized. They are sleep spindles and non sleep spindles described previously. The numbers of EEG spindles were evaluated from 2-hr period of EEG recording. Aging and Dx groups did not show any significant difference for both spindle types. Significant changes were found when dexamethasone increased number of non sleep spindle in awake stage [$F(21,2)=4.312$, $p=0.029$] and slow wave sleep stage [$F(21,2)=9.728$, $p=0.001$] (Fig. 5.7).

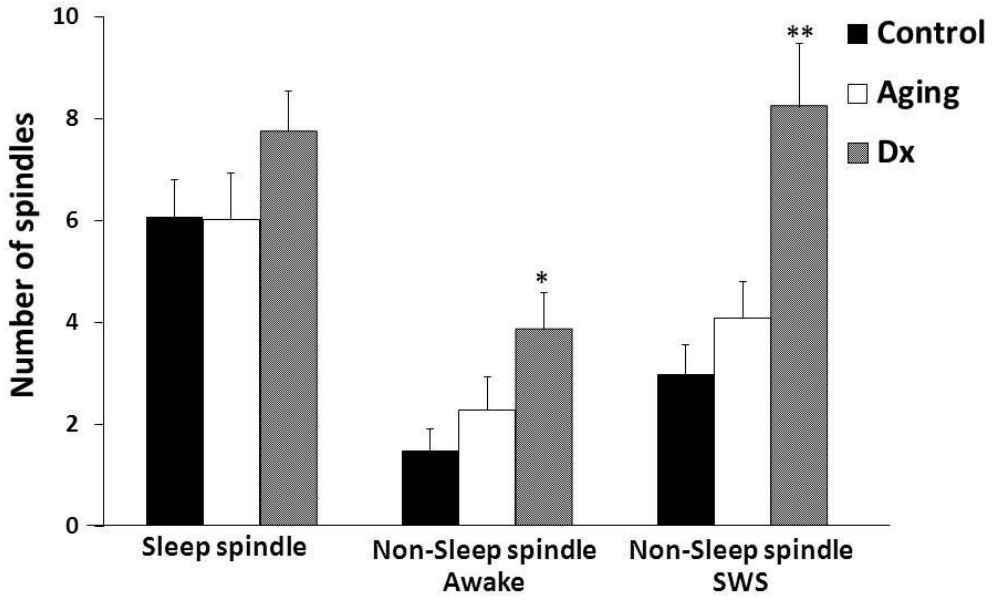

Fig. 5.7 Comparisons of spindles from 2 different neurodegeneration models and control group. Numbers of EEG spindles were counted from 2-hour EEG recording. EEG spindles were divided into 2 types from EEG spectrogram, non sleep spindle (6-10 Hz) and sleep spindle (10-14 Hz). Non sleep spindle analysis were separated into 2 stage, awake stage (AW) and slow wave sleep stage (SWS). Data are expressed as mean ± S.E.M. and differences between groups were considered using one-way ANOVA, followed by Student-Newman-Keuls method,*$p<0.05$ and **$p<0.01$ compare with control group.

5.3.4 Comparisons among spatial memory behaviors of dexamethasone induced rats, kainic acid induced rats and aging rats

Spatial memory behavior were evaluated from number of entries of a rat through each arm of Y-maze. The analysis of number of entries revealed significant decrease induced by kainic acid [$F(27,3)=14.177$, $p<0.001$] (Fig. 5.8 A). However, Y-maze test showed significant reduction in SA% in aging and Dx groups [$F(21,2)=4.125$, $p=0.033$] while that of kainic acid group was not evaluated due to insufficient movement of animals (Fig. 5.8 B).

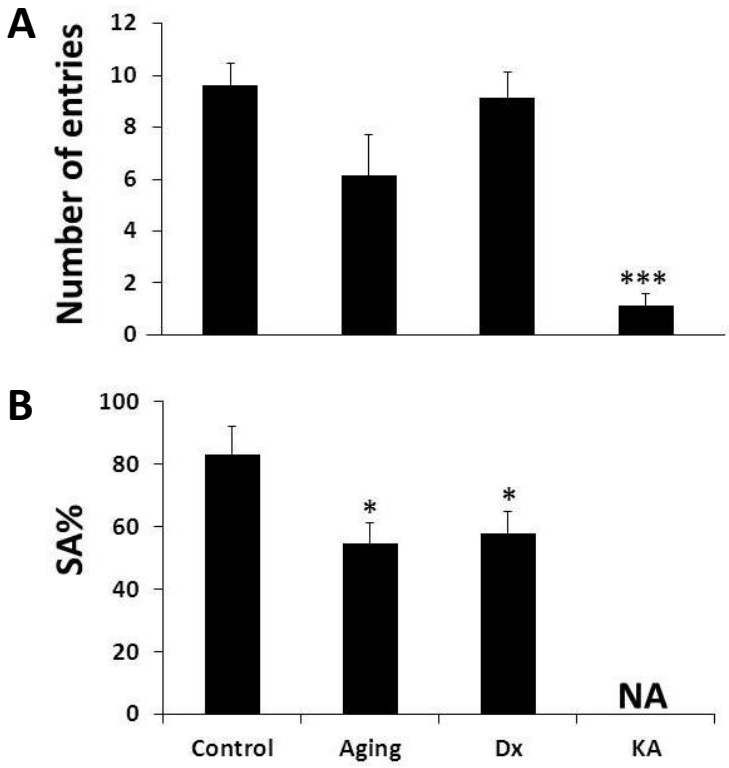

Fig. 5.8 The effects of neurodegeneration models on spatial memory behavior. Data were analyzed in terms of (A) number of entries and (B) spontaneous alteration percentage or SA%, data are expressed as mean ± S.E.M. and differences between groups were considered using one-way ANOVA, followed by Student-Newman-Keuls method, *$p<0.05$ and ***$p<0.001$ compare with control group.

5.4 Discussion

The percentage of total power demonstrates the proportion of power in each band wave compared with total power. The percentage of total power in delta band from frontal EEG was decreased in aging rats. When EEG during awake state (AW) and slow wave sleep stage (SWS) were analyzed separately, frontal delta power was found to be decreased both during awake stage and SWS stage of aging rats. Previously, EEG delta activity was commonly declined in the older group (Munch et al., 2004). Besides the absolute amplitude and absolute power of delta band were lower in aging human (aged 60 and over) than in young human (aged 20–39 years) (Hartikainen et al., 1992).

Aging is often accompanied by learning and memory problems, many of which resemble deficits associated with hippocampal damage (Driscoll et al., 2003). Age-related structural alterations in the hippocampus have been identified with diverse methods and the hippocampal formation especially vulnerable to the effects of aging. Obviously, rodents with hippocampal damage have striking impairments in learning and remembering spatial information (Morris et al., 1982).

In summary, spontaneous aging were found to have similar changes to that of neurodegeneration. In particular, the hippocampus was found to have neuronal loss that might affect behavior and finally cognitive performance. However, from the present study, electrical brain oscillation in aging animals was unique from that induced by chronic stress and excitotoxicity. This indicates that, with the use of EEG technique, the analysis of brain histology and function is critical to obtain essential details much better than any other techniques. At least, it was precise enough to distinguish electrical patterns of 3 different models. The approach to studying changes in brain oscillation, EEG technique is utilized to improve the test's ability to distinguish specific character of brain changes among different models of neurodegeneration.

5.5 Conclusion

Aging is one of critical factors that affect efficiency of the central nervous system. Neurodegeneration is commonly found in aging. However, levels of severity are dependent on individual conditions such as complicate health problems or brain damage from other pathologies. Previous studies have reported great consistency of hippocampal neuronal loss that contributes to dementia in aging. In terms of histology, brain change in aging might be viewed as same as found in other types of neurodegeneration.

However, in this study, the analysis of control and aging EEG signals clearly showed unique patterns of aging electrical brain wave in comparison to neurodegeneration induced in chronic stress and acute excitotoxicity. This particularly highlighted the advantage of EEG study that can distinguish specific patterns of neurodeneration among different methods. The details of these findings are relatively impractical to obtain from histological or behavioral studies.

GENERAL CONCLUSION

Ultimately, ideal strategy is to develop a new test that predicts neurodegeneration with high accuracy. It is critical to identify people who might be at risk. When people reach a stage of dementia, most of treatments seem to be ineffective. The main reason is that they are considered to be too far advanced in their diseases to be helped. Thus, detecting the early signs and giving early intervention before the brain is severely damaged could perhaps slow or stop the progress of the neurodegeneration.

From findings of this study, it can be clearly concluded that pattern of electrical brain wave, learning and memory behavior and brain histology of rats with induced neurodegeneration were significantly correlated. The data gave better understanding of prognosis of neurodegeneration. In particular, the analysis of specific EEG pattern gave biomarkers that predict histological change and learning behavioral dysfunction.

One of the advantages of EEG study for neurodegenerative research is that brain oscillation can be detected and monitored early enough in comparison to behavioral observation or loss of motor skills. This technique is sensitive to detect changes in electrical brain activity when pathology starts and well before loss of brain cells. It is also practical to track the progression of the diseases. This would allow preventing and help design for treatment strategy. In addition, treatment is likely to have the best outcome when the diseases are not too advanced and the brain damage is not severe. In general, neurodegeneration is detected when afflicted people are at the stage of dementia. No sufficient satisfaction has been made. It is unlikely that there would be effective medication for the diseases when neuronal loss already proceeds. So far, the development of a new test with high ability to identify those at risk is critical. It would be able for population screening and long-term preventive treatment. Ultimately, EEG technique is suitable for the application to address neurodegeneration.

REFERENCES

Abraham, I., Juhasz, G., Kekesi, K. A., and Kovacs, K. J. 1996. Effect of intrahippocampal dexamethasone on the levels of amino acid transmitters and neuronal excitability. *Brain Res.* 733(1): 56-63.

Abraham, I. M., Harkany, T., Horvath, K. M., and Luiten, P. G. 2001. Action of glucocorticoids on survival of nerve cells: promoting neurodegeneration or neuroprotection? *J. Neuroendocrinol.* 13(9): 749-760.

Algimantas Juozapavi□cius, Gytis Bacevi□cius, Dmitrijus Bugelskis, and R□uta Samaitien 2011. EEG analysis – automatic spike detection. *Nonlinear Analysis: Modelling and Control.* 16(375-386.

Alhassan, A. W., Bauchi, Z. M., Adebisi, S. S., Mabrouk, M. A., and Sabo, A. M. 2009. The effect of early administration of glucocorticoids on learning and spatial memory. *Niger. J Physiol Sci.* 24(2): 137-139.

Amaral, D. G. and Witter, M. P. 1989. The three-dimensional organization of the hippocampal formation: a review of anatomical data. *Neuroscience.* 31(3): 571-591.

Andersson, M., Hansson, O., Minthon, L., Rosen, I., and Londos, E. 2008. Electroencephalogram variability in dementia with lewy bodies, Alzheimer's disease and controls. *Dement. Geriatr. Cogn Disord.* 26(3): 284-290.

Barcaro, U., Navona, C., Belloli, S., Bonanni, E., Gneri, C., and Murri, L. 1998. A simple method for the quantitative description of sleep microstructure. *Electroencephalogr. Clin. Neurophysiol.* 106(5): 429-43

Arbel, I., Kadar, T., Silbermann, M., and Levy, A. 1994. The effects of long-term corticosterone administration on hippocampal morphology and cognitive performance of middle-aged rats. *Brain Res.* 657(1-2): 227-235.

Bains, J. S. and Shaw, C. A. 1997. Neurodegenerative disorders in humans: the role of glutathione in oxidative stress-mediated neuronal death. *Brain Res. Brain Res. Rev.* 25(3): 335-358.

Banasr, M., Chowdhury, G. M., Terwilliger, R., Newton, S. S., Duman, R. S., Behar, K. L., and Sanacora, G. 2010. Glial pathology in an animal model of depression: reversal of stress-induced cellular, metabolic and behavioral deficits by the glutamate-modulating drug riluzole. *Mol. Psychiatry.* 15(5): 501-511.

Bardgett, M. E., Jackson, J. L., Taylor, G. T., and Csernansky, J. G. 1995. Kainic acid decreases hippocampal neuronal number and increases dopamine receptor binding in the nucleus accumbens: an animal model of schizophrenia. *Behav. Brain Res.* 70(2): 153-164.

Ben-Ari, Y. 1985. Limbic seizure and brain damage produced by kainic acid: mechanisms and relevance to human temporal lobe epilepsy. *Neuroscience.* 14(2): 375-403.

Binder, S., Rawohl, J., Born, J., and Marshall, L. 2014. Transcranial slow oscillation stimulation during NREM sleep enhances acquisition of the radial maze task and modulates cortical network activity in rats. *Front Behav. Neurosci.* 7(220)

Bradbury, M. J., Dement, W. C., and Edgar, D. M. 1998. Effects of adrenalectomy and subsequent corticosterone replacement on rat sleep state and EEG power spectra. *Am. J. Physiol.* 275(2 Pt 2): R555-R565.

Bodizs, R., Kantor, S., Szabo, G., Szucs, A., Eross, L., and Halasz, P. 2001. Rhythmic hippocampal slow oscillation characterizes REM sleep in humans. *Hippocampus.* 11(6): 747-753.

Bohn, M. C., Howard, E., Vielkind, U., and Krozowski, Z. 1991. Glial cells express both mineralocorticoid and glucocorticoid receptors. *J. Steroid Biochem. Mol. Biol.* 40(1-3): 105-111.

Cai, Z. J. 1991. The functions of sleep: further analysis. *Physiol Behav.* 50(1): 53-60.

Carpentier, P., Foquin, A., Dorandeu, F., and Lallement, G. 2001. Delta activity as an early indicator for soman-induced brain damage: a review. *Neurotoxicology.* 22(3): 299-315.

Carroll, B. J., Curtis, G. C., and Mendels, J. 1976. Neuroendocrine regulation in depression. II. Discrimination of depressed from nondepressed patients. *Arch. Gen. Psychiatry.* 33(9): 1051-1058.

Chen, Z., Yu, S., Concha, H. Q., Zhu, Y., Mix, E., Winblad, B., Ljunggren, H. G., and Zhu, J. 2004. Kainic acid-induced excitotoxic hippocampal neurodegeneration in C57BL/6 mice: B cell and T cell subsets may contribute differently to the pathogenesis. *Brain Behav. Immun.* 18(2): 175-185.

Claessens, S. E., Belanoff, J. K., Kanatsou, S., Lucassen, P. J., Champagne, D. L., and de Kloet, E. R. 2012. Acute effects of neonatal dexamethasone treatment on proliferation and astrocyte immunoreactivity in hippocampus and corpus callosum: towards a rescue strategy. *Brain Res.* 1482(11-12).

Clark, B. J., Hines, D. J., Hamilton, D. A., and Whishaw, I. Q. 2005. Movements of exploration intact in rats with hippocampal lesions. *Behav. Brain Res.* 163(1): 91-99.

Coben, L. A., Danziger, W. L., and Berg, L. 1983. Frequency analysis of the resting awake EEG in mild senile dementia of Alzheimer type. *Electroencephalogr. Clin. Neurophysiol.* 55(4): 372-380.

Coburn-Litvak, P. S., Tata, D. A., Gorby, H. E., McCloskey, D. P., Richardson, G., and Anderson, B. J. 2004. Chronic corticosterone affects brain weight, and mitochondrial, but not glial volume fraction in hippocampal area CA3. *Neuroscience.* 124(2): 429-438.

Coenen, A. M. and Van Luijtelaar, E. L. 1987. The WAG/Rij rat model for absence epilepsy: age and sex factors. *Epilepsy Res.* 1(5): 297-301.

Cole, C. S. and Richards, K. C. 2006. Sleep in persons with dementia: Increasing quality of life by managing sleep disorders. *J Gerontol. Nurs.* 32(3): 48-53.

Cornell-Bell, A. H., Finkbeiner, S. M., Cooper, M. S., and Smith, S. J. 1990. Glutamate induces calcium waves in cultured astrocytes: long-range glial signaling. *Science.* 247(4941): 470-473.

Conrad, C. D., McLaughlin, K. J., Harman, J. S., Foltz, C., Wieczorek, L., Lightner, E., and Wright, R. L. 2007. Chronic glucocorticoids increase hippocampal vulnerability to neurotoxicity under conditions that produce CA3 dendritic retraction but fail to impair spatial recognition memory. *J. Neurosci.* 27(31): 8278-8285.

Czeh, B., Simon, M., Schmelting, B., Hiemke, C., and Fuchs, E. 2006. Astroglial plasticity in the hippocampus is affected by chronic psychosocial stress and concomitant fluoxetine treatment. *Neuropsychopharmacology.* 31(8): 1616-1626.

Dallman, M. F., Akana, S. F., Strack, A. M., Hanson, E. S., and Sebastian, R. J. 1995. The neural network that regulates energy balance is responsive to glucocorticoids and insulin and also regulates HPA axis responsivity at a site proximal to CRF neurons. *Ann. N. Y. Acad. Sci.* 771(730-742.

Darchia, N., Campbell, I. G., Tan, X., and Feinberg, I. 2007. Kinetics of NREM delta EEG power density across NREM periods depend on age and on delta-band designation. *Sleep.* 30(1): 71-79.

De Boer, S. F., Koopmans, S. J., Slangen, J. L., and Van der Gugten, J. 1990. Plasma catecholamine, corticosterone and glucose responses to repeated stress in rats: effect of interstressor interval length. *Physiol Behav.* 47(6): 1117-1124.

De Kloet, E. R., Vreugdenhil, E., Oitzl, M. S., and Joels, M. 1998. Brain corticosteroid receptor balance in health and disease. *Endocr. Rev.* 19(3): 269-301.

Dement, W. and Kleitman, N. 1957. The relation of eye movements during sleep to dream activity: an objective method for the study of dreaming. *J Exp. Psychol.* 53(5): 339-346.

Diamond, D. M., Branch, B. J., Fleshner, M., and Rose, G. M. 1995. Effects of dehydroepiandrosterone sulfate and stress on hippocampal electrophysiological plasticity. *Ann. N. Y. Acad. Sci.* 774(304-307.

Diamond, D. M., Fleshner, M., Ingersoll, N., and Rose, G. M. 1996. Psychological stress impairs spatial working memory: relevance to electrophysiological studies of hippocampal function. *Behav. Neurosci.* 110(4): 661-672.

Doyle, P., Rohner-Jeanrenaud, F., and Jeanrenaud, B. 1993. Local cerebral glucose utilization in brains of lean and genetically obese (fa/fa) rats. *Am. J Physiol.* 264(1 Pt 1): E29-E36.

Dringenberg, H. C., Diavolitsis, P., and Noseworthy, P. A. 2000. Effect of tacrine on EEG slowing in the rat: enhancement by concurrent monoamine therapy. *Neurobiol. Aging.* 21(1): 135-143.

Driscoll, I., Hamilton, D. A., Petropoulos, H., Yeo, R. A., Brooks, W. M., Baumgartner, R. N., and Sutherland, R. J. 2003. The aging hippocampus: cognitive, biochemical and structural findings. *Cereb. Cortex.* 13(12): 1344-1351.

Driscoll, I., Howard, S. R., Stone, J. C., Monfils, M. H., Tomanek, B., Brooks, W. M., and Sutherland, R. J. 2006. The aging hippocampus: a multi-level analysis in the rat. *Neuroscience.* 139(4): 1173-1185.

Dugan, L. L. and Choi, D. W. 1994. Excitotoxicity, free radicals, and cell membrane changes. *Ann. Neurol.* 35 Suppl(S17-S21.

Dujardin, K., Bourriez, J. L., and Guieu, J. D. 1995. Event-related desynchronization (ERD) patterns during memory processes: effects of aging and task difficulty. *Electroencephalogr. Clin. Neurophysiol.* 96(2): 169-182.

Dumermuth, G. and Molinari, L. 1987. Spectral analysis of the EEG. Some fundamentals revisited and some open problems. *Neuropsychobiology.* 17(1-2): 85-99.

Edwards, F. A. 1995. LTP--a structural model to explain the inconsistencies. *Trends Neurosci.* 18(6): 250-255.

Ellis, J. M. 2005. Cholinesterase inhibitors in the treatment of dementia. *J. Am. Osteopath. Assoc.* 105(3): 145-158.

Esch, T., Stefano, G. B., Fricchione, G. L., and Benson, H. 2002. The role of stress in neurodegenerative diseases and mental disorders. *Neuro. Endocrinol. Lett.* 23(3): 199-208.

Everse, J. and Coates, P. W. 2009. Neurodegeneration and peroxidases. *Neurobiol. Aging.* 30(7): 1011-1025.

Finkel, T. 2003. Oxidant signals and oxidative stress. *Curr. Opin. Cell Biol.* 15(2): 247-254.

Fiskum, G., Starkov, A., Polster, B. M., and Chinopoulos, C. 2003. Mitochondrial mechanisms of neural cell death and neuroprotective interventions in Parkinson's disease. *Ann. N. Y. Acad. Sci.* 991: 111-119.

Fuchs, E., Czeh, B., Kole, M. H., Michaelis, T., and Lucassen, P. J. 2004. Alterations of neuroplasticity in depression: the hippocampus and beyond. *Eur. Neuropsychopharmacol.* 14 Suppl 5: S481-S490.

Fuggetta, G., Bennett, M. A., Duke, P. A., and Young, A. M. 2014. Quantitative electroencephalography as a biomarker for proneness toward developing psychosis. *Schizophr. Res.* 153(1–3): 68–77

Ganguly, R. and Guha, D. 2008. Alteration of brain monoamines & EEG wave pattern in rat model of Alzheimer's disease & protection by Moringa oleifera. *Indian J. Med. Res.* 128(6): 744-751.

Geering, B. A., Achermann, P., Eggimann, F., and Borbely, A. A. 1993. Period-amplitude analysis and power spectral analysis: a comparison based on all-night sleep EEG recordings. *J Sleep Res.* 2(3): 121-129.

Geinisman, Y., Detoledo-Morrell, L., Morrell, F., and Heller, R. E. 1995. Hippocampal markers of age-related memory dysfunction: behavioral, electrophysiological and morphological perspectives. *Prog. Neurobiol.* 45(3): 223-252.

Giap, B. T., Jong, C. N., Ricker, J. H., Cullen, N. K., and Zafonte, R. D. 2000. The hippocampus: anatomy, pathophysiology, and regenerative capacity. *J Head Trauma Rehabil.* 15(3): 875-894.

Golomb, J., de Leon, M. J., Kluger, A., George, A. E., Tarshish, C., and Ferris, S. H. 1993. Hippocampal atrophy in normal aging. An association with recent memory impairment. *Arch. Neurol.* 50(9): 967-973.

Grosmark, A. D., Mizuseki, K., Pastalkova, E., Diba, K., and Buzsaki, G. 2012. REM sleep reorganizes hippocampal excitability. *Neuron.* 75(6): 1001-1007.

Grunwald, M., Hensel, A., Wolf, H., Weiss, T., and Gertz, H. J. 2007. Does the hippocampal atrophy correlate with the cortical theta power in elderly subjects with a range of cognitive impairment? *J Clin. Neurophysiol.* 24(1): 22-26.

Halasz, P., Terzano, M., Parrino, L., and Bodizs, R. 2004. The nature of arousal in sleep. *J Sleep Res.* 13(1): 1-23.

Hall, M., Thayer, J. F., Germain, A., Moul, D., Vasko, R., Puhl, M., Miewald, J., and Buysse, D. J. 2007. Psychological stress is associated with heightened physiological arousal during NREM sleep in primary insomnia. *Behav. Sleep Med.* 5(3): 178-193.

Hansen, I. H., Marcussen, M., Christensen, J. A., Jennum, P., and Sorensen, H. B. 2013. Detection of a sleep disorder predicting Parkinson's disease. *Conf. Proc. IEEE Eng Med. Biol. Soc.* 2013(5793-5796.

Hartikainen, P., Soininen, H., Partanen, J., Helkala, E. L., and Riekkinen, P. 1992. Aging and spectral analysis of EEG in normal subjects: a link to memory and CSF AChE. *Acta Neurol. Scand.* 86(2): 148-155.

Haynes, L. E., Griffiths, M. R., Hyde, R. E., Barber, D. J., and Mitchell, I. J. 2001. Dexamethasone induces limited apoptosis and extensive sublethal damage to specific subregions of the striatum and hippocampus: implications for mood disorders. *Neuroscience.* 104(1): 57-69.

Heffelfinger, A. K. and Newcomer, J. W. 2001. Glucocorticoid effects on memory function over the human life span. *Dev. Psychopathol.* 13(3): 491-513.

Heidenreich, K. A. 2003. Molecular mechanisms of neuronal cell death. *Ann. N. Y. Acad. Sci.* 991(237-250.

Helkala, E. L., Hanninen, T., Hallikainen, M., Kononen, M., Laakso, M. P., Hartikainen, P., Soininen, H., Partanen, J., Partanen, K., Vainio, P., and Riekkinen, P., Sr. 1996. Slow-wave activity in the spectral analysis of the electroencephalogram and volumes of hippocampus in subgroups of Alzheimer's disease patients. *Behav. Neurosci.* 110(6): 1235-1243.

Hibberd, C., Yau, J. L., and Seckl, J. R. 2000. Glucocorticoids and the ageing hippocampus. *J Anat.* 197 Pt 4(553-562.

Hoenicka, J. 2006. [Genes in Alzheimer's disease]. *Rev. Neurol.* 42(5): 302-305.

Ikonomidou, C. and Kaindl, A. M. 2011. Neuronal death and oxidative stress in the developing brain. *Antioxid. Redox. Signal.* 14(8): 1535-1550.

Inoue, M., Peeters, B. W., van Luijtelaar, E. L., Vossen, J. M., and Coenen, A. M. 1990. Spontaneous occurrence of spike-wave discharges in five inbred strains of rats. *Physiol Behav.* 48(1): 199-201.

Jan, J. E., Reiter, R. J., Bax, M. C., Ribary, U., Freeman, R. D., and Wasdell, M. B. 2010. Long-term sleep disturbances in children: a cause of neuronal loss. *Eur. J Paediatr. Neurol.* 14(5): 380-390.

Joels, M. and de Kloet, E. R. 1994. Mineralocorticoid and glucocorticoid receptors in the brain. Implications for ion permeability and transmitter systems. *Prog. Neurobiol.* 43(1): 1-36.

Jones, B. E. 2005. From waking to sleeping: neuronal and chemical substrates. *Trends Pharmacol. Sci.* 26(11): 578-586.

Kim, B. S., Kim, M. Y., and Leem, Y. H. 2011. Hippocampal neuronal death induced by kainic acid and restraint stress is suppressed by exercise. *Neuroscience.* 194(291-301.

Kim, J. J., Lee, H. J., Han, J. S., and Packard, M. G. 2001. Amygdala is critical for stress-induced modulation of hippocampal long-term potentiation and learning. *J Neurosci.* 21(14): 5222-5228.

Kumar, A., Prakash, A., and Pahwa, D. 2011. Galantamine potentiates the protective effect of rofecoxib and caffeic acid against intrahippocampal Kainic acid-induced cognitive dysfunction in rat. *Brain Res. Bull.* 85(3-4): 158-168.

Kwak, Y. T. 2006. Quantitative EEG findings in different stages of Alzheimer's disease. *J. Clin. Neurophysiol.* 23(5): 456-461.

Lancel, M. 1993. Cortical and subcortical EEG in relation to sleep-wake behavior in mammalian species. *Neuropsychobiology.* 28(3): 154-159.

Landfield, P. W., Waymire, J. C., and Lynch, G. 1978. Hippocampal aging and adrenocorticoids: quantitative correlations. *Science.* 202(4372): 1098-1102.

Lothman, E. W. and Collins, R. C. 1981. Kainic acid induced limbic seizures: metabolic, behavioral, electroencephalographic and neuropathological correlates. *Brain Res.* 218(1-2): 299-318.

Lu, J., Greco, M. A., Shiromani, P., and Saper, C. B. 2000. Effect of lesions of the ventrolateral preoptic nucleus on NREM and REM sleep. *J Neurosci.* 20(10): 3830-3842.

Luine, V., Villegas, M., Martinez, C., and McEwen, B. S. 1994. Repeated stress causes reversible impairments of spatial memory performance. *Brain Res.* 639(1): 167-170.

Lv, Y., Chu, F., Meng, H., Wang, Z., and Cui, L. 2013. A Patient with Progressive Cognitive Decline and Periodic Abnormal Waves in EEG: PLEDs of Neurosyphilis or PSDs of Creutzfeldt-Jakob Disease? *Clin. EEG. Neurosci.*

Mackenzie, L., Pope, K. J., and Willoughby, J. O. 2004. Physiological and pathological spindling phenomena have similar regional EEG power distributions. *Brain Res.* 1008(1): 92-106.

Mackenzie, L., Pope, K. J., and Willoughby, J. O. 2010. EEG spindles in the rat: evidence for a synchronous network phenomenon. *Epilepsy Res.* 89(2-3): 194-206.

Maquet, P. 2001. The role of sleep in learning and memory. *Science.* 294(5544): 1048-1052.

Martin, S. J., Grimwood, P. D., and Morris, R. G. 2000. Synaptic plasticity and memory: an evaluation of the hypothesis. *Annu. Rev. Neurosci.* 23(649-711.

Mattson, M. P. 1998. Modification of ion homeostasis by lipid peroxidation: roles in neuronal degeneration and adaptive plasticity. *Trends Neurosci.* 21(2): 53-57.

McCarty, R. and Gold, P. E. 1981. Plasma catecholamines: effects of footshock level and hormonal modulators of memory storage. *Horm. Behav.* 15(2): 168-182.

McCormick, D. A. and Bal, T. 1997. Sleep and arousal: thalamocortical mechanisms. *Annu. Rev. Neurosci.* 20(185-215.

McEwen, B. S. 2002. Protective and damaging effects of stress mediators: the good and bad sides of the response to stress. *Metabolism.* 51(6 Suppl 1): 2-4.

McEwen, B. S., Angulo, J., Cameron, H., Chao, H. M., Daniels, D., Gannon, M. N., Gould, E., Mendelson, S., Sakai, R., Spencer, R., and . 1992. Paradoxical effects of adrenal steroids on the brain: protection versus degeneration. *Biol. Psychiatry.* 31(2): 177-199.

McEwen, B. S., Weiss, J. M., and Schwartz, L. S. 1968. Selective retention of corticosterone by limbic structures in rat brain. *Nature.* 220(5170): 911-912.

McIntosh, L. J. and Sapolsky, R. M. 1996. Glucocorticoids increase the accumulation of reactive oxygen species and enhance adriamycin-induced toxicity in neuronal culture. *Exp. Neurol.* 141(2): 201-206.

Meerlo, P., Mistlberger, R. E., Jacobs, B. L., Heller, H. C., and McGinty, D. 2009. New neurons in the adult brain: the role of sleep and consequences of sleep loss. *Sleep Med Rev.* 13(3): 187-194.

Micanovic, C. and Pal, S. 2013. The diagnostic utility of EEG in early-onset dementia: a systematic review of the literature with narrative analysis. *J. Neural Transm.*121: 59-69

Moghaddam, B., Bolinao, M. L., Stein-Behrens, B., and Sapolsky, R. 1994. Glucocorticoids mediate the stress-induced extracellular accumulation of glutamate. *Brain Res.* 655(1-2): 251-254.

Montgomery, E. M., Bardgett, M. E., Lall, B., Csernansky, C. A., and Csernansky, J. G. 1999. Delayed neuronal loss after administration of intracerebroventricular kainic acid to preweanling rats. *Brain Res. Dev. Brain Res.* 112(1): 107-116.

Morairty, S. R., Dittrich, L., Pasumarthi, R. K., Valladao, D., Heiss, J. E., Gerashchenko, D., and Kilduff, T. S. 2013. A role for cortical nNOS/NK1 neurons in coupling homeostatic sleep drive to EEG slow wave activity. *Proc. Natl. Acad. Sci. U. S. A.* 110(50): 20272-20277.

Morris, R. G., Garrud, P., Rawlins, J. N., and O'Keefe, J. 1982. Place navigation impaired in rats with hippocampal lesions. *Nature.* 297(5868): 681-683.

Moser, N. J., Phillips, B. A., Guthrie, G., and Barnett, G. 1996. Effects of dexamethasone on sleep. *Pharmacol. Toxicol.* 79(2): 100-102.

Munch, M., Knoblauch, V., Blatter, K., Schroder, C., Schnitzler, C., Krauchi, K., Wirz-Justice, A., and Cajochen, C. 2004. The frontal predominance in human EEG delta activity after sleep loss decreases with age. *Eur. J Neurosci.* 20(5): 1402-1410.

Munck, A., Guyre, P. M., and Holbrook, N. J. 1984. Physiological functions of glucocorticoids in stress and their relation to pharmacological actions. *Endocr. Rev.* 5(1): 25-44.

Myhrer, T. 2003. Neurotransmitter systems involved in learning and memory in the rat: a meta-analysis based on studies of four behavioral tasks. *Brain Res. Brain Res. Rev.* 41(2-3): 268-287.

Nedergaard, M., Ransom, B., and Goldman, S. A. 2003. New roles for astrocytes: redefining the functional architecture of the brain. *Trends Neurosci.* 26(10): 523-530.

Nichols, N. R., Osterburg, H. H., Masters, J. N., Millar, S. L., and Finch, C. E. 1990. Messenger RNA for glial fibrillary acidic protein is decreased in rat brain following acute and chronic corticosterone treatment. *Brain Res. Mol. Brain Res.* 7(1): 1-7.

Nichols NR, Zieba M, Bye N. 2001. Do glucocorticoids contribute to brain aging?. *Brain Res Brain Res Rev*. 37:273-286.

O'Callaghan, J. P., Brinton, R. E., and McEwen, B. S. 1989. Glucocorticoids regulate the concentration of glial fibrillary acidic protein throughout the brain. *Brain Res.* 494(1): 159-161.

Orrenius, S., Gogvadze, V., and Zhivotovsky, B. 2007. Mitochondrial oxidative stress: implications for cell death. *Annu. Rev. Pharmacol. Toxicol.* 47: 143-183.

Pace-Schott, E. F. and Spencer, R. M. 2011. Age-related changes in the cognitive function of sleep. *Prog. Brain Res.* 191:75-89.

Palop, J. J., Chin, J., and Mucke, L. 2006. A network dysfunction perspective on neurodegenerative diseases. *Nature.* 443(7113): 768-773.

Pavlides, C., Watanabe, Y., Magarinos, A. M., and McEwen, B. S. 1995. Opposing roles of type I and type II adrenal steroid receptors in hippocampal long-term potentiation. *Neuroscience.* 68(2): 387-394.

Perlis, M. L., Smith, M. T., Andrews, P. J., Orff, H., and Giles, D. E. 2001. Beta/Gamma EEG activity in patients with primary and secondary insomnia and good sleeper controls. *Sleep.* 24(1): 110-117.

Petit, D., Gagnon, J. F., Fantini, M. L., Ferini-Strambi, L., and Montplaisir, J. 2004. Sleep and quantitative EEG in neurodegenerative disorders. *J Psychosom. Res.* 56(5): 487-496.

Pinto A, Jacobsen M, Geoghegan PA, Cangelosi A, Cejudo ML, Tironi-Farinati C, Goldstein J. 2013. Dexamethasone rescues neurovascular unit integrity from cell damage caused by systemic administration of shiga toxin 2 and lipopolysaccharide in mice motor cortex. *PLoS One*. 8(7): 1-14.

Prichep, L. S., John, E. R., Ferris, S. H., Reisberg, B., Almas, M., Alper, K., and Cancro, R. 1994. Quantitative EEG correlates of cognitive deterioration in the elderly. *Neurobiol. Aging.* 15(1): 85-90.

Prinz, P. N., Peskind, E. R., Vitaliano, P. P., Raskind, M. A., Eisdorfer, C., Zemcuznikov, N., and Gerber, C. J. 1982. Changes in the sleep and waking EEGs of nondemented and demented elderly subjects. *J Am. Geriatr. Soc.* 30(2): 86-93.

Rasmussen, T., Schliemann, T., Sorensen, J. C., Zimmer, J., and West, M. J. 1996. Memory impaired aged rats: no loss of principal hippocampal and subicular neurons. *Neurobiol. Aging.* 17(1): 143-147.

Reagan, L. P. and McEwen, B. S. 1997. Controversies surrounding glucocorticoid-mediated cell death in the hippocampus. *J. Chem. Neuroanat.* 13(3): 149-167.

Reichlin, S. 1993. Book Review. *N Engl J Med.* 329(14): 1049-1049.

Reul, J. M. and de Kloet, E. R. 1985. Two receptor systems for corticosterone in rat brain: microdistribution and differential occupation. *Endocrinology.* 117(6): 2505-2511.

Reus, V. I. and Wolkowitz, O. M. 2001. Antiglucocorticoid drugs in the treatment of depression. *Expert. Opin. Investig. Drugs.* 10(10): 1789-1796.

Rodrigues, B. J., Montplaisir, J., Petit, D., Postuma, R. B., Bertrand, J. A., Genier, M. D., and Gagnon, J. F. 2013. Electroencephalogram slowing in rapid eye movement sleep behavior disorder is associated with mild cognitive impairment. *Sleep Med.* 14(11): 1059-1063

Romano, A. D., Serviddio, G., de, M. A., Bellanti, F., and Vendemiale, G. 2010. Oxidative stress and aging. *J Nephrol.* 23 Suppl 15(S29-S36.

Roozendaal, B. 2000. 1999 Curt P. Richter award. Glucocorticoids and the regulation of memory consolidation. *Psychoneuroendocrinology.* 25(3): 213-238.

Roozendaal, B. 2002. Stress and memory: opposing effects of glucocorticoids on memory consolidation and memory retrieval. *Neurobiol. Learn. Mem.* 78(3): 578-595.

Roozendaal, B., Nguyen, B. T., Power, A. E., and McGaugh, J. L. 1999. Basolateral amygdala noradrenergic influence enables enhancement of memory consolidation induced by hippocampal glucocorticoid receptor activation. *Proc. Natl. Acad. Sci. U. S. A.* 96(20): 11642-11647.

Routbort, M. J., Bausch, S. B., and McNamara, J. O. 1999. Seizures, cell death, and mossy fiber sprouting in kainic acid-treated organotypic hippocampal cultures. *Neuroscience.* 94(3): 755-765.

Rosenzweig, E. S. and Barnes, C. A. 2003. Impact of aging on hippocampal function: plasticity, network dynamics, and cognition. *Prog. Neurobiol.* 69(3): 143-179.

Sapolsky, R. M. 1985. A mechanism for glucocorticoid toxicity in the hippocampus: increased neuronal vulnerability to metabolic insults. *J. Neurosci.* 5(5): 1228-1232.

Sapolsky, R. M. 1996. Stress, Glucocorticoids, and Damage to the Nervous System: The Current State of Confusion. *Stress.* 1(1): 1-19.

Schmidt, M. T., Kanda, P. A., Basile, L. F., da Silva Lopes, H. F., Baratho, R., Demario, J. L., Jorge, M. S., Nardi, A. E., Machado, S., Ianof, J. N., Nitrini, R., and Anghinah, R. 2013. Index of alpha/theta ratio of the electroencephalogram: a new marker for Alzheimer's disease. *Front Aging Neurosci.* 5(60): 1-6.

Schwartz, J. R. and Roth, T. 2008. Neurophysiology of sleep and wakefulness: basic science and clinical implications. *Curr. Neuropharmacol.* 6(4): 367-378.

Seed, J. A., Dixon, R. A., McCluskey, S. E., and Young, A. H. 2000. Basal activity of the hypothalamic-pituitary-adrenal axis and cognitive function in anorexia nervosa. *Eur. Arch. Psychiatry Clin. Neurosci.* 250(1): 11-15.

Siegel, J. M. 2001. The REM sleep-memory consolidation hypothesis. *Science.* 294(5544): 1058-1063.

Smith, C. 1995. Sleep states and memory processes. *Behav. Brain Res.* 69(1-2): 137-145.

Soininen, H. and Riekkinen, P. J., Sr. 1992. EEG in diagnostics and follow-up of Alzheimer's disease. *Acta Neurol. Scand. Suppl.* 139: 36-39.

Starkman, M. N., Gebarski, S. S., Berent, S., and Schteingart, D. E. 1992. Hippocampal formation volume, memory dysfunction, and cortisol levels in patients with Cushing's syndrome. *Biol. Psychiatry.* 32(9): 756-765.

Steiger, A. 2007. Neurochemical regulation of sleep. *J. Psychiatr. Res.* 41(7): 537-552.

Stein-Behrens, B. A., Lin, W. J., and Sapolsky, R. M. 1994. Physiological elevations of glucocorticoids potentiate glutamate accumulation in the hippocampus. *J Neurochem.* 63(2): 596-602.

Steriade, M. and Deschenes, M. 1984. The thalamus as a neuronal oscillator. *Brain Res.* 320(1): 1-63.

Steriade, M., Deschenes, M., Domich, L., and Mulle, C. 1985. Abolition of spindle oscillations in thalamic neurons disconnected from nucleus reticularis thalami. *J. Neurophysiol.* 54(6): 1473-1497.

Steriade, M., McCormick, D. A., and Sejnowski, T. J. 1993. Thalamocortical oscillations in the sleeping and aroused brain. *Science.* 262(5134): 679-685.

Sun, A. Y., Cheng, Y., and Sun, G. Y. 1992. Kainic acid-induced excitotoxicity in neurons and glial cells. *Prog. Brain Res.* 94: 271-280.

Swaab, D. F., Bao, A. M., and Lucassen, P. J. 2005. The stress system in the human brain in depression and neurodegeneration. *Ageing Res. Rev.* 4(2): 141-194.

Szatkowski, M. and Attwell, D. 1994. Triggering and execution of neuronal death in brain ischaemia: two phases of glutamate release by different mechanisms. *Trends Neurosci.* 17(9): 359-365.

Sze, P. Y. and Yu, B. H. 1995. Glucocorticoid actions on synaptic plasma membranes: modulation of dihydropyridine-sensitive calcium channels. *J. Steroid Biochem. Mol. Biol.* 55(2): 185-192.

Takahashi, T., Kimoto, T., Tanabe, N., Hattori, T. A., Yasumatsu, N., and Kawato, S. 2002. Corticosterone acutely prolonged N-methyl-d-aspartate receptor-mediated Ca2+ elevation in cultured rat hippocampal neurons. *J. Neurochem.* 83(6): 1441-1451.

Tesche, C. D. and Karhu, J. 2000. Theta oscillations index human hippocampal activation during a working memory task. *Proc. Natl. Acad. Sci. U. S. A.* 97(2): 919-924.

Uchida, S., Maloney, T., and Feinberg, I. 1992. Beta (20-28 Hz) and delta (0.3-3 Hz) EEGs oscillate reciprocally across NREM and REM sleep. *Sleep.* 15(4): 352-358.

Unemura, K., Kume, T., Kondo, M., Maeda, Y., Izumi, Y., and Akaike, A. 2012. Glucocorticoids decrease astrocyte numbers by reducing glucocorticoid receptor expression in vitro and in vivo. *J. Pharmacol. Sci.* 119(1): 30-39.

Valdez, L. B., Lores, A. S., Bustamante, J., Alvarez, S., Costa, L. E., and Boveris, A. 2000. Free radical chemistry in biological systems. *Biol. Res.* 33(2): 65-70.

van der Hiele, K., Jurgens, C. K., Vein, A. A., Reijntjes, R. H., Witjes-Ane, M. N., Roos, R. A., van, D. G., and Middelkoop, H. A. 2007. Memory activation reveals abnormal EEG in preclinical Huntington's disease. *Mov Disord.* 22(5): 690-695.

Verdaguer, E., Garcia-Jorda, E., Jimenez, A., Stranges, A., Sureda, F. X., Canudas, A. M., Escubedo, E., Camarasa, J., Pallas, M., and Camins, A. 2002. Kainic acid-induced neuronal cell death in cerebellar granule cells is not prevented by caspase inhibitors. *Br. J Pharmacol.* 135(5): 1297-1307.

Virgin, C. E., Jr., Ha, T. P., Packan, D. R., Tombaugh, G. C., Yang, S. H., Horner, H. C., and Sapolsky, R. M. 1991. Glucocorticoids inhibit glucose transport and glutamate uptake in hippocampal astrocytes: implications for glucocorticoid neurotoxicity. *J. Neurochem.* 57(4): 1422-1428.

Voutsinos-Porche, B., Bonvento, G., Tanaka, K., Steiner, P., Welker, E., Chatton, J. Y., Magistretti, P. J., and Pellerin, L. 2003. Glial glutamate transporters mediate a functional metabolic crosstalk between neurons and astrocytes in the mouse developing cortex. *Neuron.* 37(2): 275-286.

Vyazovskiy, V. V. and Tobler, I. 2005. Theta activity in the waking EEG is a marker of sleep propensity in the rat. *Brain Res.* 1050(1-2): 64-71.

Walder, D. J., Walker, E. F., and Lewine, R. J. 2000. Cognitive functioning, cortisol release, and symptom severity in patients with schizophrenia. *Biol. Psychiatry.* 48(12): 1121-1132.

Walker, M. P., Stickgold, R., Alsop, D., Gaab, N., and Schlaug, G. 2005. Sleep-dependent motor memory plasticity in the human brain. *Neuroscience.* 133(4): 911-917.

Wang, Q., Yu, S., Simonyi, A., Sun, G. Y., and Sun, A. Y. 2005. Kainic acid-mediated excitotoxicity as a model for neurodegeneration. *Mol. Neurobiol.* 31(1-3): 3-16.

Watanabe, Y., Gould, E., and McEwen, B. S. 1992. Stress induces atrophy of apical dendrites of hippocampal CA3 pyramidal neurons. *Brain Res.* 588(2): 341-345.

Whitnall, M. H. 1993. Regulation of the hypothalamic corticotropin-releasing hormone neurosecretory system. *Prog. Neurobiol.* 40(5): 573-629.

Winner, B., Kohl, Z., and Gage, F. H. 2011. Neurodegenerative disease and adult neurogenesis. *Eur. J. Neurosci.* 33(6): 1139-1151.

Woolley, C. S., Gould, E., and McEwen, B. S. 1990. Exposure to excess glucocorticoids alters dendritic morphology of adult hippocampal pyramidal neurons. *Brain Res.* 531(1-2): 225-231.

Wolter, T., Steinbrecher, T., and Elstner, M. 2014. Correction: Computational Study of Synthetic Agonist Ligands of Ionotropic Glutamate Receptors. *PLoS. One.* 8(3): 1-13.

Won, S. J., Kim, D. Y., and Gwag, B. J. 2002. Cellular and molecular pathways of ischemic neuronal death. *J. Biochem. Mol. Biol.* 35(1): 67-86.

Yu, S., Holsboer, F., and Almeida, O. F. 2008. Neuronal actions of glucocorticoids: focus on depression. *J. Steroid Biochem. Mol. Biol.* 108(3-5): 300-309.

APPENDIX

Table 1 R-square data of correlation among EEG patterns, leaning & memory behavior and brain structures in dexamethasone induced neurodegenerative rats. Grey box represent significant correlation, $p<0.05$.

	SA %	Delta PC AW	Theta PC AW	Alpha FC AW	Alpha PC AW	Beta FC SWS	Beta PC SWS	REM %	Non SP AW	Non SP SWS	CA1 Nu	CA3 Nu	DG Nu	PC Nu	CA1 GFAP	CA3 GFAP	DG GFAP	PC GFAP
SA %																		
Delta PC AW	0.460																	
Theta PC AW	0.256	0.448																
Alpha FC AW	0.264	0.740	0.367															
Alpha PC AW	0.408	0.758	0.554	0.718														
Beta FC SWS	0.203	0.020	0.195	0.190	0.138													
Beta PC SWS	0.008	0.538	0.329	0.290	0.324	0.056												
REM %	0.233	0.371	0.416	0.409	0.474	0.291	0.091											
Non SP AW	0.211	0.429	0.266	0.456	0.455	0.003	0.495	0.179										
Non SP SWS	0.193	0.419	0.085	0.503	0.394	0.078	0.058	0.408	0.081									
CA1 Nu	0.296	0.539	0.537	0.509	0.423	0.271	0.218	0.537	0.459	0.384								
CA3 Nu	0.307	0.237	0.295	0.255	0.222	0.021	0.167	0.216	0.261	0.317	0.244							
DG Nu	0.270	0.612	0.433	0.399	0.385	0.250	0.054	0.433	0.366	0.552	0.748	0.292						
PC Nu	0.126	0.217	0.368	0.252	0.277	0.151	0.094	0.426	0.173	0.300	0.448	0.089	0.510					
CA1 GFAP	0.550	0.310	0.253	0.208	0.267	0.274	0.002	0.227	0.112	0.103	0.342	0.148	0.222	0.144				
CA3 GFAP	0.083	0.241	0.326	0.336	0.188	0.281	0.046	0.118	0.153	0.383	0.205	0.340	0.251	0.198	0.088			
DG GFAP	0.389	0.512	0.255	0.445	0.445	0.222	0.036	0.368	0.458	0.518	0.435	0.550	0.469	0.220	0.245	0.098		
PC GFAP	0.189	0.118	0.287	0.144	0.144	0.050	0.028	0.429	0.133	0.234	0.113	0.238	0.159	0.523	0.089	0.164	0.144	

Table 2 R-square data of correlation among EEG patterns, leaning & memory behavior and brain structures in kainic acid induced neurodegenerative rats. Grey box represent significant correlation, $p<0.05$.

	No. of Entries	Delta AW	Theta AW	Delta SWS	AW %	SWS %	REM %	Sleep Lat	CA1 Nu	CA2 Nu	CA3 Nu	DG Nu
No. of Entries												
Delta AW	0.340											
Theta AW	0.300	0.355										
Delta SWS	0.259	0.688	0.516									
AW %	0.570	0.445	0.638	0.657								
SWS %	0.599	0.294	0.521	0.693	0.895							
REM %	0.220	0.311	0.319	0.339	0.640	0.234						
Sleep Lat	0.409	0.394	0.420	0.399	0.456	0.569	0.202					
CA1 Nu	0.529	0.328	0.407	0.424	0.512	0.618	0.428	0.531				
CA2 Nu	0.117	0.396	0.434	0.423	0.068	0.219	0.124	0.258	0.284			
CA3 Nu	0.316	0.246	0.347	0.350	0.518	0.434	0.584	0.338	0.563	0.364		
DG Nu	0.463	0.279	0.351	0.433	0.270	0.530	0.116	0.166	0.460	0.446	0.384	

PRINCE OF SONGKLA UNIVERSITY
15 Karnjanawanij Road, Hat Yai, Songkhla 90110, Thailand
Tel (66-74) 286958 Fax (66-74) 286961
Website : www.psu.ac.th

MOE 0521.11/ ๑๐๙๙ Ref.14/2011

December ๑๖ , 2011

This is to certify that the research project entitled "Relations among EEG patterns, learning & memory and brain structures in induced neurodegenerative rats" which was conducted by Asst.Prof.Dr. Ekkasit Kumarnsit, Faculty of Sciences, Prince of Songkla University, has been approved by The Animal Ethic Committee, Prince of Songkla University.

Kitja Sawangjaroen.

Kitja Sawangjaroen, Ph.D.
Chairman,
The Animal Ethic Committee, Prince of Songkla University

37th Congress of IUPS (Birmingham, UK) (2013) **Proc 37th IUPS, PCC144**

Poster Communications

Analysis of parietal EEG following hippocampal injection with kainic acid in rats

Acharaporn Issuriya[1], Uraporn Vangvatharanon[2], Chatchai Wattanapiromsakul[3], Ekkasit Kumarnsit[1]

1. Physiology, Faculty of science, Prince of Songkla University, Hadyai, Songkhla, Thailand.
2. Anatomy, Faculty of Science, Prince of Songkla University, Hadyai, Songkhla, Thailand.
3. Phamacognosy, Faculty of Phamaceutical Science, Prince of Songkla University, Hadyai, Songkhla, Thailand.

Electroencephalogram (EEG) pattern represents the electric activity of brain cells. Its recordings have helped clinicians for decades to diagnose specific diseases of the central nervous system. The present study characterized behaviors and EEG patterns after injection with kainic acid (KA) in rats. Male Wistar rats (300-350g, n=6) were anesthetized with 60 mg/kg Zoletil® 100 (i.m.). Assessment of depth anesthetic was evaluated by gentle toe pinch withdrawal reflex. During the surgery, the depth of anesthetic was also evaluated periodically and additional anesthetic was injected to animal that was found with any reaction of too light anesthesia. Then rats were implanted stainless steel screw electrodes on both sides of the parietal cortices (AP; -4, ML; 4) for EEG recording and a cannula for KA injection into right dorsal hippocampus (AP; -4.2, ML; 3.6, DV; 3.8). Rats were sacrificed by thiopental sodium overdose injection. Results showed that the injection of KA (1 nmol/µl) 1 µl into hippocampus (continuously 7 days) induced hyperactivity of hippocampal neurons via kainate receptor. KA administration did not induce neither increase in explorative behavior nor change in learning and memory behavior, observed in Y-maze test (5min.). EEG signals of individual rats were recorded for 2-h period through connection of recording cables. EEG signals were digitized at 400 Hz by a PowerLab/4SP system (AD Instruments) with 12-bit A/D, and stored in a PC through the Chart program software. The EEG signals were processed through 1.25 – 45 Hz band pass filter. The digitized EEG data were segmented into 1024-point (50% overlap) and the signals were converted to power spectra by the fast Fourier transform algorithm (Hanning window cosine transform). Intrahippocampal injection of KA induced paroxysmal discharges in the ipsilateral EEG. This abnormality of brain wave of frequent spikes occurred either in isolated or short bursts. Saline injection did not induce any change in EEG patterns. EEG spectral power analysis revealed the ipsilateral increase in power density (µV2/Hz) of slow wave activity (0.125-5 Hz, 18.55%) and decrease in power density of fast wave activity (23-45 Hz, 6.97%) compared to pretreatment levels ($p<0.05$,compared by T-test). The 7th day after injection (last day) rats with KA administration showed only the decrease in theta activity (4-7 Hz, 5.32%). No similar finding was observed contralaterally. This study demonstrated cortical EEG characteristics following activation of hippocampal neurons via glutamate receptor. The data suggest that EEG study is sufficiently accurate to identify brain site and time dependent effects of neurodegenerative induction.

Acknowledgements: This work was supported by Prince of Songkla Scholarship, Prince of Songkla University, Thailand

VITAE

Name Miss Acharaporn Issuriya

Student ID 5210230014

Academic background

Degree	Name of Institution	Year of Graduation
Bachelor of Science (Biology)	Prince of Songkla University	2005
Master of Pharmaceutical Science (Pharmacognosy and Pharmaceutical Botany)	Prince of Songkla University	2008

Scholarship Awards during Enrolment

Teaching Assistance scholarship, 2009

Scholarship form Prince of Songkla University Graduate Studies Grant, Prince of Songkla University, Songkhla, Thailand,

List of Publication and Proceeding

Issuriya, A., Vongvatcharanon, U., Wattanapiromsakul, C. and Kumarnsit, E. 2013. Analysis of parietal EEG Following hippocampal injection with kainic acid in rat. 37th Congress of International Union of Physiological Society. Birmingham, UK. 21-26 July 2013. PCC144.